# PATTERN FORMATION: A CRITICAL STUDY OF LIESEGANG AND HELICAL PATTERNS IN REACTION DIFFUSION SYSTEMS

A Thesis Submitted to
**UNIVERSITY OF CALICUT**
in partial fulfillment of the requirements
for the award of the degree of
**DOCTOR OF PHILOSOPHY IN PHYSICS**

By
**SHIBI THOMAS**

*Supervisor:*
**Prof.(Dr)GEORGE VARGHESE**

DEPARTMENT OF PHYSICS
UNIVERSITY OF CALICUT
KERALA, INDIA

JUNE 2016

Dr. GEORGE VARGHESE
Professor (Rtd)
Department of Physics
University of Calicut
Kerala, India.
Email:gv@uoc.ac.in

$22^{th}$ September 2017

# Certificate

Certified that the thesis entitled "PATTERN FORMATION: A CRITICAL STUDY OF LIESEGANG AND HELICAL PATTERNS IN REACTION DIFFUSION SYSTEMS" submitted by Shibi Thomas has undergone all corrections suggested by adjudicators and there are no further errors.

Dr. GEORGE VARGHESE
(Supervising Guide)

# PATTERN FORMATION: A CRITICAL STUDY OF LIESEGANG AND HELICAL PATTERNS IN REACTION DIFFUSION SYSTEMS

A Thesis Submitted to
**UNIVERSITY OF CALICUT**
in partial fulfillment of the requirements
for the award of the degree of
**DOCTOR OF PHILOSOPHY IN PHYSICS**

By
**SHIBI THOMAS**

*Supervisor:*
**Prof.(Dr)GEORGE VARGHESE**
(Director KSCSTE,Trivandrum)

DEPARTMENT OF PHYSICS
UNIVERSITY OF CALICUT
KERALA, INDIA

JUNE 2016

Dr. GEORGE VARGHESE
(Director KSCSTE, Trivandrum)
Professor (Rtd)
Department of Physics
University of Calicut
Kerala, India.

---

$27^{th}$ June 2016

# Certificate

Certified that the work presented in this thesis entitled "PATTERN FORMATION: A CRITICAL STUDY OF LIESEGANG AND HELICAL PATTERNS IN REACTION DIFFUSION SYSTEMS" is based on the authentic record of research carried out by Mrs. Shibi Thomas under my guidance and supervision in the Department of Physics, University of Calicut, Kerala and has not been included in any other thesis submitted for the award of any degree in any university and has undergone plagiarism check using URKUND software at CHMK Library, University of Calicut and found that the plagiarism results are within the limit.

Dr. GEORGE VARGHESE
(Supervising Guide)

---

Phone : +91 9447227571 Email: gv@uoc.ac.in

Dr. GEORGE VARGHESE
(Director KSCSTE, Trivandrum)
Professor (Rtd)
Department of Physics
University of Calicut
Kerala, India.

---

$27^{th}$ June 2016

# Certificate

Certified that the following articles, originated as the outcome of this research work, are published in the peer-reviewed national and international journals.

1. Shibi Thomas, George Varghese, Dora Bardfalvy, Zoltan Racz, Istvan Lagzi, Chem. Phys. Lett., 599, 159 (2014)

2. Shibi Thomas, George Varghese, Istvan Lagzi, Pramana, 78, 135, (2012)

Dr. GEORGE VARGHESE
(Supervising Guide)

---

Phone : +91 9447227571 Email: gv@uoc.ac.in

# Declaration

I hereby declare that the work presented in this thesis entitled "PATTERN FORMATION: A CRITICAL STUDY OF LIESEGANG AND HELICAL PATTERNS IN REACTION DIFFUSION SYSTEMS"is based on the original research work and is prepared independently by me under the supervision and guidance of Dr. GEORGE VARGHESE, Professor(Rtd), Department of Physics, University of Calicut, Kerala and has not been included in any other thesis submitted previously for the award of any degree in any university.

Shibi Thomas

Calicut University Campus
$27^{th}$ June 2016

# List of Publications/Conference

1. Helicoidal precipitation patterns in silica and agarose gels

   Shibi Thomas, George Varghese, Dora Bardfalvy, Zoltan Racz, Istvan Lagzi, Chem. Phys. Lett., 599, 159 (2014)

2. The width of Liesegang bands: A study using moving boundary model and simulation

   Shibi Thomas, George Varghese, Istvan Lagzi, Pramana, 78, 135, (2012)

**Conference Presentations**

1. Helicoidal Pattern formation in reaction-diffusion system, National seminar on 'Recent trends in Physics'in Govt. Arts and Science college, Calicut, 2013.

2. Recent trends in pattern formation, Kerala Science Congress, Trivandrum, 2013 [Best Poster Award].

3. Emergence of Helices in reaction-diffusion system, National seminar, Farooke College, Farooke, 2012

# *Acknowledgments*

*It is with profound joy that I present this thesis and I take this opportunity to express my sincere thanks and gratitude to those who have helped me to accomplish this work. I present this report in the name of God, the Almighty, who kindly showers His ever- flowing grace and blessings throughout my life.*

*This thesis work has been carried out under the guidance and supervision of Dr. George Varghese, Professor and former Head, Department of Physics, University of Calicut. I would like to gratefully express my sincere appreciation to him for his deep involvement, valuable guidance, unceasing encouragement and concern during my work. I express my heartfelt thank towards him for making it possible for me the successful completion of this work.*

*I am also grateful to the current and former Heads of the Department, for providing me all facilities in the Department of Physics, University of Calicut, for doing my work. I gratefully acknowledge the help and inspiration from all the teaching and non-teaching staff of the Department of Physics who have contributed to my scholastic and personal development.*

*I extend my sincere thanks to Prof. Zoltan Racz and Dr. Istvan Lagzi, Lornard Etvs University, Budapest, Hungary, for their co-operation, guidance and support. Also I express my sincere thanks to my friends, batch mates and all the research scholars for their co-operation and help. I would also like to thank my relatives and well-wishers for their moral support and all kinds of help.*

*I thank University Grants Commission and CSIR, Government of India for financially supporting me during this endeavour.*

*Words are inadequate to express my feelings for the love, support and encouragement shown by my husband, parents, brothers and sisters throughout my academic career.*

*Shibi Thomas*

# Contents

# Preface

In nature we can see a large variety of helical and helicoidal precipitation patterns. A few are double helices in DNA, tendrils in plants, ZnO nanohelices, fiber geometry of heart walls, inorganic crystals with helical structure etc. We are interested in studying the dynamics of such patterns since it leads us to know how these patterns are evolving and what is the mechanism behind it. So we tried to find out a simple system where we can easily reproduce the helical patterns with high probability. Our investigation recently find that Liesegang system are most suitable for that and we had done our studies on helical patterns in this system. Present work is about the study of Liesegang patterns, especially helical and helicoidal precipitation patterns.

Chapter 1 begins with a brief introduction about pattern formation and various patterns in physical, chemical, biological and geological systems. It describes the basic concepts like reaction-diffusion, nucleation, phase separation etc. The reaction-diffusion system exhibit different behaviour like excitable medium, bistable medium, chemical oscillation, Turing patterns and Liesegang patterns. In this review, the history of periodic precipita-

tion gives a brief introduction about Liesegang phenomena and its empirical relations. Many of the proposed theoretical models for the Liesegang phenomena are briefly explained. Lastly the chapter also outlines the exotic patterns in precipitation system and also the effect of external field, gel, gravity etc on the precipitation patterns.

Chapter 2 deals with the study of pattern formation in reaction diffusion system using moving boundary model. The moving boundary model and its assumptions are briefly explained. This model considers that the phase separation mechanism is responsible for separating the colloidal haze of precipitants into band and non-band regions. With the theoretical model so developed, the moving boundary model can easily reproduce the scaling law, time law and the width law without many assumptions. Thus the moving boundary model provides a reasonable conclusion on the spatial positioning of the periodic band structure observed in reaction diffusion systems. A remarkable feature of this model is that the asymptotic condition for the band formation can be determined. Also, this model can be used to calculate the width of the bands using a minimum of approximation, which many others were trying to find. The theoretical calculation based on the model suggests that the width of the precipitation bands depends exclusively on the concentration of the intermediate colloidal particles. Hence a better understanding of the basic facts of pattern forming process is made possible with the theoretical investigations and is also verified using computer simulations and the simulated patterns bear a characteristic nature of the experimentally observed Liesegang patterns.

Chapter 3 includes the description of experiments and analysis of patterns. A few well-known Liesegang systems are also given. Liesegang and helical patterns are observed in silica and agarose gel; the experimental sys-

tem which were used in the study. These patterns are easily reproducible also. An observed feature of the experiments is that the local pitch of the helices is always slightly larger than the local band spacing of the Liesegang patterns obtained with the same setup. In the experiments, conducted with different test tube radii, it is found that no helicoids are formed below a critical radius and at larger radii, there is more space for the evolution of more complex structures (double or triple helicoids, disordered patterns). Similar experiments in silica and agarose gel were also carried out in a quasi two dimensional geometry by placing the gel in-between two test tubes of slightly different radii, thereby creating a cylindrical gel column. This setup is called the tube-in-tube experiment and rather easier for the theoretical investigation than the single tube experiments, since they are 2D and can be transformed to tilted Liesegang bands. In mixed silica-agarose gel also we obtained both Liesegang and helical patterns but its found that the probability of getting helices are more in equal amounts of both gel.

The fourth chapter mainly deals with the helicoidal precipitation patterns. The helical precipitation patterns emerging in the wake of reaction diffusion front are studied. It is found that the formation of helical and helicoidal patterns are reproducible but had a probabilistic aspect. For a given set of experimental parameters, there is a well defined probability for helical pattern to emerge. The helices emerged from a complex interplay among the unstable precipitation modes, the motion of the reaction front, and the noise in the system. Unfortunately, the noise is not easily accessible in experiments although the probability depends sensitively on it. Many attempts are done to overcome this problem and implement controlled noise by changing the properties of the gel. The internal surface area is roughly proportional to a noise-amplitude: the larger it is the larger is the probabil-

ity of a nucleation event. In order to see the effects resulting from internal surface area changes, the helicoidal patterns in agarose and silica gels are examined and varied the internal surface area by changing the gel concentration in agarose gel and by varying the pH in the silica gel. The trends in the probability of the emergence of helices are measured and found that they are in agreement with the interpretation that the internal surface acts as an effective noise inducing nucleation. Maximizing the yield of helices can ensure by mixing equal amount of agarose and silica gels.

The final chapter contains the conclusion and the future perspectives of the present work.

# Chapter 1

# Dynamics of Pattern Formation

## 1.1 Introduction

Nature has a huge storage of miraculous patterns in both living and non-living systems. These kind of patterns ranging from simple to complex types in our surroundings. The pattern formation can arise in a variety of extended systems, like chemically reacting systems, crystallisation of solids, hydrodynamic fluids, living cells, bacterial colonies, non-linear systems etc. They are all different structures on a space time scale and may arise due to a collective and co-operative mechanism in the underlying dynamics of large number of constituent subsystems [1, 2]. These subsystems include aggregation of atoms, molecules, small particles, circuits, cells, defects and dislocations. This aggregation can interact or move in space, giving rise to various patterns. This dynamic patterns tell many stories about the macroscopic as well as mesoscopic behaviour of the underlying systems. One

might expect novel and unexpected patterns, when the interaction among the constituent subsystem is non linear.

Patterns are found in everyday life which include spreading coffee stains on a napkin to the patterns on animal coats and the spiral arms of galaxies. Patterns can be simple as well as complex type. Some of them are periodic, regular and stationary, linear where as some others are non-periodic, irregular, dynamic and non-linear which are originated mostly due to the self-organised process with the intervention of external templates. Dissipative systems have travelling wave patterns and different soliton waves give rise to novel type of spatio-temporal patterns. Perturbation of such system can also give rise to further interesting patterns. But more complex structures which can produce naturally occurring patterns arise in non-linear diffusion (especially in reaction-diffusion system) and dissipative systems and their analysis is more complicate and difficult.

Systems that shows pattern formation are very common in nature and these patterns often emerge in the wake of a moving reaction front. This moving reaction front [3, 4] play an important role in large variety of physical, biological, chemical and geological process. Front propagation has gained considerable research attention during the past years. A large number of phenomena in various fields (eg. chemical pattern formation, crystal growth, biological inversion problems) are determined by the peculiarities of various kinds of moving fronts. An important system of problems is related to the case of front propagation into unstable states [5]. Interest in these type of reaction fronts has increased recently since it has been realised that pattern formation in the wake of a moving front is a quite general phenomena. The initial stage of understanding pattern formation phenomena is the description and calculation of the specific properties of the reaction zone,

i.e., answering the question regarding where and at what rate the reaction product appears and so on [6].

A wide class of patterns include the characteristic spots and stripes on animal coats- especially in zebra, fish, tiger, mosaic on butterfly wings, annular rings in woods, hexagonal form of honey comb, rings in bacterial colonies, whorls on finger tips, mineral strata in certain rocks, branching patterns in plants and rivers etc (Figure 1.1). Many kind of patterns are also seen in wildly different natural contexts like rotating spirals appearing in a dish of reacting chemicals, soap foams, ripples in sandy deserts, in an arrhythmic human heart, regular hexagonal patterns developed on the surface of a warm pan of tomato soup (convection patterns), vegetation patterns and so on. Patterns in peacock feathers are example of one of the most exotic patterns in the biological world. Another class of patterns include- intricate, lacy ice crystals form from swirling mists, turbulence patterns in river, clouds take on regular periodic patterns that stretch for hundreds of kilometres, stock-market average and DLA( Diffusion limited aggregation) patterns are few examples of chaotic patterns. Patterns having fractal dimensions are also much interesting.

Patterns are universal and nature generate patterns when even we least expect to find them. By knowing the symmetries and their surroundings of patterns we can find out nearly everything about them [7]. These patterns tells about the emerging dynamics at the macroscopic as well as the microscopic levels of the underlying system. The miraculous patterns delight both our imagination and understanding. How does nature generate these patterns? Is there a simple mechanism or universal phenomena behind these pattern forming mechanism? What happens when we pour a thin layer of oil in a frying pan, add pepper in to it and heat it evenly it will form hexag-

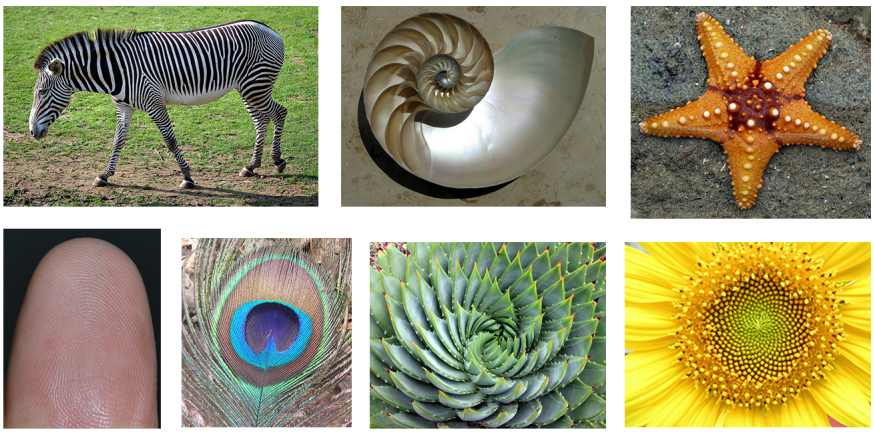

**Figure 1.1:** Different types of patterns found in nature: Zebra (photograph by Andre Karwath aka Aka,licensed under the creative commons attribution-share alike 2.5 Generic license), Nautilus shell (wikipedia commons image from the user Chris 73 and is freely available at http://commons.wikimedia.org/ wiki/ File:NautilusCutawayLogarithmicSpiral.jpg under the cc-by-sa 3.0 license), Star fish(photograph by Paul Shaffner, licensed under the creative commons attribution 2.0 generic license), Human finger pattern, Peacock pattern(photograph by Satdeep gill, licensed under the creative commons attribution-share alike 3.0 unported license), Spiral Aloe(photograph by just chaos, licensed under the creative commons attribution 2.0 generic license), Sunflower(photograph by L. Shyamal, licensed under the creative commons attribution-share alike 2.5 generic license)

onal shapes. These are a few questions which arise curiosity in lay people and expert alike [8]. Tremendous progress has been made in the last few years and several mathematical and computational techniques are used for analysing different types of patterns, both in small and in spatially extended domains in order to find answers to all these questions.

## 1.2 Basic concepts

### 1.2.1 Diffusion and reaction

Diffusion is the mechanism of transportation of particles in a fluid from an area of higher concentration to an area of lower concentration through the

pushing and bumping of the liquid or gas molecules around them, each of which is in constant random thermal motion. Diffusion can occur in either still or moving fluids [7]. Diffusion is defined as the mass flow process by which atoms or molecules change their positions relative to their neighbours within a phase under the influence of thermal energy and a gradient. This gradient may be of chemical potential resulting from a concentration gradient, or a gradient due to temperature, stress, electric field or gravitational field.

### 1.2.2 Ficks laws of diffusion

The concentration gradients are first proposed by Adolf Fick in 1855 [9]. For ideal solutions these gradients are directly related to the chemical potential gradient. Fick's first law states that,

$$\frac{dm}{dt} = -DA\frac{dn}{dx} \tag{1.1}$$

where $\frac{dm}{dt}$ is the number of moles of the diffusion particles passing through a cross sectional area $A$ perpendicular to the diffusion direction $x$ per unit time, $n$ is the concentration of the specie and $D$ is the diffusion coefficient. The negative sign shows that the mass flow is down the concentration gradient. The first law can also be written in terms of flux $J$ as,

$$J = -\frac{1}{A}\frac{dm}{dt} = -D\frac{dn}{dx} \tag{1.2}$$

Fick's second law corresponds to non-steady state flow. Consider an elemental volume of length $\Delta x$ along the diffusion distance $x$ and of unit cross-sectional area. Let the volume of such an element is $\Delta x$. The rate of

accumulation of the diffusing species within this elemental volume is $\frac{\partial n}{\partial t}\Delta x$ and can be expressed in terms of fluxes into and out of the volume,

$$\frac{\partial n}{\partial t}\Delta x = J_x - J_{x+\Delta x} \tag{1.3}$$

Substituting $J_{x+\Delta x} = J_x + \frac{\partial J}{\partial x}\Delta x$ into equation 1.3, we get

$$\frac{\partial n}{\partial t} = -\frac{\partial J}{\partial x} \tag{1.4}$$

Again substituting equation 1.2 in equation 1.4

$$\frac{\partial n}{\partial t} = -\frac{\partial}{\partial x}(\frac{-D\partial n}{\partial x}) \tag{1.5}$$

$$\frac{\partial n}{\partial t} = \frac{\partial}{\partial x}(\frac{D\partial n}{\partial x}) \tag{1.6}$$

If $D$ is independent of concentration, equation 1.6 simplifies to

$$\frac{\partial n}{\partial t} = D\frac{\partial^2 n}{\partial x^2} \tag{1.7}$$

This is linear diffusion equation.

For a reaction consisting of two chemical species, the reaction term include the product of concentration of the two chemical species and hence the reaction-diffusion equation becomes

$$\frac{\partial n}{\partial t} = D\frac{\partial^2 n}{\partial x^2} + E(n) \tag{1.8}$$

where $E$ can be a linear or non-linear function of concentration of the chemical species.

### 1.2.3 Nucleation- homogeneous and heterogeneous

Nucleation is defined as the atomic process by which atoms of a reactant rearrange their positions to form a cluster of a product phase. For thermodynamically stable state, the cluster has to be large. During nucleation process the atomic fluctuations occurring are very small, typically on the scale of 10-1000 atoms. Nucleation is the formation of a distinct thermodynamic phase and can occur in gas, liquid and solid phase.

Nucleation process are physical rather than chemical and nucleation normally occurs at nucleation sites on surfaces contacting the liquid or vapour. When the nucleation sites are provided by the suspended particles or minute bubbles, then it is known as heterogeneous nucleation. Heterogeneous nucleation occurs at preferential sites such as phase boundaries, surfaces (of container, bottles, etc.) or impurities like dust. Homogenous nucleation occurs without preferential nucleation sites and it arises spontaneously and randomly, but it requires superheating or supercooling of the medium. As compared to the heterogeneous nucleation, homogeneous nucleation occurs with much more difficulty in the interior of a uniform substance. Heterogeneous nucleation occurs much more often than homogeneous nucleation [10].

Now consider the rate of nucleation, $R$, of a critical clusters. The rate of nucleation increases when the concentration of molecule($n$) increases, but very slowly at first and here is the heterogeneous nucleation (nucleation initiated by things such as dust particles and walls) occurs. Once the molecule concentration has increased just enough to reach the point, $S_{crit}$, a sharp, almost instantaneous, increase in the nucleation rate occurs and here the homogeneous nucleation takes place (Figure 1.2), where the molecule nucleates

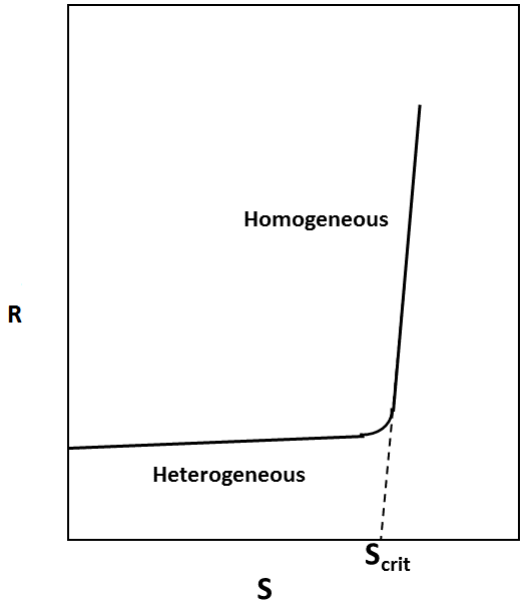


**Figure 1.2:** Rate of nucleation, $R$ versus Supersaturation $S$ [11]

with other molecules or on previously formed solid particles [11].

### 1.2.4 Phase separation

Phase separation is the conversion of a single-phase system into a multiphase-system; especially the separation of a solution into two immiscible liquids. There are two types of phase transition:($i$) changes of concentration that are initially small but extend over a wide spatial range and ($ii$) changes of concentration that are initially large but affect only a narrow spatial range. The first one is termed as spinodal decomposition and the other is nucleation and growth [12]. The theory of spinodal decomposition starts with the Gibbs free energy function, $\Delta G$. Gibbs showed that when the second derivative of the free energy of mixing is positive, then the condition for stability or metastability arises. The system is unstable when it becomes negative and if zero, the spinodal is defined.

Spinodal structures are narrow, homogenous two-phase mixtures arising from phase separation that take place under certain conditions of temperature and composition. The spinodal reaction is a spontaneous unmixing or diffusional clustering distinct from classical nucleation and growth in metastable solutions. Spinodal decomposition or continuous phase separation compose the selective amplification of long wavelength concentration waves within the supersaturated state resulting from random fluctuations. The fingerprint mechanism of spinodal decomposition is uphill diffusion and that of nucleation and growth is downhill diffusion [13].

### 1.2.5 Spinodal decomposition

The spinodal decomposition was introduced in 1999 by Antal, Droz, Magnin and Racz [14]. It is a powerful postnucleation mean-field model to describe the formation of precipitation patterns, that accounts for all the empirical laws. The counterpart of this mean-field model is the feature of fluctuations which are known to give rise to several interesting phenomena, like formation of bifurcations and helical structures (will discuss in chapter 4) [15, 16]. Here we will consider the basic aspects of spinodal decomposition mechanism.

According to the spinodal decomposition mechanism the two electrolytes, $A$ and $B$, react to produce a metastable state $C$. Thus the reaction front leaves behind a constant concentration of $C$ particles, that can move diffusively in the gel. As a result of an attractive interaction the particles can aggregate when the temperature is low enough and the density is high. On a mesoscopic level this mechanism is described by the phase separation model for the concentration of the $C$ particles, namely by the Model B of critical dynamics [17]. The system is treated as one-dimensional, due to

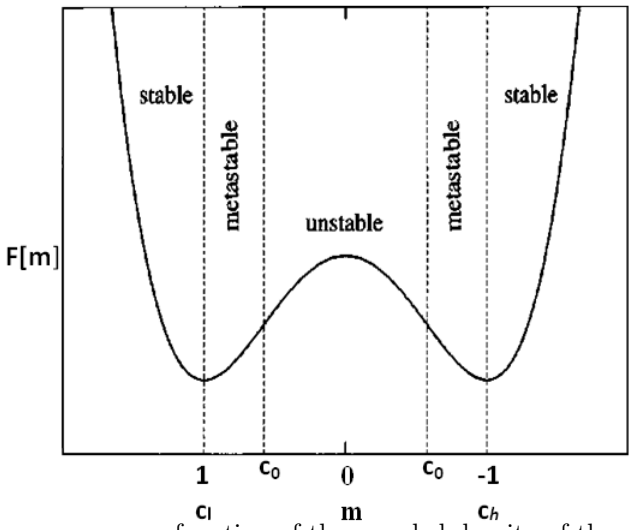


**Figure 1.3:** Free energy as a function of the rescaled density of the reaction product for the spinodal decomposition, the two minima account for the high and the low density phase and $c_0$ is the spinodal, figure taken from [14] and reproduced with permission

the uniaxial symmetry of the problem and all the relevant quantities are assumed to depend on a single space coordinate $x$. The dynamics is described by a Cahn-Hilliard equation [18, 19] with a source term $S(x,t)$, that accounts for the production of $C$:

$$\frac{\partial c}{\partial t} = -\lambda \Delta \frac{\partial F}{\partial c} + S(x,t) \tag{1.9}$$

where $\lambda$ denotes a kinetic coefficient characterizing the dynamics of the $C$ particles. $F$ is the free energy functional, that introduces the phase separation dynamics in the system and $\Delta$ is the Laplacian operator.

We shall assume the simplest analytical form of free energy, $F$, since experimentally it is not possible to measure the free energy of this system,. The free energy should describe the phase separation process and contain a minimal number of parameters. Now let us assume the following Ginzburg-

Landau form of the free energy [14, 20]:

$$F[m] = -\frac{1}{2}\epsilon m^2 + \frac{1}{4}\gamma m^4 + \frac{1}{2}\sigma(\nabla m)^2 \tag{1.10}$$

$m$ being the shifted and rescaled concentration $m = (2c - c_h - c_l)/(c_h - c_l)$ (Figure 1.3). The parameters of the model, namely $\epsilon$, $\gamma$ and $\sigma$ have their own physical meaning and can be fitted by comparing with experiments. The parameter $\epsilon$ should be bigger than zero to insure that the system is in a critical regime where phase separation takes place. This parameter can be considered to describe the deviation from the critical temperature of the system. The parameters $\sigma$ is a measure of the surface tension of the bands and $\sigma > 0$ ensures the stability against short wavelength fluctuations. To obtain an overall stability of the system the parameter $\gamma$ has also to be positive and the ratio $\gamma/\epsilon$ is related to the minima of the free energy, $m_h = \sqrt{\gamma/\epsilon}$ and the spinodal values $m_s = \pm\sqrt{\gamma/3\epsilon}$.

Figure 1.4 gives a general idea of pattern formation. The last band act as a sink for the neighbouring particles above $c_l$ density. Thus the $C's$ produced in the front end increases the width of the last band. This continuous untill the front moves far enough so that density in it reaches the spinodal value. Then the spinodal instability sets in and a new band appears.

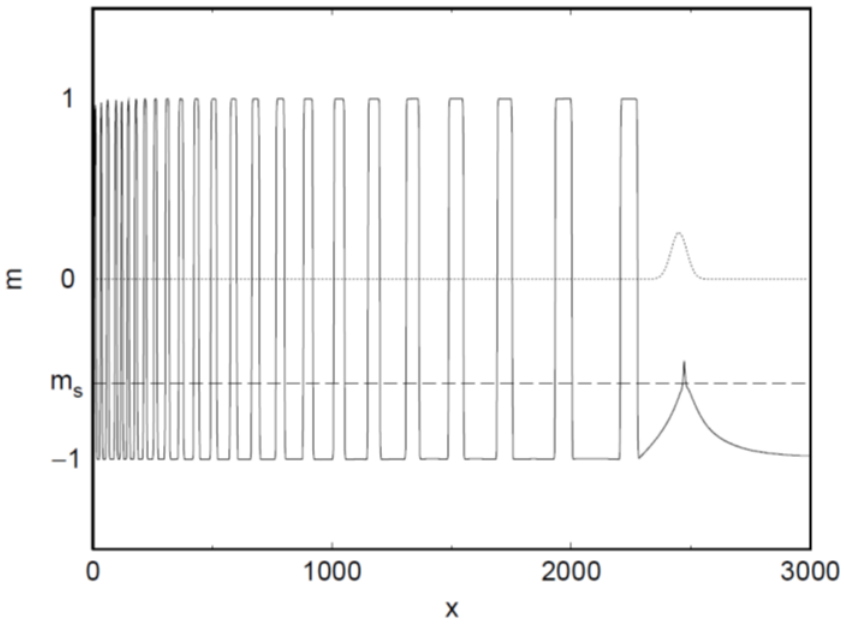


**Figure 1.4:** Liesegang pattern formation in spinodal decomposition, figure taken from [20] and reproduced with permission

The formation of the bands is described in a deterministic way and no fluctuation are taken into account in the spinodal decomposition model. Without any noise terms the formation of the bands is based on the spinodal decomposition, that takes place in the unstable regime. There are situations where the patterns are spontaneously formed without any concentration gradients present in the system and can be described in a nucleation and growth scenario where the patterns are created by a ripening process, starting from a homogeneous system [16].

### 1.2.6 Periodic precipitation

The periodic precipitation (PP) is a generic term for material deposition process which occur intermittently in terms of time or space or (generally) both [21]. This type of process represents a typical oscillatory reactions, with practical implications in crystal growth and material preparation. Periodic precipitation is a beautiful, intriguing and dynamically rich phenomenon and can be used for potential application in material science [22], if effective techniques to control and design these patterns can be found.

### 1.2.7 Linear stability analysis

Linear stability analysis of a uniform state was first carried out in 1952 by Alan Turing [23]. He suggested the radical and highly stimulating idea that reaction and diffusion of chemicals in an initially uniform state could explain morphogenesis, how biological pattern arise during growth. Linear stability analysis is a useful step toward understanding how the properties of a non-equilibrium system depend on various parameters [24]. This analysis also suggest a way to classify non-equilibrium systems in regard to their pattern forming tendencies. The key steps in linear stability analysis are:

1. Obtain the evolution equation of the system
2. Rewrite the evolution equations in dimensionless form to reduce the number of parameters and to obtain the parameters in dimensionless form.
3. For a given system, find explicitly at least one time independent state, $u_0$.
4. Linearise the evolution equations about the uniform base state $u_0$ to obtain the linear evolution equations for an infinitesimal perturbation.
5. Solve the linearised equations and obtain the wave vector dependence of growth rate.
6. Analyse the solution by studying the real and imaginary part of growth rate.

Using this analysis we can able to predict when will a spatially uniform time-independent state becomes unstable to tiny perturbations and also get

the details of the growing spatial structures such as its characteristic length and time scales.

### 1.2.8 Symmetry breaking phenomena

Breaking of the spatial symmetry of a medium was first predicted by Alan M. Turing [23], mainly due to diffusive aspects. When soluble reactants such as inorganic ions and cations react, symmetric patterns can arise in simple chemical precipitation systems when the particles move only by diffusion. The helix formation is caused by the breaking of symmetry due to initial conditions [25]. Microscopic fluctuations are often relevant at macroscopic level of observation because they make symmetry breaking possible and are responsible for triggering complex patterns. Noise and fluctuations play a key role in symmetry breaking. One of the main characteristic of the reaction-diffusion systems is that, they exhibit spontaneous symmetry breaking and self-sustained patterns are formed under some circumstances [26]. Chirality is also encountered in a host of every day examples where asymmetry occurs.

## 1.3 Self-organisation and pattern formation

Self-organisation and spontaneous pattern formation has a great and highly increasing relevance in the natural and life science. Over the past decades, various self-organisation phenomena have been reported: precipitation patterns, self-oscillating systems,travelling waves and Turing patterns. A variety of self-organization structures are wide spread in nature. In various biological systems patterns are manifested in the lamellar rings in bones, the pigmentation of the iris, the coloured shapes on butterflies wings, spiral

waves in cardiac fibers, the stripes in zebreas and tigers. Geological patterns found in a wide variety of sedimentary rocks and stratifications in the agate structure are a few examples. The phenomenon of periodic precipitation is one of the most interesting manifestations of self-organization is the periodic precipitation which is generated by a moving reaction-diffusion precipitation front [27].

The mechanism of biological self-organisation occurring from an initially homogeneous solution are not so clear. Two possible theoretical approach might account for biological self-organisation [28]. First one is based on static interactions and statical physics between entities that are not involved in chemical or biochemical reactions and the second one is based upon non-linear chemical dynamics and cooperative phenomena involving reacting species. Usually, a solution of reacting chemicals or biochemicals does not self-organise and theoreticians have predicted that the non-linear properties such as self-organisation may arise due to some particular types of chemical or biochemical reactions that are far from equilibrium.

In 1952 Turing published an article predicting that in some reaction, a stationary chemical pattern could spontaneously arise from an initially homogeneous solution. This pattern arises from a combination of reaction and diffusion and the patterns that form are made up of the periodic variations in the concentration of some reactants. Structures of this type are called reaction-diffusion or Turing structures. Turing structure is recognised as the significant model for explaining pattern dynamics on animals skin. Turing also reported that if the diffusion coefficients of species are not same, then homogeneous state of chemical species may lose its stability [23]. Classical Turing patterns emerge as a result of this, which consist of stationary equidistant spots and stripes, such structures are supposed to appear in

various biological systems. Lagzi et al., proposed a new mechanism based on the coupling of a simple auto-catalytic front with precipitation process producing Turing Patterns [29].

## 1.4 Reaction diffusion system

Living organisms and natural systems respond to external changes in an unpredictable way. Since it involves an infinitude of variables, which are commonly hidden and thus interaction between the medium and the environment is extremely complicated. In chemical reactions different substances react and produce new substances and in ecological problems, different species interact with each other. The robustness of this natural phenomena is in contradiction with the difficulty of their understanding and knowledge, if one uses the classical tools of mathematics, physics and chemistry to model these events.

The problem changes drastically when the non-linear interactions are taken into account. This process reveals new complicated behaviours, and leads to a better agreement between modelling equations and real systems [26]. A couple of successful attempts are done to translate the biological world in terms of non-linear equations and the reaction-diffusion systems played here a key role.

Reaction-diffusion systems have been shown to exhibit a lot of different behaviours which are summarised in the following way:

1. Excitable medium- A medium becomes excitable [30] when a perturbation larger than given threshold applied to a system, then it grows and makes a large and non-trivial excursion in the space of variables.

This process constitute a "state of excitation", where the system remains for a while and this state is able to perturb its neighbouring due to diffusive process, leaving the steady state and making the same cycle, but with a delay in time. Thus a wave of excitation travels trough the medium. Most common examples of excitable systems are neurons and cardiac tissue, due to the important role of waves plays in the fibrillation mechanism.

2. Bistable system- A bistable system is endowed with more than one steady state (typically two stable steady states and one unstable) [31]. Mainly due to their capacity for storage of information, the importance of these kind of systems is huge. A large amount of systems exhibit two steady states in the biological world. For instance, bistable behaviour of inhibitory neurons play a crucial role in controlling impulse traffic through the amygdala.

3. Chemical oscillations- The chemical waves and oscillations was published in 1991 by Anatol M. Zhabotinsky [32]. The first discovery of oscillations in a homogeneous chemical reaction was obtained accidentally by W. C. Bray at the University of California at Berkeley in 1921. He observed periodic changes in the color in the production of oxygen bubbles. Hundreds of chemical oscillating reactions of different types such as Ph Oscillators, Calcium Oscillators, etc are found in now a days.

4. Turing patterns- Alan M. Turing [23] proposed the theory of morphogenesis which made a lot of impact on theoretical developments in pattern formation and reaction-diffusion systems. Turing showed that, for an open system containing two reacting substances, provided

one of them diffuses much faster than the other, then stationary concentration patterns may spontaneously develop. Turing mechanism is still treated as a prototype for the formation of coherent patterns in non equilibrium systems [33].

5. Liesegang patterns- Liesegang patterns are quasi-periodic precipitation patterns arise in the wake of a moving reaction front. Although they appear only in particular physiochemical conditions, such structures are widespread in nature and found in systems ranging from biological (population of bacteria) to geological structures (structures in agate rocks). Liesegang bands additionally require a fast precipitation and growth process.

The diffusion time and reaction time are two fundamental time scales characterizing the diffusion-reaction systems. The process is said to be diffusion limited if the reaction time is much shorter than the diffusion time. The whole process often results in pattern formation in such cases. One of the best example for such a diffusion-limited reaction is the so-called Liesegang phenomenon [34].

## 1.5 History of Periodic precipitation

The periodic precipitation process known as 'Liesegang phenomenon'has now been investigated for more than 100 years. Although during the $20^{th}$ century the phenomenon caught the attention of many scientists from different fields and hundreds of papers have been published, still it lacks completion. Liesegang patterning is a special type of chemical pattern formation in which the spatial order is formed by the density fluctuation of a weakly

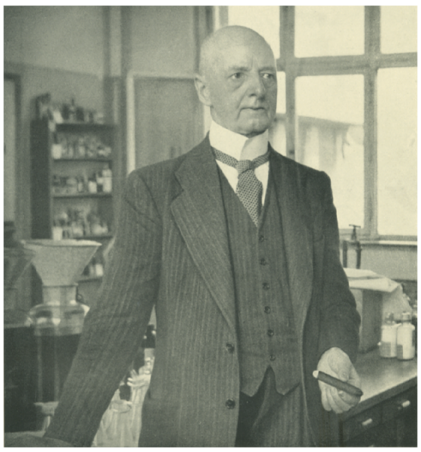

**Figure 1.5:** R. E. Liesegang (Wikipedia Commons image, freely available at https:// en.wikipedia.org/wiki/File:Liesegang.png and the image is in the public domain)

soluble salt. A best example for this kind of system is the reaction of silver nitrate ($AgNO_3$) and potassium dichromate ($K_2Cr_2O_7$) [35].

The chemical patterning was first discovered in 1855 by Frederic Ferdinard Runge. As a reaction mechanism he has used simple filter paper wet by an electrolyte solution. He published a whole book about his patterns 'self painting pictures'. But Runge's discovery was unfortunately too early and nobody paid attention to his work and hence precipitate patterns have fallen into oblivion until 1896 [35]. In that year Raphel Eduard Liesegang, a German photographer and Chemist, was doing a lot of experiments and accidently he covered a glass plate with a layer of gelatin impregnated with potassium dichromate [36]. Then he pour a small drop of silver nitrate in the center. As a result of diffusion, silver dichromate was precipitated in the form of a serious of concentric rings with varying spacings. Liesegang's observations were published in 1896 in the Naturwissenschaftliche Wochenzeitschrift with the title 'Ueber einige Eigenschaften von Gallerten'[36].

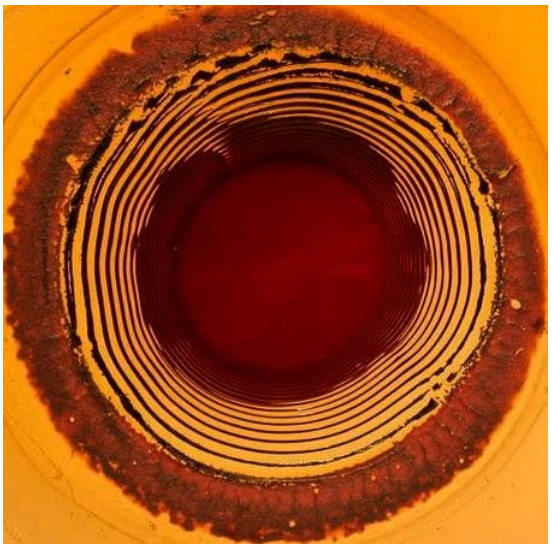

**Figure 1.6:** Silver dichromate patterns, figure taken from www.insilco.hu and reproduced with permission

## 1.6 Simple Liesegang experiment

Depending on the geometry of the system used, Liesegang precipitation patterns can be bands (in an uniaxially-symmetric configuration) or rings (in a circular configuration). In a typical experiment, two reactants are initially separated in space, with the inner electrolyte $B$ homogeneously dissolved in a gel column while the outer electrolyte $A$ is kept in an aqueous solution.

At time $t = 0$, the outer electrolyte is brought into contact with the end of the gel column and since the initial concentration $a_0$, of $A$ is chosen to be much higher than that of $B$ (typically $a_0/b_0 \approx 100$), $A$ invades the gel and a reaction front emerges which advances along the column. The motion of this moving front and the amount of product $C$ left behind the front are the important factors since they determine the input for the precipitation processes. The reaction product $C$ may be the product of further intermediate reactions (e.g. $A + B \rightarrow C' \rightarrow ... \rightarrow C$), As a result of phase separation

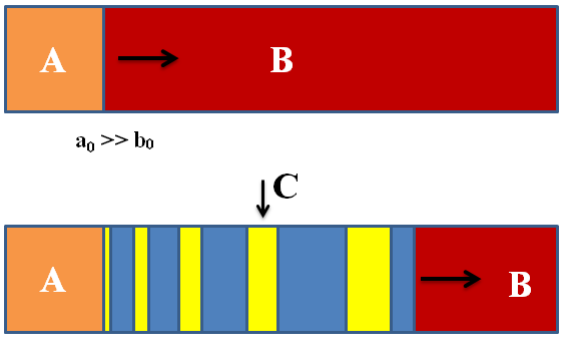


**Figure 1.7:** Schematic representation of formation of bands

mechanism insoluble precipitate are formed when the local concentration is above some threshold value.

Soon after Liesegang's experimental observations Wilhem Ostwald proposed a theoretical explanation for the emergence of the rings [37], which is still the basis of most of the modern theories. The bands appear only at some particular positions $x_n$ at certain time $t_n$, which obey simple generic rules. In 1903, Morse and Pierce [38], calculated the formation time of the bands, and according to them the position of the band and its time of formation are related by a simple equation, often called time law. This was given by,

$$x_n^2 \propto t_n \tag{1.11}$$

where $x_n$ is the distance of the $n^{th}$ precipitation band from the gel-solution interface. This relation is similar to the well known Einstein-Smoluchowski relation for Brownian motion interpreted in terms of random walk in a homogeneous space. The time law reflects the diffusive behaviour of the outer electrolyte into the gel matrix. The next law is, due to Jabalczynski [39], called the spacing law which reflects another important property of the bands. According to this law, the spatially ordered patterns obeys a

geometric series.

$$x_{n+1} = \Gamma x_n \tag{1.12}$$

where $\Gamma$ becomes a constant when the number of the bands are large. The spacing between the bands usually increases as $n$ increases. The constant referred to as the spacing coefficient is normally greater than unity and is generally expressed as $(1 + p)$ where $p$ lies between 0 and 0.5, which are in good accordance with experimental results. Matalon and Packter [40] proposed a detailed understanding of the spacing law. They collected various experimental results for $p$ and found a functional dependence on the concentration of both reactants, $a_0$ and $b_0$ . This relation is known as the Matalon-Packter law and it has the form,

$$p = R(b_0) + S(b_0)\frac{b_0}{a_0} \tag{1.13}$$

where $R$ and $S$ are dimensionless decreasing functions of $b_0$ and is obtained mathematically also. It is also observed that the width of the bands increase with $n$ and obey the width law,

$$w \sim x_n^{\alpha} \tag{1.14}$$

where the exponent $\alpha$ is close to 1. Many values for $\alpha$ have been published, it is difficult to calculate the value of alpha, since number of bands is limited and width $w_n$ of the bands are small compared to their positions $x_n$.

Until now, more attention has been paid to the spacing law since its coefficients are directly derivable from the concentration profiles of reacting species. On the other hand the width law has largely been ignored for many reasons. Without having resources to sophisticated digitizing methods, it

is very difficult to make precise measurements of the width of bands. The time law is a simple consequence of a diffusion process. All these empirical laws cannot be explained so easily and a few theoretical models are proposed based on diffusion and reaction dynamics to explain the pattern formation. However none of them explain all the distinguishable features of bands.

## 1.7 On the threshold of theories

Several competing theories have been proposed for describing the mechanism of Liesegang phenomena. The dependence of the concentration of inner and outer electrolytes arises as a major problem. All the theories of Liesegang pattern formation follow how the diffusive reagents $A$ and $B$ turn into final immobile precipitate $D$,

$$A + B \longrightarrow ...C... \longrightarrow D \tag{1.15}$$

where $...C...$ accounts for the various intermediate stages due to the formation of $D$ [40]. Reaction-diffusion models with thresholds are the earliest models describing Liesegang pattern formation. Ostwald [37] explain the pattern formation on the basis of super saturating liquids. He proposed that the precipitation is not a result of a complete reaction but it arise spontaneously when the concentration product $P$ of the reactive species reaches a critical concentration $P_{crit}$. Most of the theoretical models are based on an analytical study or numerical solution of differential equations.

### 1.7.1 Ion product saturation model

In this model, the precipitation takes place without any intermediate stage, i.e., there is no $C$ stage and hence this is the first and easiest quantitative model for Liesegang pattern formation. As in Ostwald model, nucleation $A + B \rightarrow D$ occurs when the local concentration of the product $P = ab$ (it is the concentration of D, which is the product concentration) reaches the threshold $P_{crit}$. The precipitate $D$ will grow and deplete their surrounding of $A$ and $B$. As the reaction front moves further, the product concentration around the immobile precipitate decays until band formation becomes impossible. Wagner [41] and Prager [42] had shown that these ingredients yield patterns which obey the time law and spacing law.

### 1.7.2 Nucleation and growth model

This model introduce an intermediate state $C$ to the reaction-diffusion process $A + B \rightarrow C$ from the nucleation and growth process $C \rightarrow D$. This model is called nucleation and growth model because the formation of $D$ depends on the nucleation and accumulation of $C$ rather than on the product concentration of $A$ and $B$. This model was first proposed by Keller et al., [43] by studying reaction-diffusion equations and confirmed the time law and spacing law. They calculate the positions $x_n$ of the bands without apriori assuming band formation and stopping of the band growth. The first numerical solutions for nucleation and growth model were presented by Dee [44]. He used a similar technique as Ross et al., [45] and calculated the nucleation and growth criterion by classical nucleation theory. Using this model, Dee confirmed the spacing law and the width law and due to lack of computational techniques this model has no information about the

Matalon-Packter law.

### 1.7.3 Induced sol coagulation model

Induced sol coagulation model is a variant of single intermediate compound theory and the compound $C$ is assumed to be the sol and this sol coagulates if the following two conditions are satisfied: $(i)$ concentration of $C$ exceeds a supersaturation threshold $C \geqslant P_{crit}$ and $(ii)$ the local concentration of the outer electrolyte $(a)$ is above a critical coagulation concentration $(p)$, $a > p$. The bands are formed as a result of the nucleation and growth of the precipitate combined with the motion of the front where $a = p$ [46].

Models of Liesegang band formation envisage an important role for sol flocculation in certain cases. They are evidently complex, involving reagent diffusion, sol formation, sol particle diffusion and adsorption as well as electrostatic space charges. A comprehensive analysis of the interplay between these components has not yet been attempted. Separate parts of the process have been extensively studied on a qualitative basis, mostly in the context of colloid and flocculation research.

### 1.7.4 Competitive growth model

In competitive growth model, the precipitates $D$ can dissolve with a probability decreasing with increasing size of the precipitates [47]. According to the competitive particle growth theory, this is due to a thermodynamical instability caused by the non-homogeneous size distribution of sol particles. Flicker and Ross (1974) pointed out that, due to the surface tension large crystallites are less soluble than small ones and will therefore grow at the expense of the latter [48]. This happens for crystallites and any colloidal

particles that might exist before crystallites as such are formed. The descriptive equations have to be solved numerically and some assumptions had to be made to establish the 'symmetry breaking'conditions which brought periodic solutions. A more detailed analysis has been given by Lovett et al., [47] who obtained explicit solution on the basis of their own pattern of assumptions. The diffusion controlled growth rate of a spherical particle of radius $R$, is given by,

$$\frac{dr}{dt} = \frac{DC_\mu}{\rho r\left[\chi - 1 - \frac{2\xi}{\rho rkt}\right]} \tag{1.16}$$

where $D$ is diffusion constant, $\rho$ is density of precipitated particle, $t$ is time, $\chi$ is supersaturation and $\xi$ the surface energy of crystallite. $C_\mu$ is the true equilibrium concentration of the reaction product. It is seen that $\frac{dr}{dt}$ is positive only when $R > R_{crit}$ such that,

$$R_{crit} = \frac{2\xi}{\rho\chi kt} \tag{1.17}$$

only then can particle grow, otherwise they dissolve. The competitive particle growth can seen in crystal system on a macroscopic scale and the fact that the crystals in each layer are more or less of the same size is in harmony with the model.

Comparing all four supersaturation models, the nucleation and growth model is considered as a reference model since it is the model which briefly explains the Matalon-packter law in the simplest way. Although it needs an intermediate state C, the model is basically suitable for analytical and numerical studies. The sol coagulation model and the competitive growth model, could explain some more details but they are not sufficient to explain all the empirical laws. Thus many more general information are missing in

the theories and final theory is yet to evolve. Attempts are however made by researchers to formulate the theories of patterning based on phase separation mechanisms and a few of them are briefly described below.

### 1.7.5 The spinodal decomposition model with Cahn-Hillard dynamics

When the Liesegang patterns are formed once, they become frozen forever, i.e., they do not evolve any more on any reasonable time scale. All the above described models have some conceptual problems due to the threshold parameters controlling the growth of the bands which are difficult to grasp theoretically and not easy to control experimentally. Also the description of how the band formation could be manipulated in a desired way is bit difficult. Furthermore the specific models might seem insufficiently universal. To overcome all these problems a new model free of thresholds and reaction-diffusion equation was suggested by Antal et al., [14] which is mainly based on a phase separation mechanism that takes place in the formation of bands. No coarsening of the band is experimentally observed, this process should takes place at very low temperature. The phase separation dynamics is a well understood problem [49]. When one quenches a system having a phase transition below the coexistence curve, the system separates into two phases and if it takes place near the coexistence curve, the system will be in a metastable state. Small droplets of the minority phase are formed and grow with time and is a slow process due to the presence of an activation energy and this is called homogeneous nucleation. On the other hand when one quenches the system far from the coexistence curve, the system will be in an unstable state and no activation energy involved and the phase separation starts immediately and this process is called spinodal

decomposition and the spinodal line separates the two regimes (nucleation and spinodal decomposition).

The mechanism of phase separation can be described as, consider the $A + B \rightarrow C$ reaction-diffusion process having a moving reaction- diffusion front and the front put down locally some $C$ particles. Once deposited, $C$ particles diffuse and small cluster of particles nucleate and aggregate behind the front. The nucleation is an activated process and its characteristic time scale $\tau_{nucl}$ is large at low temperature. If $\tau_{nucl}$ is much larger than the time $\tau_{front}$ needed by the front to put out the local concentration $c_0$ then the system reaches the unstable state, ie, crosses the spinodal line. Once the spinodal line is crossed, the phase separation takes place on a short time scale and a domain formed by $C$ particles is rapidly formed at or behind the front, hence the formation of a Liesegang band. The spinodal decomposition model can start with the $C$ particles. Their dynamics are described by a simple phase separating equation taking particle conservation into account. The specific dynamics were introduced by Cahn and Hillard [18]. In Cahn-Hillard equation the concentration of $C$ particles is represented by $c$ and the so called 'magnetization'$m$ is defined as

$$m = c - \frac{(c_l + c_h)}{2} \tag{1.18}$$

the Cahn-Hillard equation is,

$$\frac{\partial m}{\partial t} = -\lambda\Delta[\epsilon m - \Gamma m^3 + \sigma\Delta m] + R(x,t) \tag{1.19}$$

here $R(x,t)$ is the source term introducing new $C$ particles into the system via the $A + B \rightarrow C$ reaction and $\Delta$ is the Laplacian operator. Using this model it is possible to produce Liesegang patterns satisfying the spacing law

in agreement with the Matalon-packter law. The spinodal decomposition model can also be implemented for sophisticated condition such as the effect of an additional electric field also.

### 1.7.6 The Kinetic Ising model with Glauber and Kawasaki dynamics

A different approach to model the phase separating dynamics was recently proposed by Magnin et al., [50] along the lines of the kinetic Ising model for ferromagnet's. Empty and occupied lattice sites are denoted with down and up spins. The initial state is empty and the moving reaction front flips the down spins at a given rate. This process can be described by Glauber dynamics [51] while the diffusion is described by a spin exchange process or Kawasaki dynamics [52]. The rate of exchanges entering into Glauber and Kawasaki dynamics are governed by a heat bath at temperature $T$. The local magnetization $m$ and particle density $n$ are related by $m = 2n - 1$.

To explain model qualitatively, suppose that the spins are down, as the reaction front leaves behind a constant density $n_0$ of $C$ particles, the spin flipping front produces a local magnetization $m_0 = 2n_0 - 1$. As time evolves the local state moves from $s_u$ (spin up) towards $s_d$ (spin down). The system crosses successively the coexistence line and spinodal line and ends up into the unstable states domain where phase separation takes place. Thus a spin up domain is rapidly formed at or behind the front. The time scale for nucleation is much larger than the time needed by the front to put the system in the unstable state domain and the the mechanism is possible because of low temperature. The new band acts as a sink for the up-spins in its vicinity. Thus the local magnification decreases and the front is no longer

in the unstable domain. However, when the front has moved far enough, the depleting effect of the band disappears. The front can bring again the system into the unstable domain and a new band is formed the formation of the precipitates is modelled by a combination of spin-flip and spin-exchange dynamics. The Hamiltonian with ferromagnetic coupling $l > 0$ between the spins $\sigma_r$ at site $r$, modelling the attraction of the $C$ particles.

$$H = -l\Sigma_{r,r'}\sigma_r\sigma'_r \tag{1.20}$$

Glauber dynamics are used to add the $C$ particles in an initial state in which all spins are down. The spins flip rate $w_r$ at site $r$ is given by

$$w_r = R(r,t)\frac{(1-\sigma_r)}{2} \tag{1.21}$$

where $R$ is the source term. $2D$ and $3D$ simulations have been reported for this model [50] but are not yet good as the experimentally obtained ones due to fluctuations and this indicates that the model needs further investigation.

### 1.7.7 Lattice gas simulations

Lattice gas simulations can serve as a computational experiment to check how the mean-field solutions can be applied to experimental data and moreover how fluctuations might cause deviations from these solutions. As in the case of separation of the two processes in the nucleation and growth model, the lattice- gas simulation consist of two stages. In the first stage the $C$ particles are generated and the second stage simulates the precipitation of $C$ particles by rules comparable with cellular automata. All empirical laws describing Liesegang pattern formation, i.e., the time law, the spacing

law, the Matalon-Packter law and the width law can be well understood on the basis of the nucleation and growth model. A good correlation between experimental observations, simulation results and mean-field models can be obtained only if a constant offset $\kappa$ between measured and theoretically assumed band positions is taken into account. Due to the effects of fluctuations on Liesegang pattern formation, an additional modification of the Matalon-Packter law are necessary especially in small-scale systems.

A new scenario for the formation of Liesegang patterns is proposed by J. George et al., [3, 4] and they interpreted the periodic pattern formation in a gel column as a moving boundary problem. They reformulated the empirical laws on the basis of moving boundary assumptions and more meaningful explanations are given. Their equations are found to be in good agreement with experimental observations.

Another phenomenological description of periodic precipitation on the basis of chaos theory is due to the "butterfly effect"[53]. A butterfly fluttering its wings in Beijing can cause a hurricane on the other side of the world. Using this concept in our Liesegang system, it indicated that minor changes in chemical composition(concentration, ion species, gel media) or the micro environment(temperature, pressure, pH) may lead to a very different kind of patterns with a variety of shape, colour, appearance and structure. These results may give new insights into different forms of precipitation in gallstone [53].

## 1.8 Exotic patterns in precipitation systems

More complex structural features have been noted during the study of Liesegang systems: these include secondary structures (the separation of one

band into several closely adjacent thinner bands), segmentation of concentric rings into radially aligned convex sections [54], spirals instead of concentric rings [55] and helicoidal precipitation bands instead of set of parallel bands [54]. The helicoidal precipitation phenomena is often rare, because for occurrence of symmetry breaking due to initial condition of a rather spherical shape, so that at least a part of one curl of the helix can initially appear in the test tube. Continuous helical pattern were observed experimentally in test tubes with relatively large radius [56]. T. Karm et al., [57] reported the mechanism of revert spacing in $Pb(NO_3)_2/K_2CrO_4$ system and this occurs mainly due to adsorption mechanism and more over the spacing laws are all reversed compared to the normal banding. In $NaOH/CuCl_2$ system [58] a wide variety of spatial patterns are formed by varying the concentration of outer and inner electrolyte and different patterns like Liesegang patterns, multi-armed spirals, cardioid like patterns, irregular "cabbage-like"patterns etc are formed. Also it is found that, in strong base like $NaOH$ very dense bands are formed where as weak base like $(NH_4OH)$ produces a rather loose pattern and the spacing coefficient is large compared to the other [59]. Complex motion of precipitation front are also described by Lagzi et al., [60].

Periodic precipitation in a gaseous reaction-diffusion system occurs in $NH_3/HCl$ [61] system. The gaseous $HCl$ and $NH_3$ diffuse from the opposite sides of a test tube and react in silica aerogel rods, a porous matrix. The reaction further leads to solid $NH_4Cl$ precipitates in the form of sheet-like structures which are very thin, densely spaced and parallel to each other. Recently the formation of bilaterally symmetric 'face-like'deposits are also obtained due to the reactions mechanism by the properties and concentrations of soluble reactants placed symmetrically relative to a mid

line and due to the temporal and spatial distributions arising from the initial times and positions of reactant [62].

### 1.8.1 Propagating patterns

Liesegang patterns remained stationary and locked in their respective positions once they are formed. But in some systems they appear as dynamic due to the reason that the precipitate can redissolve in excess diffusing electrolyte due to complex formation. As a result the whole pattern propagates through system during the band formation process due to precipitation and band disappearance due to re-dissolution drive by complex formation. Several experimental studies on such periodic precipitation patterns with redissolution exist in the literature include the $Co(OH)_2/NH_3$ [63], $Cr(OH)_3/Cr(OH)_4$ [64], $Al(OH)_3/Al(OH)_4$ [65], $CoCl_2/NH_4OH$ [66] etc. Further experimental studies were performed on these systems based on observations, macroscopic measurements of spacing laws and various microscopic techniques to study the dynamic behaviour of this propagation phenomena. In the $Co(OH)_2$ propagation, it is noted that the number of bands exhibits chaotic oscillation with time. The variation of the velocity of propagation of patterns are studied and found that at higher concentration of the outer electrolyte like ($NH_4OH$), the pattern propagates faster and slower at higher concentration of the inner electrolyte like, ($CoCl_2$). Also the propagation velocity of the front increases when an electric field is applied in the same direction of the propagation of the front [67].

### 1.8.2 Precipitate patterning involving two salts

In addition to the single banded precipitate system deals upto here there are double banded systems too. It is found that different system have different patterning trends and arises due to the potential patterning properties of chemical reaction schemes involving two precipitates. The experiments on two-precipitate pattern formation gives ideas behind the possible reaction schemes actually involved in precipitation process and also suggests interesting experiments for eventual conclusions. Experimental results shows that there are systems showing "correlated"patterns (with bands overlap) or "anti-correlated"(with band alternation) patterns. In the few systems studied, $Co(OH)_2/Mg(OH)_2$, MnS/CuS etc yields alternation of bands of two salts and $PbI_2/PbF_2$ yields a dominant overlap between the bands [66].

The mixing of precipitation kinetics to diffusion mechanism in gel media reveals new perspectives of rich and complex dynamics of pattern formation phenomena. The obtained precipitate patterns continue to exhibit fascinating features with novelty and originality. A greater variety is anticipated when the experiments are extended to systems involving more than two precipitates. Periodic precipitation experiments find most feasible and interesting application in 'Geochemical Self-Organisation'due to the similarities they found in the banding structure seen in several rocks (zebra-like and other patterns). A nice example is the alternation of dark dolomite $CaMg(CO_3)_2$ with pure $CaCO_3$(white) in Zebra spa rock [68]. Surprisingly enough in addition to the doublets in Liesegang pattern formation, J. George et al., [69] reported the emergence of triples also. They studied the precipitation mechanism of multiple phases of calcium phosphate simultaneously into Liesegang bands in silica gel. They found dynamic triplet precipitate

patterns inside the gel column at pH below 6.86 and it is also found that all bands in the triplet were in precise geometric series and satisfies the spacing law. Moreover the triplet itself behaves as a system obeying the geometric law.

### 1.8.3 Effect of electric field

The effect of electric field on evolution of Liesegang patterns have been studied by many researchers with several electrolyte systems in different gels. The study of Sultan and Halabieh [70] found that the effect of varying field strength on front propagation in the $NH_4OH/CoCl_2$ system in gelatine gel studied the dependence of band position on the formation time by,

$$x_n = f_1(E)t^{1/2} + f_2(E)t + f_3(E) \tag{1.22}$$

where $f_1$, $f_2$ and $f_3$ are the parameters depending on the electric field strength, $E$. Lagzi and Izsak [71] found that as the strength of electric field increases, then the spacing coefficient and the thickness of the precipitation bands decrease. This observation is just opposite to that observed by Sultan and Halabieh [70] and this difference is due to the dependence of inner electrolyte. Another result of their experiment suggest that the width law also holds in electric field with little approximations. Lagzi also observed that the total number of bands increases to a maximum value and then decreases as electric field strength increases. As electric field strength is varies, a cross over from moving bands to precipitation wave is also noted . Also the spacing coefficient, that describes the overall structure of a Liesegang bands decreases with increasing field strength are also verified using both simulation and real experiments.

In $Mg(OH)_2$ system also studies were carried out in the absence and presence (in positive and negative) of electric field [72]. It is found that under the effect of positive field a wide span of patterns occurs compared to the field free case and in the negative field a successions of rings of unpredictably variable thickness and unusual time sequence are observed. Recently the effect of alternating electric field in $Co(OH)_2$ were studied and noted that band spacing increases with spacing number, but reaches a plateau at large spacing numbers. Also at low applied voltage the band spacing increases with increase in frequency and at higher voltage band spacing become independent of field frequency. The effect of concentration of inner electrolyte ($Co^{2+}$) exactly opposes that found under DC electric field, ie., the band spacing decreases with increasing concentration.

Flexible control of precipitation patterns is proposed by I.Bena et al.,[73] and showed that patterns resulting from reactions among charged agents can be controlled by a time dependent electric current. Experimentally they demonstrated the pattern control using $AgNO_3/K_2Cr_2O_7$ in gelatin gel.

### 1.8.4 Effect of gel

Gel has an important role in study of pattern formation. Gel is treated as a solution in the thermodynamical point of view, but for its mechanical character it is regarded as a solid. Due to this dual nature gel exhibits many feature which are absent neither in solid nor in liquid. Gels are prepared from both organic and inorganic materials and are hence made of cross linked homopolymers and exhibits very large volume change either by absorbing or by ejecting solvents depending on external conditions. This change in

volume has been treated as a discontinuous volume phase transition which arises mainly due to an imbalance in hydrophilic and hydrophobic interactions [74]. For the hydro gel, the liquid part of gel is water. The various kinds of gels which are used in many physico-chemical applications include agar-agar gel, gelatine gel, clay etc. The physical properties of gel depend on several factors like polymer concentration, free energy change per solvent molecule, osmotic pressure and temperature. The swelling character of the gel is determined by the osmotic pressure. The importance of gel matrix in Liesegang experiment is to prevent convection of sols and sedimentation of the precipitate [75].

Same chemical reaction can result in different precipitate due to difference in composition and structure of different gel and also due to undesirable impurities. A typical example is the precipitation of silver chromate in agarose gel or silica gel typically produces small, randomly distributed crystals, and in gelatin produces periodic bands [76]. In few systems, crystals or bands can be produced in same type of gel, and the morphological transition between randomly spaced crystals and bands is due to relative rates of heterogeneous and surface nucleation [77]. The formation of bands was strongly inhibited by the presence of a small amount of fatty acids. The number of bands usually decreases in the presence of amino acids where as increases in the presence of alcohol. The solubility of the salt increases by the hydrogen ion concentration of the solution increases. Thus Liesegang phenomena have striking affect due to the hydrogen ion concentration of the gel. The concentration of the gel has a remarkable influence on precipitation system. Thus gel acts as the medium of diffusion and hence therefore enables precipitants to agglomerate into patterns.

### 1.8.5 Effect of gravity

The effect of gravity on pattern formation was investigated by V. Holba et al., [78] in gelatin and agar gel. Spacing coefficient of Liesegnag bands was measured in the parallel and anti-parallel orientation to the gravitational field in one species with all other parameters fixed. The mean values of spacing coefficient indicate the effect of gravity and it is found that there is only a little difference between the spacing values in parallel and anti-parallel direction.

The Liesegang patterns arises from a spatially continuous regimes of colloid in a long time after nucleation has occurred and the mass of such aggregate is very small to be influenced by the gravitational field to a measurable extent. Gravity has its influence only when the crystal mass is large enough to overcome elasticity modulus of the gel matrix.

### 1.8.6 Effect of fluctuation

L. Jahnke et al., [79] studied the effect of fluctuation on Liesegang patterns and results shown that irrespective of the origin of noise in either thermal motion of particles or in impurities, stabilize the formation of patterns. Contrary to the intuition the precipitation structures are not disturbed by the fluctuations, but the regime of stable pattern formation is rather expanded. The empirical laws of pattern formation are also verified in large fluctuation system. The attractive application of the effect of fluctuation is to control the pattern formation without affecting the the reaction-diffusion process.

In general, fluctuations induced by heterogeneous nucleation decreases the spacing-law coefficient $p$ and increase the number of Liesegang bands. Hence it is possible to change the number or spacing of bands without chang-

ing the properties or concentrations of the reactants involved in the pattern formation process, one only need to change the level of impurities or defects in a sample. In contrast to thermal fluctuations, such changes can be realized with spatial variations. Hence it may be possible to obtain equidistant band formation without interfering with the chemical reactions. Such designed Liesegang pattern formation can be used, for example, in optics, where the spacing and the widths of the bands directly affect absorption and scattering of light.

## 1.9 Conclusion

The study of emergence of spatial patterns are vast, complex and is far from complete. Thus the mechanism of spatio-temporal pattern formation in natural and in laboratory systems are interesting subjects for study. Both physicists and chemists have speculated on the kinetics and dynamics of the systems and developed few interesting models. The patterns, which are formed in laboratory systems, called Liesegang patterns, attracted our interest and the study of these patterns will help us to reveal the mystery of many natural phenomena.

Even though a lot of theoretical and experimental studies have been made to understand the Liesegang phenomena, all of them have their own defects and none of them can explain all the experimental observation and conditions related to the formation of patterns. The mechanism underlying this pattern formation phenomena is still ambiguous and hence attracted many scientists and young researchers. Several challenging problems still remain open in this fascinating field of pattern formation in non-equilibrium systems. The rest of the chapters include our recent works in the field of

pattern formation.

# Chapter 2

# A study of Liesegang bands using moving boundary model

## 2.1 Introduction

The pattern formation in reaction diffusion systems was studied in a another way by assuming a concept different from the moving reaction front mechanism. As the reaction front advances in to the zone progressively, a virtual migration of the two phases that contain reactants A and B takes place. Here the moving boundary model consider that the phase separation mechanism is responsible for distributing the colloidal precipitant particles into band and non-band regions. In this model the band separation and its width are related to concentration of the reacting components and it also provides a critical condition for formation of bands in reaction diffusion systems.

## 2.2 Moving boundary model

All the theories discussed in chapter 1 on Liesegang phenomena share some common features to show how the diffusive reagents $A$ and $B$ turn into a final immobile precipitate $D$ in a diffusion stream.

$$A + B \rightarrow D \tag{2.1}$$

Some theorists suggests an intermediate compound ($C'$) formation from the reagents, before the end product is formed [37].

$$A + B \rightarrow C' \rightarrow D \tag{2.2}$$

There are two main categories of proposed models: pre-nucleation model is based on Lifshitz-Sloyzov instability mechanism. The model explains the band formation on the support of a feedback process between the nucleation and diffusion transport [37, 41, 42]. When the product of the reagent ion concentrations attains a saturation threshold value, the nucleation of the precipitated particles occurs. This is a non-equilibrium process and result in the lowering of the supersaturation level. When the concentration product is less than the threshold limit, further nucleation is impossible [80]. This product attains the threshold value again when the front proceeds more into the medium and the nucleation of the precipitate take place. Sequential repetition of this process results periodic pattern formation in the system. Based on this model, Wagner and Prager predicts sharp periodic band formations.

The second model is based on a post-nucleation droplet coarsening processes [47, 81, 82]. The moving nucleation front produces an intermediate

compound; a homogeneous haze of colloids, with the rate proportional to the reactants local concentration product [80] . A first order type phase separation mechanism that takes place inside the colloid separates them into regions of different matter densities. In the later stages of phase separation, several stochastic fluctuations results in the growth of crystals and generates a bunch of bands in the system. The precipitation bands appears by the agglomeration of the intermediate colloidal particles if the electrolyte concentration exceeds certain critical value [80],[46]. The colloidal particles are not stable against disturbances in the medium [83]. Venzl concludes the Liesegang band formation process through three characteristic steps: at first a continuous homogeneous colloid is formed, then the coarsening takes place and finally the dynamics of colloidal haze leads to formation of bands [84].

The moving boundary model, proposed by J.George and G.Varghese tackle the problem slightly differently. Though it supports the intermediate colloidal particle formation, it describes the pattern formation process as a result of virtual movement of the boundary of both inner and outer electrolytes [3]. This model also propose a phase separation mechanism for the band formation. The formation of intermediate colloidal particles prior to band formation with the moving boundary model, easily predicts the dependence of the width of the Liesegang patterns on concentration of electrolyte. One of the remarkable features of this model is that it upholds all the existing laws once the boundary migration concept is introduced. Thus a better and easy understanding of the basic concepts of precipitation patterns is possible with this model. The main approximations used in the moving boundary model [3],

1. The initial concentration of the outer electrolyte $C_{A0}$ should be higher

than the initial concentration $C_{B0}$ of the inner electrolyte and also the value of $C_A(x = 0, t)$ is fixed at the boundary of two electrolytes. In experiments, $0.005 \leq C_{B0}/C_{A0} \leq 0.1$.

2. The gel-solution interface, which is the boundary between the two electrolytes is located at the $x = 0$, in the $y - z$ plane. The $B$ type ions are considered to be uniformly distributed in the gel column and its initial concentration values are:

$$C_A = C_{A0}, C_B = 0; x < 0, t = 0 \tag{2.3}$$

and

$$C_A = 0, C_B = C_{B0}; x > 0, t = 0 \tag{2.4}$$

3. When the reaction front moves in to the gel column, the concentration of $A$ type ions changes and at the band position

$$C_A = C_{A0}; 0 < x \leq x_n, t \sim t_n \tag{2.5}$$

This is valid only when the reservoir concentration $C_{A0}$ of $A$ type ions is much higher compared to the initial concentration value $C_{B0}$ of $B$ type ions.

4. The boundary layer shifts from one band to the other with a uniform speed since the movement of the particles from one band to the other is almost uniform.

In the gel medium, the concentration profile of $A$ type ions is represented by [3],

$$C_A(x,t) = C_{A0}e^{-\gamma(x-x_n(t))/\xi_{n+1}}, x_n \leq x \leq x_{n+1} \tag{2.6}$$

here $\gamma > 0$, is a constant and $\xi_{n+1}$ is the separation distance between two consecutive bands.

The concentration profile of $B$ type ions inside the gel medium is disturbed by the reaction-diffusion process, and can be represented by

$$C_B(x,t) = \nu C_{B0}e^{-\sigma(x_n(t)-x)/\xi_n} + C_{B0}(1-\nu' e^{-\sigma(x-x_n(t))/\xi_{n+1}}) \tag{2.7}$$

where $\nu$ is a constant for a given system. The first part of the RHS of the equation (2.7) gives the idea of amount of $B$ type ions which have penetrated the band in the negative $x-$direction. The parameter $\nu$ will be very small, since the fraction of penetrated components in this direction are very less. And also the parameter $\nu'$ in the second term represents the factor of $C_{B0}$ which is dropped from its initial level during the precipitation of the reaction product $C^*$. Using the criteria for band formation in the ion product theory [3],

$$C_A(x,t)C_B(x,t) \mid_{x_n,t_n} = C^* \tag{2.8}$$

and

$$\frac{\partial}{\partial x}C_A(x,t)C_B(x,t) \mid_{x_n,t_n} = 0 \tag{2.9}$$

Putting the values of $C_A(x,t)$ and $C_B(x,t)$ from equations (2.6) and (2.7) in equations (2.8) and (2.9), we will get [3],

$$(\nu - \nu' + 1)C_{A0}C_{B0} = C^* \tag{2.10}$$

and

$$\nu'\left(\frac{\gamma}{\sigma}+1\right)=\frac{\gamma}{\nu}+\nu\left(\frac{\gamma}{\sigma}-\frac{\xi_{n+1}}{\xi_n}\right) \tag{2.11}$$

Substituting $\frac{\xi_{n+1}}{\xi_n}=1+p$ and $\frac{\gamma}{\sigma}=\alpha$, we get,

$$\nu(\alpha-(1+p))+\alpha=\nu'(\alpha+1) \tag{2.12}$$

Eliminating $\nu'$ from equation (2.10) and by substituting in equation (2.12)

$$p=\frac{KC^*}{\nu C_{B0}^2}+\frac{K\alpha C^*-(1+2\nu)C_{B0}^2}{C_{A0}(K\nu C_{B0})}, \tag{2.13}$$

which is the Matalon-Packater law and here $K=\frac{C_{A0}}{C_{B0}}$. It is now possible to estimate the values of the positive constants $\nu$ and $\nu'$ . Assume that the two concentration profile indices are same and put the value of $C^*$ in equation (2.10), we get

$$p=C_{B0}^2\alpha(\nu-\nu'+1)-\frac{(1+2\nu)}{\nu C_{B0}^2} \tag{2.14}$$

and hence

$$p=\frac{(1-2\nu')}{\nu} \tag{2.15}$$

If we take the upper limit for $p=0.5$, the value of $\nu$ and $\nu'$ will become respectively 0.05 and 0.493 [80]. Also if $p$ takes the lowest limiting value i.e., $p\sim 0$ similar to equidistant band system, one of the constants attains $\frac{1}{2}(\nu)$ and the other constant turns out ambiguous. Thus the limiting values of the constants can be fixed and it help us to understand the reaction dynamics. As $\nu'$ becomes 0.493, it implies that due to the formation of the reaction product ($C^*$), 49.3% of $C_{B0}$ had been eliminated from its initial concentration level . Even though this a large value, the thick bands formed near the gel-solution interface, still validates this approximation. The constant $\nu$,

which is a very small, represents the quantity of penetration of $B$ type ions in to the negative direction. Here $\nu \sim 0.05$ describes a very low penetration of the $B$ type ions in the backward $(-x)$ direction [80].

## 2.3 Determination of width of bands

The determination of the width law is possible using the moving boundary concept. One of the important observed features of the intermediate species theory is that the particles to be precipitated in the band is originated as a system of continuous homogeneous colloidal particles [46],[85], [86]. A phase separation mechanism that taking place in the medium separates the colloidal precipitant particles into band and non-band regions. Various methods were proposed to explain the phase separation phenomena. Droz et al., studied the phase separation phenomenon using spinodal decomposition mechanism [49],[14] and also by the behaviour of a moving reaction front [80]. The moving reaction front creates the colloidal particle and small bunch of particle nucleate and segregate behind the reaction front. When the outer electrolyte $A$ reacts with the inner electrolyte $B$, an intermediate compound $C$ of constant concentration $c_0$ is formed and all the colloidal particles appear on and near the band, then the concentration of intermediate particles falls of rapidly. The phase separation phenomena separates the homogeneous colloidal precipitant particles of uniform initial concentration $c_0$ into a band and a gap having concentration, $c_{ba}$ and $c_{ga}$ respectively[80]. Using the rules of conservation of matter,

$$w_n c_{ba} + (\xi_n - w_n) c_{ga} = \xi_n c_0 \tag{2.16}$$

here $w_n$ is the nth band width. The width of the nth band in terms of concentration becomes

$$w_n = \frac{(c_0 - c_{ga})}{(c_{ba} - c_{ga})}\xi_n \tag{2.17}$$

or

$$w_n = f_c\xi_n \tag{2.18}$$

where

$$f_c = \frac{(c_0 - c_{ga})}{(c_{ba} - c_{ga})} \tag{2.19}$$

is the width coefficient. Thus according to the above equation the width of precipitation bands strongly depends on intermediate colloidal particle concentration.

For the calculation of the value of $f_c$, simple approximations used are [80].

1. The $A$ type particles will move towards the positive x-direction during the diffusion process and a small fraction of type $B$ particles will move towards the negative x-direction. The remaining $B$ type particles having concentration, $(1-\nu)C_{B0}$ , found in the diffusion zone are participating in the reactions.

2. The amount of colloidal precipitants produced will be a another fraction of the remaining electrolytes. Thus we assume that $\mu(1-\nu)C_{B0}$ as the amount of the colloidal precipitants formed.

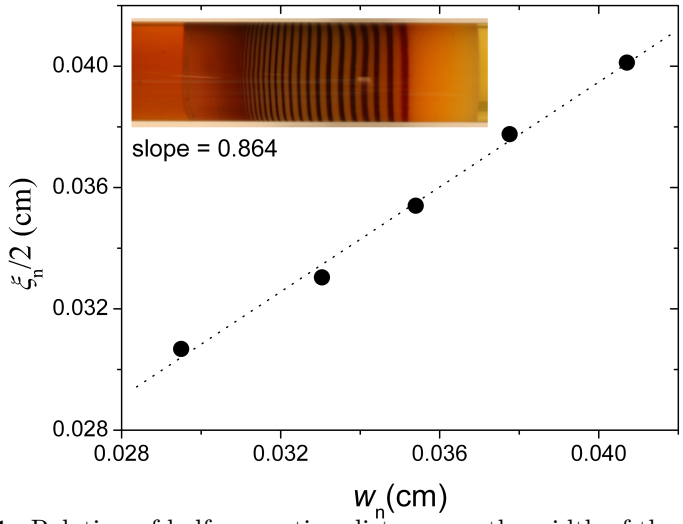


**Figure 2.1:** Relation of half separation distance on the width of the band for few bands in silver dichromate system. The outer (silver nitrate) and inner (potassium dichromate) electrolyte concentrations are 0.25 M and 0.0036 M, respectively.

3. The colloidal precipitants aggregate on the band is a further fraction of the total colloidal precipitants formed; $\lambda(1-\nu)C_{B0}$.

4. The gap contains all the remaining particles.

Equating the total concentration of colloidal particles generated $c_0$, and the concentration of the precipitant particles on the band $c_{ba}$ [80], we obtain

$$c_0 = \mu(1-\nu)C_{B0} \tag{2.20}$$

$$c_{ba} = \lambda(1-\nu)C_{B0} \tag{2.21}$$

Substituting these in equation (2.18), the width coefficient becomes

$$f_c = \lambda/(2\lambda - \mu) \tag{2.22}$$

Most of the colloidal particles seems to segregate on the bands and the gap contains a very few colloidal particles [80]. The width coefficient

$f_c$ becomes zero, when $\lambda = 0$, which is the no band condition. The width coefficient $f_c$ becomes negative, when $\lambda$ takes the values between $0 \leq \lambda \leq 0.5$ and the band formation is forbidden. When $\lambda = 0.5$, $f_c$ behaves anomalously and it holds the value 0.5 asymptotically. Thus we conclude that $\lambda \geq 0.5$ is a critical condition [80] for sustained band formation. Based on these, the width coefficient can be approximated as,

$$f_c \approx \frac{1}{2} \tag{2.23}$$

when $\mu \ll \lambda$ and $\lambda = 1$ as special case and patterns are simulated for this condition. Thus we can conclude that,

$$w_n = \frac{\xi_n}{2} \tag{2.24}$$

Hence width of the bands are almost equal to the half separation distance and is true only for small values of n [80]. As n increases the contribution of $\mu$ in equation (2.22) becomes prominent and the band width becomes smaller than this value.

## 2.4 Analysis of patterns

The experimental data by Lagzi et al., is taken for our analysis with permission and its details according to the authors were:

- Diffusion medium: gelatin gel
- Outer electrolyte (silver nitrate) concentration:$0.25M$
- Inner electrolyte (potassium dichromate) concentration: $0.0036M$

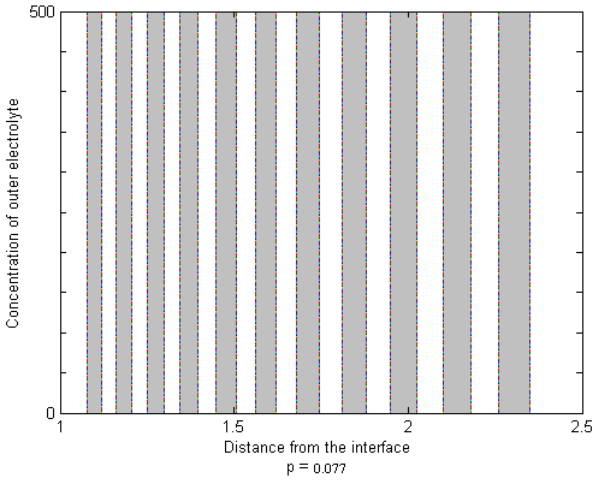


**Figure 2.2:** Simulated pattern for spacing coefficient p = 0.5. The Y -axis represents the concentration in milli moles per litre and the distance is taken along the x- axis in cm.

In the experiment, well defined Liesegang bands, obeying the geometric sequence, were seen at regular intervals in the gel medium. It is also noted that the width of the bands were approximately equal to the half separation distance (Figure 2.1), and it supports the theoretical predictions using the moving boundary model.

## 2.5 Simulation of the patterns

Usually in the computer simulation of Liesegang patterns the major task is to solve a set of coupled reaction-diffusion equation. The Fick's law was solved numerically in most of the simulation studies and the concentration profiles were plotted. We propose a different method here since the moving boundary model gives a new solution for the spacing coefficient. Here we are interested only in the structure of patterns, mainly in the spacing and width

of the bands [80]. The band position can be calculated using the formula,

$$x_n = x_0(1+p)^n \tag{2.25}$$

where n is the number of bands. As discussed earlier, p can have a multiple of values depending on the concentration of the electrolytes [80]. We have chosen two values for p in our simulation, one is the upper limit and the other value obtained experimentally. The position of the bands can be calculated using the above equation but it doesnt contain any idea on the width of bands. The theoretical approximations using moving boundary model give some idea on the width of the bands.

The simulation algorithm have the following steps [80]:

1. Choose the value of $p$, then calculate the constants $\nu$ and $\nu'$.
2. Calculate the position of the the band using spacing law, by assuming $x_0 = 1$.
3. By assuming the concentration $C_{A0}$ is fixed, the above process continues for successive ten steps.
4. Calculate the separation distance for each band and then compute the width of the bands using equation (2.25) and (2.24).
5. Then the bands are plotted using above steps.

Using the above algorithm two dimensional(2D) band structures were plotted by a Matlab programme. Simulated patterns resembles the Liesegang type patterns . The obtained pattern obeys all empirical laws of the experimentally observed patterns. In the simulation 2D patterns were obtained for

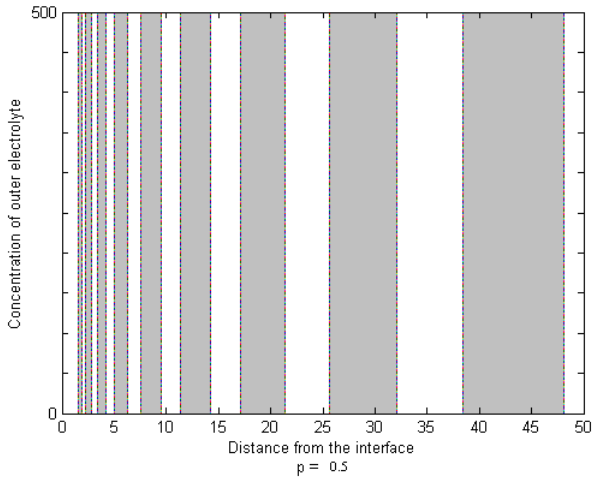


**Figure 2.3:** Simulated pattern for spacing coefficient p = 0.077. Y -axis represent the concentration in milli moles per litre and the distance is taken on x-axis is in cm.

$p$ values 0.077 and 0.5, respectively (Figure 2.2 and Figure 2.3). The maximum value in the Y-axis correspond to the initial concentration of outer electrolyte ($C_{A0}$). This concentration does not vary between $x_n$ to $x_n + w_n$, as stated in the moving boundary model and the concentration of A type ions falls of to zero beyond this point. This process repeats periodically in space and hence the patterns are formed. The separation distance and the width of the bands increases, as $p$ increases. Hence different electrolyte concentration yield different precipitation patterns. A similar approach is possible for $\lambda$ ranging from 0.5 to 1 [80].

## 2.6 Conclusion

The pattern formation mechanism in reaction diffusion system was investigated theoretically by introducing a new concept of boundary migration. The moving boundary model reproduced the scaling law, time law and the width law without making much assumption. It also gave a satisfactory

explanation on the spatial positioning of the periodic band structure seen in reaction diffusion systems. The dependence of the width of the precipitation bands on the concentration of the intermediate colloidal particles were theoretically calculated using this model. Hence a better understanding of the basic facts of pattern formation process was made possible with the theoretical investigations and was also verified using computer simulations. Simulated patterns bear the characteristic nature of the experimentally observed Liesegang patterns. Another remarkable feature of this model is that the asymptotic condition for the band formation can be determined. Also this model calculate the width of the bands with little approximations, which many others were trying to find. The concentration dependence of the width of the bands for different spacing coefficients were plotted. The intermediate colloid formation process was once more confirmed in the model and it was found to be useful in discussing many other phenomena, especially the self-sustained patterns.

# Chapter 3

# Experiments

## 3.1 Introduction

Liesegang experiments are simple and cheap to perform and this chapter gives a brief introduction about Liesegangs experiment and list a few Liesegang systems too. We performed the experiments in silica and agarose gel and in both cases we obtained both liesegang and helical patterns. The experimental setup and methods in silica, agarose, mixed(silica-agarose) gel and the tube-in-tube experiments are briefly explained. Comparison of the probability of helicoids in both gel are also studied.

The physical and chemical properties of the diffusion medium effects the pattern formation. The main function of a gel is to maintain a diffusion controlled system by eliminating convection and to hold precipitates in place and preserve the pattern that forms. Precipitation of silver chromate in agarose gel or silica gel typically produces small, randomly distributed crystals, and in gelatin produces periodic bands [87] which is probably a result of the differing chemical compositions of these gels. In some systems,

crystals or bands can be produced in the same type of gel, and morphological transition between crystals and banding is related to relative rates of heterogeneous and surface nucleation [88], which also depend on the chemical properties of the medium or the presence of chemical species that do not take part in reactions. Gradients of factors such as temperature or pH that affect precipitation can give rise to revert or equidistant spacing of precipitates [89].

During the precipitation in gel system, various types of structures are formed. The precipitation pattern formation in lead iodide, Toramaru et al.,[90] describe the transition of periodic patterns to tree like structures. At higher gel concentration ordinary Liesegang bands are formed whereas at lower gel concentration tree like crystal aggregates are formed. The two major difference they found is that in the number density and surface nucleation. The precipitation band have number density $10^3$ times higher than tree-like crystal structure and surface nucleation is absent in periodic precipitation. At higher nucleation rate in higher gel concentration, individual crystal growth is relatively suppressed and as a result Liesegang bands consisting of higher number density of tiny crystals is developed. On the other hand at lower gel concentration, due to lower number density nucleation is suppressed there by allowing each nucleated crystal to large crystals.

## 3.2 Gels

Gels are commonly used in periodic precipitation experiments due to their small pore size prevents bulk movements of fluid while allowing diffusion of small molecules and ions, and prevents precipitates greater than a certain size from moving from their sites of formation. Silica gel is the most geo-

chemically plausible gelatinous material. Silica hydro-gel is formed by the reaction between sodium silicate solution and an acid [87]. The gel is therefore an inorganic matrix of polymerized acidified silicate that contains some leftover silicate ions in solution and also anions of the acid used to create the gel. Agar is a complex polysaccharide matrix extracted from algae [91]. Agarose consisting mainly of methylated cellulose, is purified from agar to have a very low ionic content and therefore lower conductivity suitable for use in gel electrophoresis, therefore creating a charge-neutral diffusion controlled environment. Various gels differ in the method of preparation and the gel point also varies for different gels. We are using silica and agarose gel in our experiments. Thus depending on the method of preparation gels are classified into two:

1. Chemical gel: Gel formed by chemical reaction such as hydrolysis or polymerisation. Eg: Silica, polyacrylamide etc.

2. Physical gel: Gel which is obtained by physical process such as cooling. Eg: gelatin, agarose, clay etc.

## 3.3 Liesegang systems

There are a bunch of systems which exhibit Liesegang patterns. Same chemical system in different gels shows different patterns due to the physical and chemical properties of the gel. A few Liesegang systems, revert spacing system, doublets and triplet system and gaseous diffusion system are given below.

- $AgNO_3/K_2Cr_2O_7$ in gelatin gel [36]

- $MgCl_2/NH_4OH$ in PVA gel [34]

- $Pb(NO_3)_2/KI$ in agar-agar gel [92]
- $MgSO_4/NH_4OH$ in gelatin [72]
- $CoCl_2/NH_4OH$ in gelatin [67]
- $Pb(NO_3)_2/K_2CrO_4$ in agar [57] [revert spacing]
- $NaOH/CuCl_2$ in PVA gel [58]
- $CuSO_4/Na_2CrO_4$ in silica gel [93]
- $NaOH/Cu(NO_3)_2, NaOH/AgNO_3$ in PVA or agar gel [94]
- $Ba(NO_3)_2/(NH_4)_2MoO_4$ in silica gel [95]
- $CaCl_2/H_3PO_4$ (triplets), $Pb(NO_3)_2/KF$ in silica gel [4]
- $MgCl_2/NaOH$ in PVA gel
- $K_2CrO_4/CuCl_2$ in agarose [96]
- $AlCl_3/NaOH$ in agarose [97]
- $K_2CrO_7/AgNO_3$ in gelatine [98]
- $KI/PbNO_3$ in agarose [99]
- $HCl/NH_3$ in silica aerogel(gaseous diffusion)[61]

## 3.4 Precipitation patterns in silica gel

The structure and properties of silica gel has been studied very deeply [100, 101]. When sodium meta silicate dissolves in water, monosilicic acid is produced in accordance with the chemical reaction shown below. This is a reversible process and the by-product is the strong alkali NaOH remains

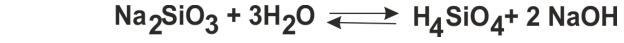

in the solution. This is the reason for the alkaline habit of the solution. The mono-silicic acid liberates the hydroxyl ions and polymerises as shown below: This happens again and again until a three dimensional network of

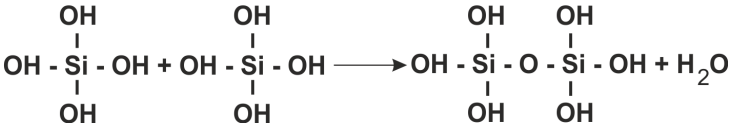

Si - O links is established and the silicon oxygen linkage is extremely strong and which is irreversible. A section of the cross-linked polymer is shown below

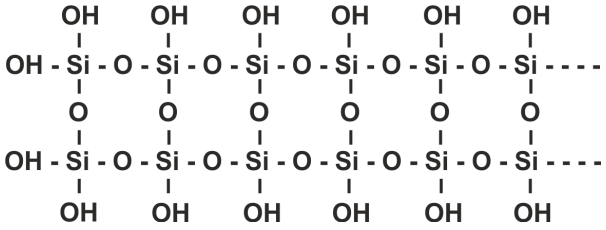

### 3.4.1 Preparation of silica gel

A gel of desired density was prepared using sodium meta silicate solution (Stock solution). Stock solution was prepared by mixing, few grams of sodium meta silicate(Loba) in doubly distilled water. Relative density of the Stock solution measured by specific gravity bottle method was 1.08.

Now, to prepare Stock solution of given relative density (say 1.03), we have to mix proper volume of initially prepared Stock solution with distilled water. To know the required volume of water to be added, plot a graph between relative density and volume of distilled water to be added. Since density and volume has linear dependence, simple interpolation technique

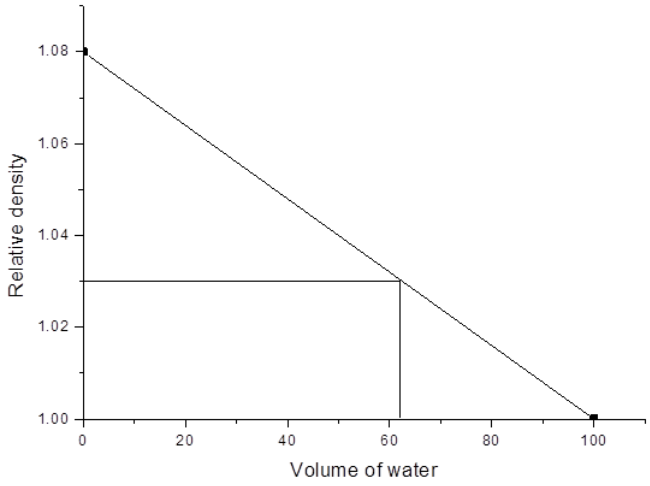


**Figure 3.1:** Relative density versus volume of water

allow us to calculate the required volume of water for any relative density between 1 and 1.08 as shown in Figure 3.1. From the graph it is clear that volume of water required to make gel of relative density 1.03 from initial Stock solution of relative density 1.08 (measured value) is 63 *ml*. That is, 63 *ml* of water is to be added to 37 *ml* of initial Stock solution to prepare a gel of relative density 1.03.

Silica gel is prepared by combining two solutions: (i) an acid solution (dilute HCl) + potassium chromate solution and (ii) sodium silicate solution prepared by diluting silica powder (Loba) to doubly distilled water. Drop by drop of (ii) is added to (i) slowly by continuous stirring and set the solution for desired pH and poured into test tubes. The tubes were then sealed and kept undisturbed for 24h. Polymerisation begin immediately as soon as silicic acid is formed. The gelling process itself takes an amount of time, which can vary from hours to days, depending on the nature of material and its temperature.

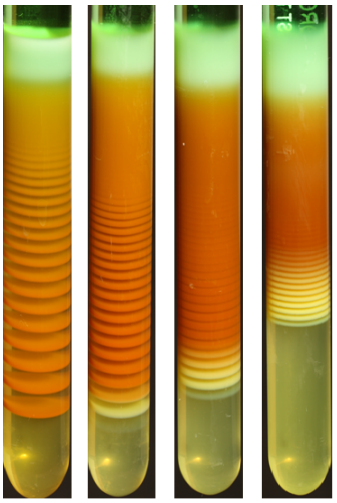

**Figure 3.2:** Liesegang patterns in silica gel having different pH value; 7, 8, 9, 10 respectively

### 3.4.2 Liesegang and helical patterns in silica gel

Stock's solution of desired relative density (1.03) was prepared in doubly distilled water. $0.01M$ solution of $K_2CrO_4$( Merk) was taken in a beaker and add drop by drop of Stock's solution to it by continuous stirring. Gelation was induced by decreasing the pH of the system by adding $HCl$ [102] . Pour this solution in to different test tube radii and kept them undisturbed for 24 hrs till the gelation was complete. After complete gelation pour the solution of $CuCl_2$(Merk, 0.5M) gently on the top of the gel. After some time a light green precipitate is formed and the test tubes were closed and kept undisturbed for the reaction to take place.

The experiments were done out at room temperature and at pH 7. Experimental results shows that both normal Liesegang (Figure 3.2) and helicoidal (Figure 3.3) patterns are obtained. The experiments were done in ten different test tubes to calculate the probability and also at different pH values 8, 9, 10. It is found that as the pH increases the initial plug also

**Figure 3.3:** Helical patterns in silica having diameters 8mm and 12mm

increases and the spacing coefficient decreases[102]. That is the patterns become more closely spaced as the pH increases (Figure 3.2) since the pH affects the pore size and the internal surface area of the gel. When the same set of experiments were carried out in a thermostatic temperature bath at $35^0C$, more probability of obtaining helicoidal precipitation patterns are found. So here the thermal noise promotes the formation of helicoidal precipitation patterns [102].

## 3.5 Precipitation patterns in agarose gel

Agarose is a polysaccharide extracted from seaweed. It is typically used at concentrations of 0.5 to 2 percent. Its structure is shown in Figure 3.4. The higher the agarose concentration the "stiffer"the gel. Agarose is available as a white powder which dissolves in near-boiling water, and forms a gel when it cools [103]. Agarose gels and melts at different temperature, and the gelling and melting temperature varies depending on the type of agarose. Usually

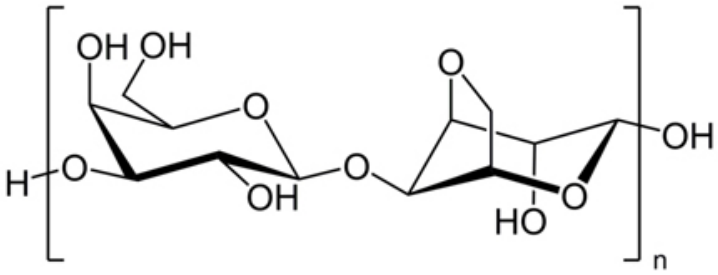


**Figure 3.4:** Structure of agarose

**Figure 3.5:** Liesegang patterns in agarose gel having test tube diameters 8mm, 12mm, 18mm

agaroses has a gelling temperature of $35-45^0C$ and a melting temperature of $85-95^0C$. The melting and gelling temperature may be dependent on the concentration of the gel. The gelling portion of agar-agar has a double helical structure. Double helices aggregate to form a three-dimensional structure framework which holds the water molecules within the interstices of the framework [103].

### 3.5.1 Liesegang and helical patterns in agarose gel

Agarose (Type I, Sigma Aldrich) is a fine white powder and its 1 % concentration with potassium chromate ($K_2CrO_4$, Sigma Aldrich) as inner electrolyte is prepared by dissolving them in doubly distilled water . The resulting solution was heated to $90^0$ C while constantly stirring it until a homogeneous solution was obtained. The precipitation reaction includes the mechanism

$$Cu^{2+}(aq) + CrO_4^{2-}(aq) \rightarrow CuCrO_4(s) \tag{3.1}$$

in 1 % agarose gel. Pour the solution into test tubes and after complete gellation, on top of this gel $CuCl_2$ ( which serves as outer electrolyte) is gently poured. Since the outer electrolyte concentration is larger than that of the inner electrolyte, the reaction front diffuses into the gel medium, and a regular Liesegang pattern of precipitation bands (Figure 3.5) forms in the wake of the front. Frequently, helicoids (Figure 3.6) evolve from the same macroscopic experimental conditions. To study this intriguing phenomenon and to quantify its stochastic mechanism, the concentration of the outer electrolyte ($a_0$) and inner electrolyte ($b_0$), the temperature ($T$) of the system and the radius of the test tube ($R$) are changed and hence determined the probability of the emergence of single helicoids using 10 independent experiments for each set of parameters.

### 3.5.2 Spacing coefficent

To generalize the concept of spacing coefficients for helices, it is required to study the Matalon-Packer law for the helicoidal patterns. By defining $x_n$ as

**Figure 3.6:** Helical patterns in agarose gel having test tube diameters 8mm, 12mm, 18mm

the position of the nth crossing of the helix at a given point (Figure 3.7), for large n $x_{n+1}/x_{n-1} = p_n$ should converge to the spacing coefficient p. The helices are often characterized by their pitch and it is very clear from experiments (Figure 3.7) that as the distance from the initial junction of the electrolytes increases, the pitch of the helices also increases. The local pitch $q_n = x_{n+1} - x_n$ can be determined and can be expressed through the spacing coefficient as $q_n = x_{n+1} - x_n = px_n$.

Figure 3.8 depicts the connection of the spacing coefficient as a function of $a_0$ for both bands and helices in experiments. The experimental data for bands and helices are close to each other and the helices having a bit larger spacing coefficients. Also the experimental data for both the Liesegang bands and helicoidal patterns have same type of curves and can be fitted to the Matalon-Packter law (refer equation 1.13 in chapter 1). Not only the

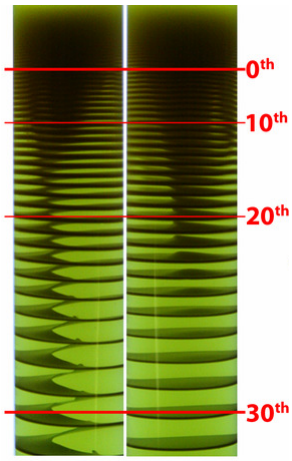


**Figure 3.7:** Variation of spacing coefficient for hellicoids and Liesegang patterns in experiments

band spacing of the patterns but the local pitch of the helices follows the Matalon-Packter law.

From the experiments, it is observed that the local pitch of the helices is little larger than the local band spacing of the Liesegang bands found in the same experimental setup. This slight variation can be explained by assuming that the bands and the helices have the same local precipitate concentrations and widths. It is noted that the amount of precipitate found in a band is always less than that in the corresponding part of the helix, since the moving reaction front leaves behind a constant concentration of Cs which are further collected into a band or a tilted band (helix). Hence it can be elucidated that the pitch of the helix should be larger than the spacing of bands to collect the same amount of C particles.

### 3.5.3 Effect of radius of tube

We performed experiments by varying the radius of the test tube(Figure 3.9). Surprisingly it is noted that no helicoids are formed below a critical radius

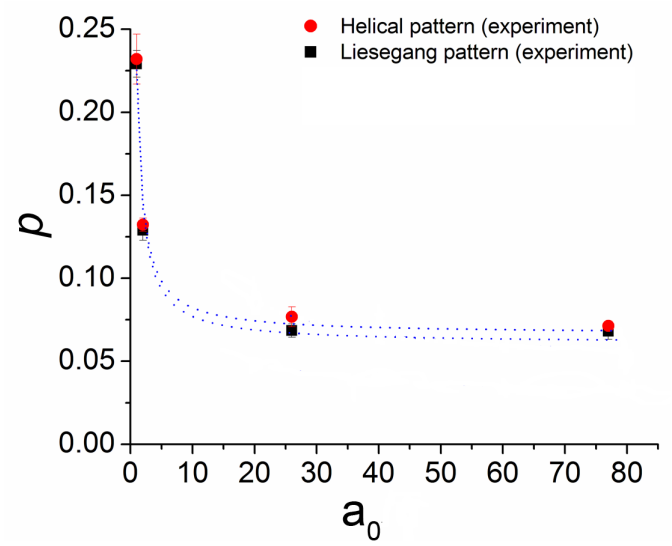


**Figure 3.8:** Dependence of spacing coefficient on $a_0$. Matalon-Packter law is equally valid for Liesegnag bands and helices

($R_{crit} = 1.5\ mm$), Figure 3.11. Also there is a maximum probability of getting helicoids at $R = 8mm$. As the radius of the test tube increases, there is much probability for the evolution of more complex structures (double helices (Figure 3.10), triple helicoids, disordered patterns). From the graph also its very clear that there are no helicoids below $R = 1.5\ mm$ and the maximum probability of helices are at $R = 8\ mm$.

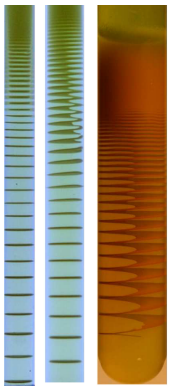

**Figure 3.9:** Effect of radius of tube on precipitation patterns for R = 1.5, 2, 8 mm respectively

**Figure 3.10:** Double helical patterns for R = 10 mm in agarose gel

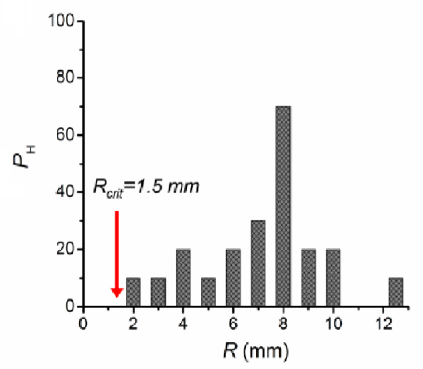


**Figure 3.11:** Graphical representation of effect of radius of tube on precipitation patterns

The experimental values for different test tube radii and their probabilities are tabulated in Table 3.1 .

**Table 3.1:** Probability of the emergence of helical pattern $P_H$ in experiments where the test tube radius $R$ was the only parameter varied

| R(mm) | 1.5 | 2 | 3 | 4 | 5 | 6 | 7 | 8 | 9 | 10 | 12.5 |
|---|---|---|---|---|---|---|---|---|---|---|---|
| pH | 0 | 0.1 | 0.1 | 0.2 | 0.1 | 0.2 | 0.3 | 0.7 | 0.2 | 0.2 | 0.1 |

### 3.5.4 Effect of temperature

We performed experiments by varying the temperature of the system and keeping all other parameters constant. The experimental values are tabulated in Table 3.2. While investigating further about helices, its noted that a fast front(eg., by selecting large $a_0$) can create an unstable state in the wake of the reaction front by placing the system deep in the misibility gap(eg., by an appropriate choice of $b_0$). Choosing the right temperature is very difficult which itself requires further extensive studies.

In the experiments, Liesegang and helicoidal precipitation patterns emerged in gel medium in the test tubes. Here the planar diffusion front of the outer electrolyte diffuses into the gel medium produces a series of precipitation bands called the regular Liesegang pattern. The helicoidal precipitation pattern emerge in the same experimental set up shows the stochastic behaviour of this phenomenon. To study the various properties of Liesegang and helicoidal precipitation patterns, we performed ten independent set of experiments with same condition.

## 3.6 Tube-in-tube experiment

The experiments which were described earlier in silica and agarose gel were also carried out in a quasi two-dimensional geometry by placing the gel in-between two test tubes of slightly different radii, thereby creating a narrow cylindrical gel column Figure 3.12. This setup is called the tube-in-tube experiment and its procedure is briefly explained below. The tube-in-tube experiments are rather easier for the theoretical investigation than the single tube experiments, since they are 2D patterns and can be easily transformed

**Table 3.2:** Probability of the emergence of helical pattern $P_H$ in experiments where the temperature $T$ is the only parameter varied

| T($^0$ C) | 8.5 | 24 | 60 |
|---|---|---|---|
| pH | 0.2 | 0.7 | 0.3 |

**Figure 3.12:** Tube-in tube helical patterns of silica and agarose gel

to tilted Liesegang bands.

In the case of agarose gel, first the given amount of agarose(Type-1, Sigma Aldrich) is dissolved with the potassium chromate(Sigma Aldrich) in double distilled water. The mixture was heated to $90^0$ C under constant stirring until a homogeneous solution was obtained and pour this solution in to test tubes. After a few minutes insert a test tube having smaller radius into the bigger test tube, where we poured the homogeneous solution. Keep the inner test tube exactly middle of the bigger test tube by slight adjustments so that the cylindrical gel column is formed between the two test tubes. After few hours the outer electrolyte is poured in between two tubes, and one can observe the formation of regular Liesegang bands, single helices, as well as double helices. Triple helices and more complex patterns also emerge for large enough tube radius. Similar experiment were done for silica gel also.

## 3.7 Comparison of helical precipitation patterns

The helicoidal patterns are formed in both agarose and silica gel. The helicoidal patterns in silica evolve more rapidly than in agarose gel. In silica gel as the pH increases, the spacing coefficient decreases and the bandwidth increases but it happens vice versa in agarose gel. In silica gel as the pH decreases the probability of getting helicoids increases [102]. In agarose medium by increasing the gel concentration, the probability of helicoidal patterns increases, simultaneously the probability of Liesegang and distorted helicoids decreases, and further increase in agarose concentration leads to decrease in the probability of helicoidal patterns . This behaviour of patterns can be qualitatively explained by considering that the gel can introduce randomness into the system. The concentration of the gel can be treated as a factor that is proportional to the noise. At low noise (at low agarose concentration), the Liesegang pattern dominates and the probability of helicoids go to zero. At large noise, the system becomes chaotic, the probability of Liesegang goes to zero, and distorted helicoids start to dominate [102].

## 3.8 Patterns in mixed silica-agarose gel

In this experimental set up 1% agarose powder(Type1, Sigma Aldrich) was added to $0.01M$ solution of potassium chromate ($K_2CrO_4$, Merk). The resulting solution was heated to $90^0C$ while continuously stirring until a homogeneous solution was formed [102]. Take some amount (10 ml) of above prepared solution in a beaker and add 90 ml of SMS to it and mix well. The resulting solution was poured into test tubes for 3 hours for

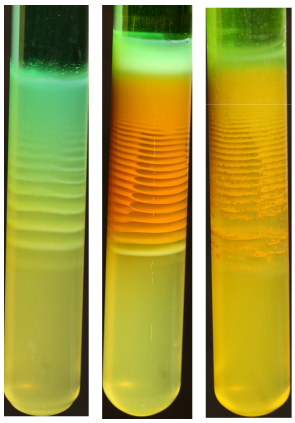

**Figure 3.13:** Effect of impurity on patterns- 10 ml agarose, 50 ml agarose, 80 ml agarose in silica are shown

complete gelation. The solution of $CuCl_2$(Merk, 0.5 $M$) was then poured gently over the top of gel after the polymerisation. The test tubes were then closed and kept undisturbed for the reaction to take place. Repeat the same procedure for different volume of silica gel, say 50 $ml$ and 20 $ml$ in to 50 $ml$ and 80 $ml$ of agarose gel. Experiments shows that different type of patterns were formed in different volume of silica gel, which differ in spacing and bandwidth (Figure 3.13). Another interesting result is that the probability of helices are large in equal amounts of both gel, i.e., at 50 $ml$ of silica and agrose gel [102].

## 3.9 Conclusion

The Liesegang and helical precipitation patterns were obtained at specific conditions and patterns were easily reproducible too. Our experiments showed that self organised precipitates could be produced in porous media under a variety of conditions. Although the chemical conditions in our experiments were different from what would be excepted in natural situations, this experimental work showed how physical and chemical properties

of a porous or permeable medium could affect the morphology of precipitates produced.

# Chapter 4

# Helical precipitation patterns

## 4.1 Introduction

Helices and helicoids are present from nano- to macroscale and a few examples includes nanohelices in ZnO [104], helical structures of inorganic crystals and macromolecules [105, 106], precipitation helicoidal patterns [15, 107, 108] and fibre geometry of heart walls [109]. Chiral patterns have been the central topic of a large number of studies in natural sciences, engineering as well as in the artistic domain. The emergence of chirality at meso- and macro-scale is a complex process which may proceed principally in distinct routes. Firstly, the chirality is present in the microscopic building blocks and the symmetry is just transcribed to a higher level of spatial organization [110]. Secondly due to the presence of chiral media, achiral microscopic units may assemble into chiral objects [111]. Finally, achiral microscopic units may self-organize into a chiral structures through symmetry breaking process [107].

To understand more about the origin of helicoidal patterns, further

studies were made in the formation of precipitation patterns in the wake of reaction-diffusion fronts [87, 112]. The motivation behind this investigation stems from the simple correlations of helicoidal precipitation patterns in the plane perpendicular to the axis. Since the Liesegang phenomena in gel systems are well studied [87, 112], this knowledge helps to know more about the emergence of helicoidal patterns in precipitation systems. Hence using well defined experimental and theoretical approaches makes it easier to develop the dynamics behind the formation of helical structures.

## 4.2 Theory

Most of the theories about the Liesegang pattern combine the properties of reaction front and the mechanism of precipitation i.e. in which way the reaction product, $C$, becomes the precipitate. The peculiarities of the moving reaction front have been studied both theoretically [6, 113] and experimentally [114, 115],but the mechanism behind the precipitation is more debated. Several methods have been proposed based on the pre- and post-nucleation mechanisms, and their merits and demerits are subjects of discussion even today. Theories which incorporate both dynamics also exist[116, 117], the simplest one [14] is based on the Cahn-Hilliard equation [18, 19] and on its generalization with conserved noise added [118]. The Cahn-Hilliard equation features both the fast spinodal-decomposition and slower nucleation-and-growth processes. When the phase separation dynamics is linked with the diffusing (decelerating) reaction zone, which provides a slowly increasing time scale, this model allows regimes where the pre- or the post-nucleation dynamics dominates the pattern formation.

In the Liesegang experiment, a reaction front arises due to the inhomo-

geneous distribution of the electrolytes $A$ and $B$. The reaction mechanism proceeds into the gel medium where the inner electrolyte ($B$) is homogeneously distributed. After complete gelation the outer electrolyte (A) having much higher concentration is gently poured on the top of the gel. Assume a second-order irreversible reaction $A + B \rightarrow C$, the moving front proceeding in to the gel medium can be represented by the set of equations

$$\frac{\partial a}{\partial t} = D_A \Delta a - kab \tag{4.1}$$

$$\frac{\partial b}{\partial t} = D_B \Delta b - kab \tag{4.2}$$

where the diffusion coefficients ($D_A, D_B$) and the reaction rate $k$ have been taken as 1 by an suitable choice of the length and time scales (see Appendix 1). The moving reaction front, described in terms of the spatio-temporal properties of the formation rate of $C's(ab)$, is narrow and it moves into the gel diffusively. The phase separation mechanism takes place since the moving reaction front back out a constant concentration of $C's(c_0)$, where $c_0$ is a function of $D$ and $b_0/a_0$. Assuming that the system having concentration $c_0$ is unstable, the phase separation process distributes $C's$ into regions having high- ($c_h$) and low-concentrations ($c_l$) and can be represented using the Cahn-Hilliard equation:

$$\frac{\partial c}{\partial t} = -\lambda_0 \Delta \left[ \frac{\delta f}{\delta c} \right] + kab + \eta_{c_0} \tag{4.3}$$

Here $\lambda_0$ is a kinetic coefficient, $f$ is the free energy driving the phase separation, $kab$ is the source term specifying the creation of $C$ particles by the front, and $\eta_{c_0}$ represents thermal noise effects which conserve the total number of C particles.

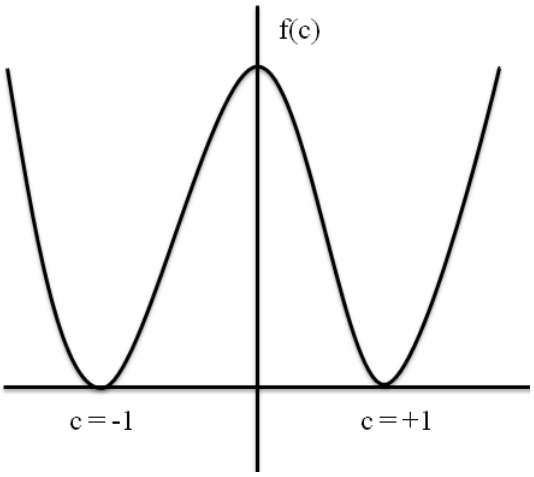


**Figure 4.1:** Landau Guinzburg free energy

In order to have phase separation, the free energy $f(c)$ should have two minima corresponding to the low $(c_l)$ and high $(c_h)$ concentrations of $C's$ in homogeneous equilibrium states (Figure 4.1). It should also have a surface tension term preventing the formation of singularities at interfaces. As a convenient form with minimal number of parameters, one can take $f$ as a Landau-Ginzburg free energy which is symmetric about $\hat{c} = (c_h + c_l)/2$

$$f(c) = -\frac{\epsilon}{2}(c - \hat{c})^2 + \frac{\gamma}{4}(c - \hat{c})^4 + \frac{\sigma_0}{2}(\nabla c)^2 \tag{4.4}$$

where $\epsilon, \gamma$ and $\sigma_0$ are phenomenological parameters, and the minima of $f(c)$ are fixed at $c_h$ and $c_l$ by setting $\sqrt{\epsilon/\gamma} = (c_h - c_l)/2 \approx c_h/2$ , assuming that $c_h > c_l$ i.e. the gaps between the bands have very low steady-state concentration of $C's$ (in usual Liesegang experiments). Measuring concentration, time, and length in units of

$$\bar{c} = \frac{c_h - c_l}{2}, \tau = \frac{1}{k\bar{c}}, l = \sqrt{\frac{D}{k\bar{c}}} \tag{4.5}$$

and, furthermore, making a shift in the concentration of $C's$

$$m = \frac{c - (c_h + c_l)/2}{(c_h - c_l)/2} \approx \frac{c}{\bar{c}} - 1 \tag{4.6}$$

and one obtains the equation

$$\frac{\partial m}{\partial t} = -\lambda\Delta[m - m^3 + \sigma\Delta m] + ab + \eta_c \tag{4.7}$$

where $\lambda = \lambda_0\epsilon/D, \eta_c = \eta_{c_0}/k\bar{c}^2, \sigma = \sigma_0 k\bar{c}/D$, are respectively the modified kinetic coefficient, conserved noise and surface tension.

where $m$ is concentration of $C's$ modified by $(c_h + c_l)/2$ and rescaled by $\bar{c} = (c_h - c_l)/2$ . Thus the concentration $m = (2c - c_h - c_l)/(c_h - c_l) = 1$, for $c = c_h$ and $m = -1$ for $c = c_l$. The parameter $\tau_u \approx \sigma/\lambda$ explains the characteristic time scale of the formation of unstable modes in the Cahn-Hilliard equation. Relative comparison of $\tau_u$ with the time the reaction front traverses through a region determines whether the nucleation-and-growth process or spinodal decomposition process dominates the formation of patterns.

Note that adding the noise component $\eta_c$ is important since the helical pattern formation is a symmetry-breaking phenomena which does not happen without the presence of noise. Noise widens the available regions of the meta- and unstable states, and makes useful the earlier morphological phase diagrams of Liesegang patterns. Note that patterns resulting from noiseless Cahn-Hilliard dynamics in the wake of a front moving with fixed velocity have been much studied [119, 120]. Complex morphologies, have been obtained only from various initial conditions or from dynamical movement of the reaction front. The model having no noise contribution shown

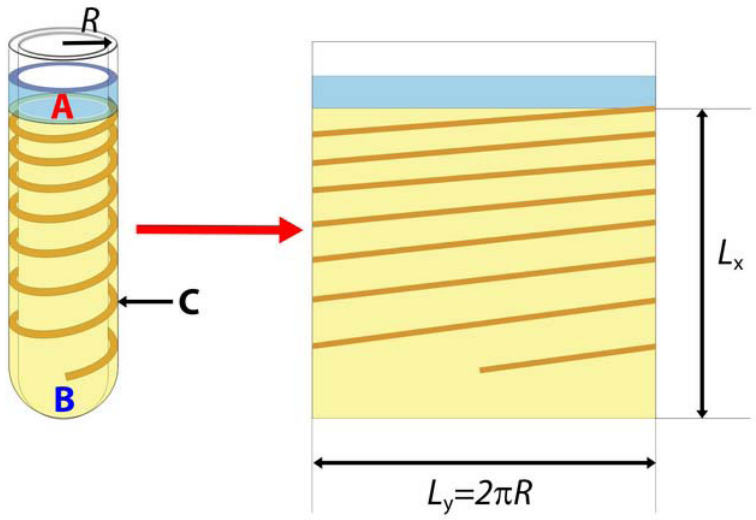


**Figure 4.2:** Transformation of the three dimensional "tube-in-tube"experimental set up into a two dimensional domain.

to reproduce the properties of the regular Liesegang patterns [14, 20].

From theoretical point of view, the tube-in-tube experiments are the easy to describe. When the test tube radii are very similar, it can be cut vertically and open as shown in Figure 4.2, and assume the thin layer of the gel as an effectively two-dimensional rectangular strip of width $L_y = 2\pi R$, and length equal to the tube length $L_x$. The equations 4.1,4.2 and 4.7 were studied in rectangle of size $L_x L_y$ with the reaction front moving in the direction of x-axes and were solved by applying the method of lines. This involves spatial discretization on a rectangular grid and the integration of the subsequent ordinary differential equations by the forward Euler method. The conserved noise $\eta_c$ was included by changing Cs to neighbouring sites at a rate $\eta_c = r\sqrt{c}$, here r is a random number uniformly distributed in an interval $[-\eta, \eta]$. Band periodicity enabled us to use periodic boundary conditions in the y direction (Figure 4.2). At the lower edge $(x = L_x, y)$ of the test tube we used no-flux boundary conditions. Since the concentration

of the outer electrolyte(A) is kept at a constant value $a(x = 0, y, t)$, we used Dirichlet boundary condition at the upper edge $(x = 0, y)$ of the test tube, where as Neumann (no-flux) boundary conditions are used for B and C. The simulation patterns indicate that both helices and Liesegang emerge in a wide range of parameters and the patterns are in good accordance with the experimental patterns, Figure 4.3.

**Figure 4.3:** Simulated and experimental helical and Liesegang patterns

## 4.3 Probability of emergence of helices

From experimental and simulation results it is clear that a fast motion of the front, large diameter of the tube, and a sufficient amount noise promotes the formation of helices. A physical picture is obtained by measuring the probabilities of helix/helicoid formation in Liesegang experiments, by varying the experimental parameters such as the initial concentration of outer electrolyte or inner electrolytes, the radius of the test tube, and the temperature of the system. The experimental setup and the initial conditions do not break chirality at the macroscopic level and the helices/helicoids emerge with large probabilities (greater than 50% for some parameter range). Also it is find

that the probabilities are well defined and are reproducible for a given set of parameters. These studies suggest that the origin of helicoidal patterns is due to an intrinsic property of the dynamics of the system and not related to the noise fluctuations and asymmetry of the initial conditions. It is also clear that the formation of unstable modes, the reaction front dynamics, and noise fluctuations together leads to helical precipitation patterns.

## 4.4 Results and Discussion

Several experimental and theoretical studies have been reported by various groups to clarify the emergence of helices in Liesegang-type setups [87, 121]. From our experiments it is clear that the formation of helical and helicoidal patterns was reproducible but had a probabilistic aspect [102]. There is a well-defined probability for the helical pattern to emerge, for a given set of experimental parameters. The probability of helical patterns based on the initial concentration of the inner and outer electrolytes and on the size of the system was measured. The helical patterns were obtained from a complex interplay of the unstable precipitation modes, the reaction front motion and the noise fluctuation in the system. Although the probability depends sensitively on the noise in the system, it is not easily accessible in experiments. While changing temperature, the noise amplitude also changes but it depends on a number of other important parameters like reaction rates, diffusion constants, precipitation thresholds etc and hence it is practically impossible. Various attempts were proposed to overcome this problem and our present work implement control of noise amplitude by changing the properties of the gel [102].

In usual way the gel is treated as an inert medium in the theoretical

study of Liesegang-type experiments [20, 25, 44, 45, 117]. It is also noted that changing the concentration of the gel medium leads to precipitation patterns with distinct spacing and width laws and leads to different kind of precipitation patterns [77, 90, 96, 102]. A simple explanation for these effects is that the gel serves as a network of quenched impurities behaving as nucleation centers [122]. The density of nucleation centres are characterized by the internal surface of the gel(larger surface area implies larger nucleation density) which defines the rate of nucleation in the system [102]. This implies that the internal surface area is proportional to the amplitude of noise. When the internal surface area is large, the probability of a nucleation event is also large. To study the effects resulting from internal surface area changes, the helicoidal patterns in agarose and silica gels are examined by changing the internal surface area by varying the concentration of agarose gel and pH in the silica gel [123–125]. The experimental trends in the probability of helices formation are noted and found in terms with the argument that the internal surface serves as an a noise inducing nucleation center. The yield of helices can be increased by mixing both silica and agarose gels and the highest value of 90% yield was obtained at 0.5% agarose concentration [102].

Figure 4.4 shows that helicoidal precipitation patterns are formed in both agarose and silica gel. To investigate the cause of the internal surface area, the gel concentration in agarose and pH of silica gel are varied. In agarose gel, the internal surface is found to be proportional to the concentration of gel [123, 124]. For silica gel, the acidity (pH) influence the pore size and the internal surface area which is proportional to 1/pH [125, 126]. Varying these two parameters gives a controllable way to 'fine-tune'the property of gels in these two different gel column [102]. It is noted that in agarose

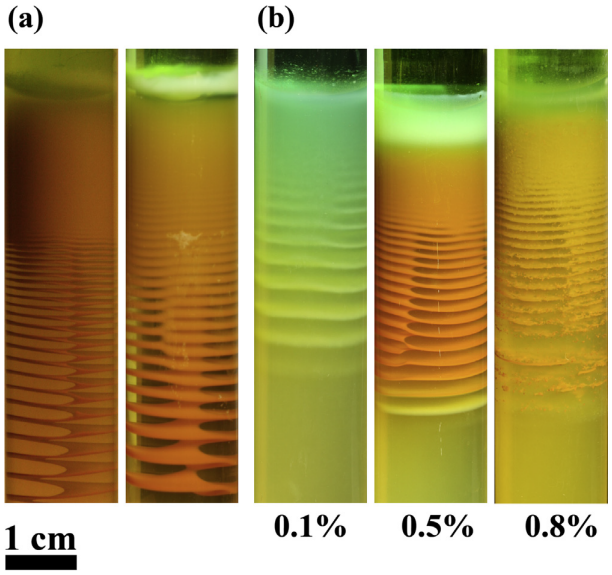


**Figure 4.4:** Various precipitation patterns in agarose, silica and mixed gels. (a) Helicoidal patterns in 1% agarose gel (left) and in silica gel having pH = 7(right). (b) Precipitation patterns in mixed gels haing pH = 7, numbers below each test tubes gives the amount of agarose in silica gels.

gel the maximum probability ($P_H = 0.6$) of the emergence of single helicoids occurs at 0.75% of gel concentration. Also parallel with this the probability of Liesegang patterns decreases with increasing concentration of gel and the probability of distorted helicoids also decreases (Figure 4.5a). For silica gel, it is found that maximum probability ($P_H = 0.5$) of helicoidal patterns occurs at pH 7 and at lower and higher pH values the probability of helices decreases (Figure 4.5b).

The theory behind formation of helix in the wake of a moving reaction front combines the properties of reaction front together with the dynamics of the pattern formation through pre- and post nucleation phenomena [102]. The phase separation mechanism is described by the noise added Cahn-Hilliard equation where its source is obtained from the reaction diffusion equations [14, 18, 20, 118]. This phase separation theory has been successful in formulating the established regularities of Liesegang patterns, and it

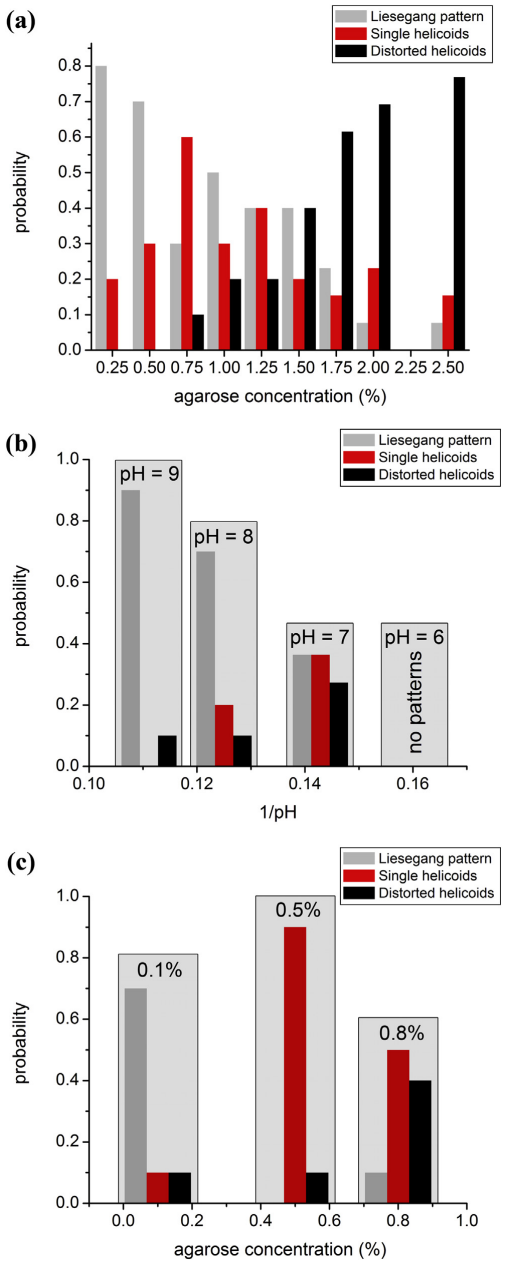


**Figure 4.5:** Variation of the probability of precipitation patterns obtained from ten experiments for each set of parameters for Liesegang patterns , single helicoids and distorted helicoids (a)in agarose gel where the concentration was changed,(b)in silica gel where the pH was varied, (c)in mixed gel where the concentration of agarose was changed

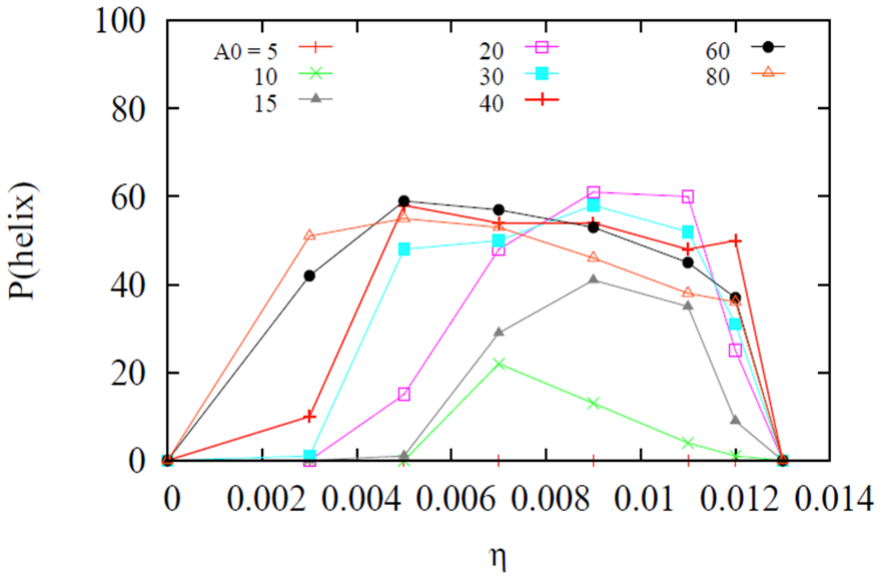


**Figure 4.6:** Probability of helices as a function of noise

also support the methods for controlling the growth of patterns by varying external fields and boundary conditions [20, 89, 127]. In precipitation systems, gel restricts the convection of solutions as well as the sedimentation of precipitate [102]. Few recent studies [77, 90, 96] have shown the strong influence of gel in pattern formation system which is in agreement with our experimental results.

In theoretical studies, the effect of gels in pattern formation becomes highly nontrivial and only a few reports in this direction [89, 96] are known. Gel helps to lower the nucleation threshold and thus provides the internal surfaces for nucleation [122]. These internal interfaces promotes nucleation in the same way as increasing noise helps achieving thresholds in the nucleation processes [102]. Since parallels may be drawn between the effects of internal interfaces and noise, the theoretical difficulties associated with gels

can be overcome by interpreting the experimental results in terms of the probability of helical pattern formation, $P_H$, to the amplitude of the noise $\eta$ (Figure 4.6). The probability of helices, $P_H$ is negligible in the $\eta \longrightarrow 0$ limit, and it increases with $\eta$ to a point that $P_H > P_L$ (probability of Liesegang patterns), and then $P_H$ decreases due to more complicated (distorted chiral and random) structures. It is clear from Figure 4.5, the same kind of changes in $P_H$ occurs if the noise is replaced by internal surface areas [102]. These arguments are phenomenological and their validity could be tested only by a more precise theory.

The variation of the purity of the supporting medium is found to strongly influence the control and engineering of precipitation patterns. Only a few experimental papers have been reported so far where the effect of the gel composition on the morphology of precipitation patterns was investigated [77, 90, 96]. In the present study, experiments were carried out in a mixed silica-agarose gel media(discussed in section 3.8) with different amounts of agarose in order to maximize the probability of helicoidal pattern formation [102]. Experimental result shows that presence of another gel can strongly influence the helicoidal pattern formation (Figure 4.4b and Figure 4.5c). As the amount of agarose increases, the probability of the emergence of helicoids increases up to 0.9 and hence the helicoids formed with certainty. Further increase in the amount of agarose leads to decrease of $P_H$, and it is still high (0.5). More explanation of this result based on experimental and theoretical assumptions is bit problematic and is due to lack of the idea on physical and chemical properties of hybrid and mixed gels [102].

Additionally, this experiment also gives an idea about the origin of helicoidal structure formation in gel system. The precipitation pattern for-

mation process can proceed in two ways [102]. First route involves the template transformation of a micro- or mesoscopic helical structure (e.g., organogel fibers) onto a new higher level structure(e.g., inorganic crystal) [111]. Second route involves the symmetry breaking where building blocks having no chiral structures self-organize into highly ordered helical/helicoidal structures [105, 128]. The general perception for emergence of chiral morphology in crystals at micrometer scale is a twisted assembly of achiral building blocks directed by mass transport. In these type of structures the diameter of the helices is almost equivalent to the size of the achiral blocks [105, 128]. The microstructure(building blocks) of helicoidal patterns in agarose are determined using SEM and observed that the precipitation helicoidal patterns contains $\sim$ 1$\mu$m size mono-disperse spherulite-like particles (Figure 4.7). These structures appear to be achiral and hence it can be concluded that the macroscopic helicoidal structures, which has four orders of larger size, emerged as a result of symmetry breaking [102].

To study the building blocks of the precipitate patterns in silica gel, dried solids from the helicoidal band regions were collected and powder XRD measurements are used to determine the particle size [102]. The powdered sample was kept in the sample holder and the XRD values were measured in a 2 $\theta$ range from $10^0$ to $80^0$ in steps of $0.1^0$. It is observed that crystals containing copper were present from the positions and intensities of the diffraction peaks (Figure 4.8). The average size of the crystallite (d) can be calculated from the line broadening using the Scherrer equation, $d = \frac{0.9\lambda}{\beta cos\theta}$, where $\lambda$ is the waelength of X-ray ($1.5406A^0$)and $\beta$ is the line broadening at half the maximum intensity (at $0.29^0$ and $0.42^0$ for the first and second peak, Figure 4.8). It is found that the average particle size is of the order of few nanometers ($\sim$ 25 nm). This result is completely different from the

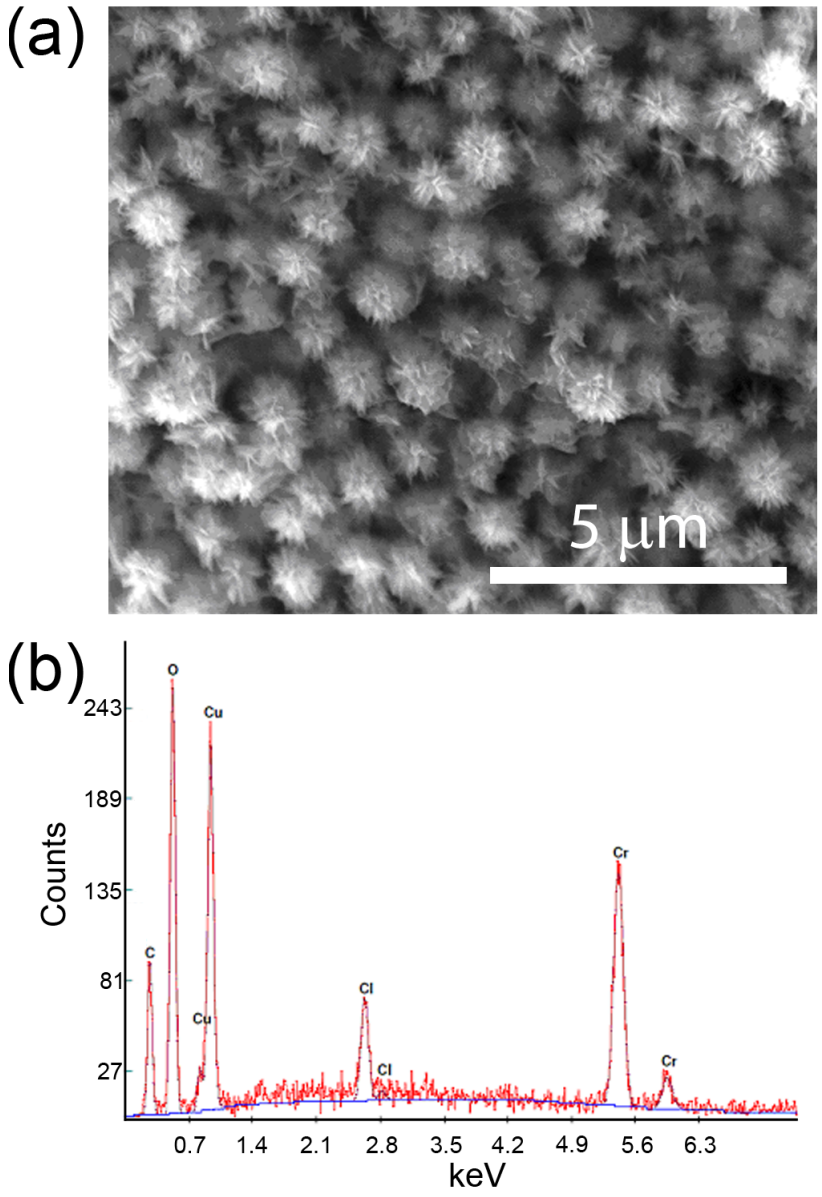


**Figure 4.7:** (a) SEM micrograph of $CuCrO_4$ helicoidal precipitations patterns in agarose gel (b) EDS spectrum of precipitation helicoid in 1% agarose gel

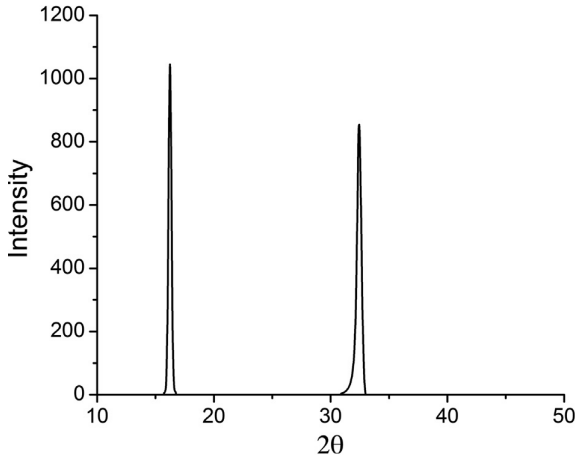


**Figure 4.8:** Powder XRD pattern of precipitation bands in silica gel. The line broadening at half the maximum intensity (which were $0.29^0$ and $0.42^0$) for the first ($2\theta = 16.23^0$) and second ($2\theta = 32.39^0$) peak, respectively

spherulites ($\sim 1\mu$ m) observed in agarose gel [102]. Thus the scale obtained in case of silica gel sets only a lower limit for the emergence of chirality.

## 4.5 Conclusion

The formation of helicoidal patterns in agarose and silica gel were studied by varying the internal surface area of the gel through its concentration and pH. The probability of the formation of helices in silica and agarose gel were found to have same trends with the maximum probability happening at intermediate internal surface areas. It is noted that the probability can be increased by mixing silica and agarose gel in a particular ratio. These results implies that the properties of the gel media on pattern formation are very relevant in understanding the process.

# Chapter 5

# Conclusion

## 5.1 Conclusion

Self-organization and pattern formation in reaction-diffusion system have significant relevance in natural and life science. Recently the interest has been increasing in both experimental and theoretical study of various types of chemically generated patterns. The important reason is that they are expected to provide new bottom-up, self-assembling technologies for engineering bulk patterns in microscopic and mescoscopic scales. A detailed study of the mechanism responsible for pattern formation is a key element in developing technological application and it helps in constructing the suitable tools for the control of the characteristics of the emerging patterns.

Controlling and designing new chemical structures are one of the most important scientific challenges in material science. Precipitation structures arise from ion or nano-particles are the main promising candidates for designing bulk structures for catalysis, energy production and electronics. The control of precipitation patterns by applying electric field opens a wide range

of new possibilities of reaction front and in designing new patterns.

Liesegang patterns are interesting research topic since simple patterns arise out of complicated reaction diffusion mechanism. Many kinds of precipitation patterns ranging from large crystals to periodic bands of similar crystalline particles to continuous colloidal precipitates have been found in gel diffusing experiments, whereas periodic banding only occurred in a narrow concentration range. Among these precipitation patterns, we explored the parameter space of the helical/helicoidal patterns. We also found that the origin of helicoidal patterns is not due to the noise and asymmetry of the initial condition but the production of unstable modes, the reaction front dynamics and the noise together leads to the formation of helicoidal precipitation patterns.

In moving boundary model of Liesegang patterns, band formation is a consequence of the phase separation phenomena taking place in the colloidal particles. It was found that the equation connecting the band width and spacing of bands strongly depends on the concentration of the reacting particles. The moving boundary theory also suggest a condition for formation of bands in reaction diffusion systems.

Liesegang and helicoidal patterns evolve from the same macroscopic conditions in both silica and agarose gel. We studied the behaviour of this process by changing the inner and outer electrolyte concentration, the temperature of the system and the test tube radius. We studied the effect of these parameters by measuring the probability of helices using ten independent experiments. We further examined the micro structure of helicoids to ascertain that the origin of macroscopic helices is in symmetry breaking and not due to the chirality of the microscopic building blocks (spherulite par-

ticles having micron size). Also it is found that the pitch of the helices are always larger than that of the bands. In mixed-gel also we observed high probability of obtaining helicoids.

We studied the helicoidal precipitation pattern formation by changing the internal interface of agarose and silica gel. Internal surface area is changed by varying by the gel concentration in agarose and pH in silica. The helices formation probability in both gel media showed same trends with the maximum probability at intermediate internal surface areas. Our results indicate that the pattern formation process strongly depends the peculiarity of the gel media. Our experiments also shows that self organized precipitation patterns can be produced in porous media under a variety of physical and chemical conditions. Even though chemical conditions in our experiments were different from what would be excepted in natural situations, our experiments showed how physical and chemical properties of a porous or permeable medium could affect the morphology of precipitates produced.

Our findings revealed that the emergence of helical and helicoidal patterns were reproducible with a finite, well-defined probability depending on the parameters of the system. The understanding of helical and helicoidal patterns in reaction diffusion systems is important since it help in designing and engineering similar helical and helicoidal and helical structures in other chemical and physical systems which could have unique physical and chemical properties.

## 5.2 Future aspects

Finding the right temperature for the emergence of helicoids is an important problem, since noise plays a major role in the emergence of helices. Also to find whether any other chemical system can reproduce the helices with high probability and hence to study the dynamics.

There is ample space for future works in this area; such as, to develop the theory of helices using the 'pulled-front' formalism and the analytical calculations of helical structure, to study the dynamics of the helicoids under the influence of external filed. If we control the emerging patterns in an external filed, we can easily engineer them under the influence of such fields. Also to check whether the helicity changes when we reverse the applied field. We know that a charged particle when placed in a crossed electric and magnetic field will follow a helical path. So here it is much interesting to check what happens when a reaction-diffusion system is placed in such fields and also to study the probability of helices/helicoids in a crossed electric and magnetic field.

# References


[1] M. Lakshmanan and S. Rajasekar. *Non Linear Dynamics - Integrability, Chaos and Patterns.* Springer-Verlag, Heidelberg, 2003.

[2] M. Daniel, K. M. Ramizhmani, and R. Sahadevan(Eds). *Non Linear Dynamics - Integrability and Chaos.* Narosa Publishing House, New Delhi, 2000.

[3] J. George and G. Varghese. *Chem. Phys. Lett.*, 362:8, 2002.

[4] J. George and G. Varghese. *J. Coll. Inter. Sic.*, 282:397, 2005.

[5] I. Bena, M. Droz, K. Martens, and Z. Racz. *J. Phy. Conds. Matter*, 19:065103, 2007.

[6] L. Galfi and Z. Racz. *Phy. Rev. A*, 38:3151, 1988.

[7] Rebecca B Hoyle. *Introduction to Pattern Formation - An introduction to methods.* Cambridge University Press, Cambridge, 2006.

[8] Lui Lam(Ed). *Introduction to Non-linear Physics.* Springer-Verlag, New York, 1997.

[9] A. Fick. *Ann. der. Physik*, 94:59, 1855.

[10] Lecture notes. www.eng.uath.edu/ lzang/images/lecture-10.pdf, 12.pdf.

[11] J. M. Shinn. PhD thesis, Colorado state University, 2012.

[12] W.D. Kingery, H.K. Bowen, and D.R. Uhlmann. *Introduction to Ceramics, $2^{nd}$ Edn.* John Wiley and Sons, New York, 1976.

[13] E. P. Favvas and A. CH. Mitropoulos. *J. Eng. Sci. Tech. Rev.*, 1:25, 2008.

[14] T. Antal, M. Droz, J. Magnin, and Z. Racz. *Phy. Rev. Lett.*, 83:2880, 1999.

[15] O. Giraldo, S. L. Brock, M. Marquez, S. L. Suib, H. Hillhouse, and M. Tsapatsis. *Nature*, 405:38, 2000.

[16] H. K. Henisch. *Periodic Precipitation.* Pergamon Press, New York, 1991.

[17] P. C. Hohenberg and B. I. Halperin. *Rev. Mod. Phys.*, 49:435, 1977.

[18] J. W. Cahn and J. E. Hilliard. *J. Chem. Phys.*, 28:258, 1958.

[19] J. W. Cahn. *Acta Metall.*, 9:795, 1961.

[20] Z. Racz. *Physica A*, 274:50, 1999.

[21] M. Lappa, D. Castagnolo, and L. Carotenuto. *Phys. A*, 314:623, 2002.

[22] B. A. Grzbowski. *Chemistry in motion:Reaction diffusion system for Micro and Nanotechnology.* John Wiley and Sons, New York, 2009.

[23] A. M. Turing. The chemical basis of morphogenesis. *Philos. Trans. R. Soc. London, Ser. B*, 237:37, 1952.

[24] M. Cross and H. Greenside. *Pattern formation and dynamics in non-equilibrium systems.* Cambridge University press, New York, 2009.

[25] D. S. Chernavskii and A. A. Polezhaev. *Physica D*, 54:160, 1991.

[26] D. G. Migues. PhD thesis, Niversidade De Santiago De Compostela, Spain, 2004.

[27] T. Karam and R. Sultan. *J. Chem. Phys.*, 412:7, 2013.

[28] J. Tabony, N. Glade, J. Demongeot, and C. Papaseit. *Langmuir*, 18:7196, 2002.

[29] I. Lagzi and D. Karman. *Chem. Phys. Lett.*, 372:831, 2003.

[30] K. Showalter, R. Noyes, and H. Turner. *J. Am. Chem. Soc.*, 101:7463, 1979.

[31] M. C. Cross and P. C. Hohenberg. *Rev. Mod. Phys.*, 65:851, 1993.

[32] A. M. Zhabotinsky. *Chaos*, 1:379, 1991.

[33] J. D. Murray. How the leopard gets its spots. *Scientific American*, 80:March, 1988.

[34] E. Karpati-Smidroczki, A. Buki, and M. Zrinyi. *Colloid. Polym. Sci.*, 273:857, 1995.

[35] J. R. I. Hepburn. *Nature*, 112:439, 1923.

[36] R. E. Liesegang. *Naturw. Wochschr.*, 11:353, 1896.

[37] W. Ostwald. *Lehrbuch der Allegemeinen Chemie.* Engelmann, Lieipzig, 1897.

[38] H. W. Morse and G. W. Pierce. *Z. Phys. Chem.*, 45:589, 1903.

[39] K. Jablczynski. *Bull. Soc. Chim Fr.*, 33:1592, 1923.

[40] A. Packter and R. Matalon. *J. Coll. Sci.*, 10:46, 1955.

[41] C. Wagner. *J. Coll. Sci.*, 5:85, 1950.

[42] S. Prager. *J. Chem. Phys.*, 25:279, 1956.

[43] J. Hallett V.W Keller, C.V McKnight. *J. Cryst.Gr*, 49:458, 1980.

[44] G. T. Dee. *Physica D*, 23:340, 1986.

[45] M. E. Levan and J. Ross. *J. Phys. Chem.*, 91:6300, 1987.

[46] S. Shinohara. *J. Phys. Soc. Jpn.*, 29:1073, 1970.

[47] R. Lovett, P. Ortoleve, and J. Ross. *J. Chem. Phys.*, 69:947, 1978.

[48] M. Flicker and J. Ross. *J. Chem. Phys.*, 60:3458, 1974.

[49] J. D. Gunton and M. Droz. *Lecture notes in Physics*, volume 83. 1983.

[50] T. Antal, M. Droz, J. Magnin, A. Pekalski, and Z. Racz. *J. Chem. Phys.*, 114:3770, 2001.

[51] R. J. Glaber. *J. Math. Phy.*, 4:294, 1963.

[52] K. Kawasaki. *Phy. Rev.*, 145:224, 1966.

[53] Q. Peng, J.-G. Wu, R. D. Soloway, T.-D. Hu, W.-D. Huang, Y.-Z. Xu, L.-B. Wang, X.-F. Li, W.-H. Li, D.-F. Xu, and G.-X. Xu. *Inc. Biospect.*, 3:195, 1997.

[54] S. C. Muller, S. Kai, and J. Ross. *Science*, 216:635, 1982.

[55] R. E. Liesegang. *Z.Phys.Chem.*, 88:1, 1914.

[56] A. A. Polezhaev and S. C. Muller. *Chaos*, 4:631, 1994.

[57] T. Karam, H. El-Rassy, and R. Sulatn. *J.Phys. Chem. A*, 115:2994, 2011.

[58] P. Hantz. *J. Phys. Chem. B.*, 104:4266, 2000.

[59] B. Chopaed, M. Droz, J. Magnin, Z. Racz, and M. Zrinyi. *J. Phys. Chem. A*, 103:1432, 1999.

[60] I. Lagzi, P. Papai, and Z. Racz. *Chem. Phys. Lett.*, 433:286, 2007.

[61] M. A. Einarsrud, F. A. Maa, A. Hansen, M. Kirkedelen, and J. Samseth. *Phys.Rev. E*, 57:6, 1998.

[62] J. Petruska and L. M. Barge. *Chem. Phys. Lett.*, 556:315, 2013.

[63] L. Badr and R. Sultan. *J. Phy. Chem. A*, 113:6581, 2009.

[64] N. Hilal and R. Sulatn. *Chem. Phys. Lett.*, 373:183, 2003.

[65] A. Volford, F. Izsak, M. Ripszam, and I. Lagzi. *J. Phys. Chem. B*, 110:4535, 2006.

[66] R. F. Sultan, N. K. Al-Kassem, A. H. Sultan, and N. N. Salem. *Phys. Chem.Chem. Phys.*, 2:3155, 2000.

[67] R. F. Sultan. *Phys. Chem. Chem. Phys.*, 4:1253, 2002.

[68] H. J. Kurg, K. H. Jacob, and S. Dietrich. *Fractals and Dynamic Systems in Geoscience*. Springer Verlag, Berlin, 1994.

[69] J. George and G. Varghese. *J. Materials Sci.*, page 5557, 2005.

[70] R. Sultan and R. Halabieh. *Chem. Phys. Lett.*, 332, 2000.

[71] I. Lagzi and F. Izsak. *Phys. Chem. Chem. Phys.*, 5:4144, 2003.

[72] L. Badr, H. El-Rassy, S. El-Joubeily, and R. Sultan. *Chem. Phys. Lett.*, 492:35, 2010.

[73] I. Bena, M. Droz, I. Lagzi, K. Martens, Z. Racz, and A. Volford. *Phys. Rev. Lett.*, 101:075701, 2008.

[74] T. Isemura and S. Hirotsu. *Bull. Chem. Soc. Japan*, 14:179, 1939.

[75] A. Buki, E. K. Smidroczki, and K. Zrinyi. *Progs. Colld. Polym. Sci*, 20:110, 1996.

[76] L. M. Barge, K. H. Nealson, and J. Petruska. *Chem. Phys. Lett.*, 293:340, 2010.

[77] I. Lagzi and Ueyama. *Chem. Phy. Lett.*, 468:188, 2009.

[78] V. Holba and F. Fusek. *Collect. Czech. Chem. Commun.*, 65:1438, 2000.

[79] L. Jahnke and J. W. Kantelhardt. *Europhysics Lett.*, 84:48006, 2008.

[80] S. Thomas, G. Varghese, and I. Lagzi. *Pramana*, 78:135, 2012.

[81] P. Strickholm J. Chadam P. Ortoleva R. Feeney, S. L. Schmidt. *J. Chem. Phys.*, 78:293, 1983.

[82] V. V. Slyozov I. M. Lifshitz. *J. Phys. Chem. Solids*, 19:35, 1961.

[83] G Venzl. *J. Chem. Phys.*, 77:1308, 1982.

[84] G. Venzl. *J. Chem. Phys.*, 85:2006, 1986.

[85] G. Varghese J. George. *J. Coll. Interface Sci.*, 282:397, 2005.

[86] D. A. B Young. *Coll. Polym. Sci.*, 278:464, 2000.

[87] H. K. Henisch. *Crystals in gels and Liesegang rings.* Cambridge University Press, Cambridge, 1988.

[88] I. Lagzi and D. Ueyama. *Chem. Phys. Lett.*, 468:188, 2009.

[89] T. Antal, I. Bena, M. Droz, K. Martens, and Z. Racz. *Phys. Rev. E*, 76:046203, 2007.

[90] A. Toramaru, T. Harada, and T. Okamura. *Physica D*, 183:133, 2003.

[91] C. D. Viljoen, B. D. Wingfield, and M. J. Wingfield. *Biotech. Tech.*, 7:723, 1993.

[92] S. C. Muller, S. Kai, and J. Ross. *J Phys. Chem.*, 8:4078, 1982.

[93] A. H. Sharbaugh lll and A. H. Sharbaugh. *J.Chem. Edu.*, 6:589, 1989.

[94] P. Hantz. *J. Chem. Phys.*, 117:2002, 14.

[95] J. George, I. Paul, P.A. Varughese, and G. Varghese. *Pramana*, 60:1259, 2003.

[96] I. Lagzi. *Langmuir*, 28:3350, 2012.

[97] A. Volford, F. Izsak, M. Ripszam, and I. Lagzi. *Langmuir*, 23:3, 2007.

[98] I. Lagzi. *Phys. Chem. Chem. Phys.*, 4:1268, 2002.

[99] M. Ripszam, A. Nagy, A. Volford, F. Izsak, and I. Lagzi. *Chem. Phys. Lett.*, 414:384, 2005.

[100] C. B. Hurd and H. A. Letteron. *J. Phy. Chem.*, 38:663, 1932.

[101] G. H. Alexander. *J.Amer. Chem. Soc.*, 75:5655, 1953.

[102] S. Thomas, G. Varghese, D. Bardfalvy, I. Lagzi, and Z. Racz. *Chem. Phys. Lett.*, 599:159, 2014.

[103] https://en.wikipedia.org/wiki/Agarose.

[104] P. X. Gao, Y. Ding, W. J. Mai, W. L. Hughes, C. S. Lao, and Z. L. Wang. *Science*, 309:1700, 2005.

[105] H. Imai and Y. Oaki. *Angew. Chem. Int. Ed.*, 43:1363, 2004.

[106] D. S. Su. *Angew. Chem. Int. Edit.*, 50:4747, 2011.

[107] S. C. Muuller, S. Kai, and J. Ross. *Science*, 216:635, 1982.

[108] R. V. Suganthi, E. K. Girija, S. N. Kalkura, H. K. Varma, and A. Rajaram. *J. Mater. Sci.-Mater M.*, 20:131, 2009.

[109] P. Savadjiev, G. J. Strijkers, A. J. Bakermans, E. Piuze, S. W. Zucker, and K Siddiqi. *Proc. Nat. Acad. Sci. USA*, 109:9248, 2012.

[110] J. M. Lehn, A. Rigault, J. Siegel, J. Harrowfield, B. Chevrier, and D. Moras. *Proc. Natl. Acad. Sci. USA*, 84:2565, 1987.

[111] J. H. Jung, Y. Ono, K. Hanabusa, and S. Shinkai. *J. Am. Chem. Soc.*, 122:5008, 2000.

[112] S. C. Muller and J. Ross. *J. Phys. Chem. A*, 107:7997, 2003.

[113] T. Antal, M. Droz, J. Magnin, Z. Racz, and M. Zrinyi. *J. Chem. Phys.*, 109:9479, 1998.

[114] C. Leger, F. Argoul, and M. Z. Bazant. *J. Phys. Chem. B*, 103:5841, 1999.

[115] C. N. Baroud, F. Okkels, L. Menetrier, and P. Tabeling. *Phys. Rev. E*, 67:060104, 2003.

[116] D. S. Chernavskii, A. A. Polezhaev, and S. C. Muller. *Physica D*, 54:160, 1991.

[117] M. Chacron and I. A. L. Heureux. *Phys. Lett. A*, 263:70, 1999.

[118] A. Volford, I. Lagzi, F. Molnar, and Z. Racz. *Phys. Rev. E*, 80:055102, 2009.

[119] P. Hantz and I. Bir. *Phys. Rev. Lett.*, 96:088305, 2006.

[120] E. M. Foard and A. J. Wanger. *Phys. Rev E*, 85:011501, 2012.

[121] R. E. Liesegang. Ueber einige eigenschaften von gallerten. *Naturwiss. Wochenschr.*, 11:353, 1896.

[122] J. Rahbani, A.R. Behzad, N.M. Khashab, and M. Al-Ghoul. *Electrophoresis*, 34:405, 2013.

[123] M. Maaloum, N. Pernodet, and B. Tinland. *Electrophoresis*, 19:1606, 1998.

[124] M. Maaloum, N. Pernodet, and B. Tinland. *Electrophoresis*, 18:55, 1997.

[125] S. Ulku, D. Balkose, and H. Baltacboglu. *Colloid Polym. Sci.*, 271:709, 1993.

[126] D. Dollimore and G.R. Heal. *J. Appl. Chem.*, 12:445, 1962.

[127] I. Bena, M. Droz, I. Lagzi, K. Martens, Z. Racz, and A. Volford. *Phys. Rev. Lett.*, 101:075701, 2008.

[128] Y. Oaki and H. Imai. *J. Am. Chem. Soc.*, 126:9271, 2004.

# Appendix I

## A.1 Derivation of $\frac{\partial a}{\partial t}$

For the reaction $A + B \longrightarrow C$, the reaction diffusion equation has the form

$$\frac{\partial a}{\partial t} = D_A \Delta a - kab \tag{A.1}$$

$$\frac{\partial b}{\partial t} = D_B \Delta b - kab \tag{A.2}$$

For $C$ assuming phase separation mechanism, we get

$$\frac{\partial c}{\partial t} = -\lambda \Delta [\epsilon c - \gamma c^3 + \sigma \Delta c] + kab \tag{A.3}$$

Using the method of rescaling we can normalise one or more parameters in an equation equal to particular value such as 0 or 1. These change of variables can create additional factors which are mere constants. Thus the new parameters in above euations are $t \to t'\tau, x \to lx', a \to b_0 a', c \to b_0 c'$, where $\tau$ and$b_0$ are constants and hence the equations A.1 and A.2 becomes,

$$\frac{\partial a'}{\partial t'} = \frac{D_A \tau}{l^2} \Delta' a' - b_0 \tau k a' b' \tag{A.4}$$

$$\frac{\partial b'}{\partial t'} = \frac{D_B \tau}{l^2} \Delta' b' - b_0 \tau k a' b' \tag{A.5}$$

Taking $\frac{D_B \tau}{l^2} = 1$ and $b_0 \tau k = 1$ Then above equations become,

$$\frac{\partial a'}{\partial t'} = \frac{D_A}{D_B} \Delta' a' - a' b' \tag{A.6}$$

$$\frac{\partial b'}{\partial t'} = \Delta' b' - a' b' \tag{A.7}$$

Assuming $D_A = D_B = 1$ and dropping all the prime sign, we get equation

$$\frac{\partial a}{\partial t} = \Delta a - ab \tag{A.8}$$

$$\frac{\partial b}{\partial t} = \Delta b - ab \tag{A.9}$$

Similarly we can do for $C$ particles also.

# Appendix II

## B.1 Publications

Chemical Physics Letters 599 (2014) 159–162

Contents lists available at ScienceDirect

Chemical Physics Letters

journal homepage: www.elsevier.com/locate/cplett

# Helicoidal precipitation patterns in silica and agarose gels

Shibi Thomas [a], George Varghese [b], Dóra Bárdfalvy [c], István Lagzi [c,*], Zoltán Rácz [d]

[a] Department of Physics, University of Calicut, Kerala, India
[b] Kerala State Council for Science Technology and Environment, Trivandrum, Kerala, India
[c] Department of Physics, Budapest University of Technology and Economics, 1111 Budapest, Hungary
[d] MTA-ELTE Theoretical Physics Research Group, Budapest, Hungary

ARTICLE INFO

*Article history:*
Received 28 January 2014
In final form 17 March 2014
Available online 24 March 2014

ABSTRACT

Helicoidal patterns grown in agarose and silica gels were studied using reaction–diffusion–precipitation processes with components $CuCl_2/K_2CrO_4$. We measured the probability $P_H$ of the emergence of helicoids as the internal surface area of the gels was varied by changing the concentration for agarose and by modifying pH for silica. In addition, the effects of mixing the two gels were also investigated. Our main result is that the surface area effects parallel the effects of noise, namely increasing the surface area initially enhances the formation of helicoids but further increase leads to downturn in $P_H$ due to proliferation of random patterns.



## 1. Introduction

Helical structures can be observed in a wide variety of natural and man-made systems [1–9]. Their emergence from a homogeneous background is a basic and rather complex problem due to the symmetry breaking that takes place at the initial stages of their evolution. Interest in chiral morphology, however, comes also from engineering applications since chirality is known to affect the physical properties of materials [10]. In particular, understanding and controlling helical structures are expected to be relevant in developing bottom-up fabrication techniques using nonlinear chemical kinetics [11,12].

Recently, we carried out a series of experimental and theoretical studies [9,13,14] in order to clarify how helices were formed in Liesegang-type setups where pattern emerged in the wake of a reaction–diffusion front [15,16]. We found that the formation of helical and helicoidal patterns was reproducible but had a probabilistic aspect. Namely, for a given set of experimental parameters, there was a well-defined probability for the helical pattern to emerge. The dependence of the probability on the initial concentration of the inner- and outer electrolytes, and on the size of the system was measured and compared successfully with a theory [9]. The theory suggested that the helices emerged from a complex interplay among the unstable precipitation modes, the motion of the reaction front, and the noise in the system. Unfortunately, the noise is not easily accessible in experiments although the probability depends sensitively on it. For example, changing temperature is not a practical way of changing the noise amplitude since it simultaneously changes a number of important parameters (diffusion constants, reaction rates, precipitation thresholds, etc.) and the delineation of the various effects is practically impossible. The present work grew out of our attempts to overcome this problem and implement controlled noise by changing the properties of the gel.

In general, the gel is considered as an inert background in the theoretical treatments of Liesegang-type experiments [17–21]. At the same time, it is known that changing the concentration or the chemical composition of the gel leads to patterns with distinct spacing- and width laws and, frequently, to qualitatively different precipitation phenomena [22–24]. The simplest rationalization of these effects is that the gel provides a network of quenched impurities acting as nucleation centers [25]. Then the internal surface of the gel defines the density of nucleation centers (larger surface area corresponding to larger density of nucleation centers) which governs the general nucleation rate in the system. This view suggests that the internal surface area is roughly proportional to a noise-amplitude: the larger it is the larger is the probability of a nucleation event.

In order to see the effects resulting from internal surface area changes, we examined helicoidal patterns in agarose and silica gels and varied the internal surface area by changing the gel concentration in agarose gel and by varying the pH in the silica gel [26–28]. We measured the trends in the probability of the emergence of helices and found that they were in agreement with the interpretation that the internal surface acts as an effective noise inducing nucleation. We also searched for ways of maximizing the yield of helices by mixing agarose and silica gels, and the maximum value

* Corresponding author. Fax: +36 1 463 1896.
*E-mail address:* lagzi@vuk.chem.elte.hu (I. Lagzi).

http://dx.doi.org/10.1016/j.cplett.2014.03.041
0009-2614/

of 90% yield was obtained at 0.5% agarose concentration. The mixing results, however, do not readily submit to a simple interpretation in terms of an effective noise.

## 2. Experimental

Agarose gel was prepared by addition of a prescribed amount of agarose powder (Type1, Sigma Aldrich) to a 0.01 M solution of $K_2CrO_4$ (Merck). The mixture was heated to 90 °C under continuous stirring until a homogenous solution was obtained. The resulting solution was then poured into test tubes for 3 h.

We prepared silica gel by the following method. A solution was prepared from sodium metasilicate (Merck) and potassium chromate (Merck) in such way that the obtained solution had relative density of 1.03 and the concentration of potassium chromate was 0.01 M. Gelation was induced by decreasing the pH of the solution by adding HCl drop by drop. We also prepared mixed silica–agarose gel with various amounts of agarose by adding hot agarose gel solution to the silica gel prior the polymerization. We poured these solutions in test tubes and kept them undisturbed for 24 h till the gelation process was completed.

After gelation process we gently poured the solution of copper (II) chloride (Merck, 0.5 M) on the top of the gel. The test tubes were closed and kept undisturbed apart from visually observing the appearance of the precipitation pattern. The experiments were carried out at room temperature (27 ± 0.3 °C).

## 3. Results and discussion

### 3.1. Comparison of helicoidal patterns in agrose and silica gel

Experimental results displayed in Figure 1a indicate that helicoidal patterns are formed not only in agarose as shown previously [9] but also in silica gel. In order to investigate the effect of the internal surface area, we changed the gel concentration in agarose gel and the pH of the silica gel. In agarose, the internal surface of the gel can be considered to be proportional to the gel concentration [26,27]. On the other hand, in silica gel, acidity (pH) affects the pore size and the internal surface area, and the internal surface area is proportional to 1/pH [28,29]. Changing these two parameters gives a simple and experimentally controllable way to 'fine-tune' the gel property in these two chemically different gels. In agarose gel we found that the probability ($P_H$) of the emergence of single helicoids has a maximum ($P_H = 0.6$) at gel concentration of 0.75%, meanwhile the probability of Liesegang patterns decreases, parallel with this, the probability of distorted helicoids decreases, with increasing gel concentration (Figure 2a). In case of silica gel we have also maximum probability of getting helices ($P_H = 0.5$) at pH 7. This probability decreases rapidly at lower and higher pH (Figure 2b).

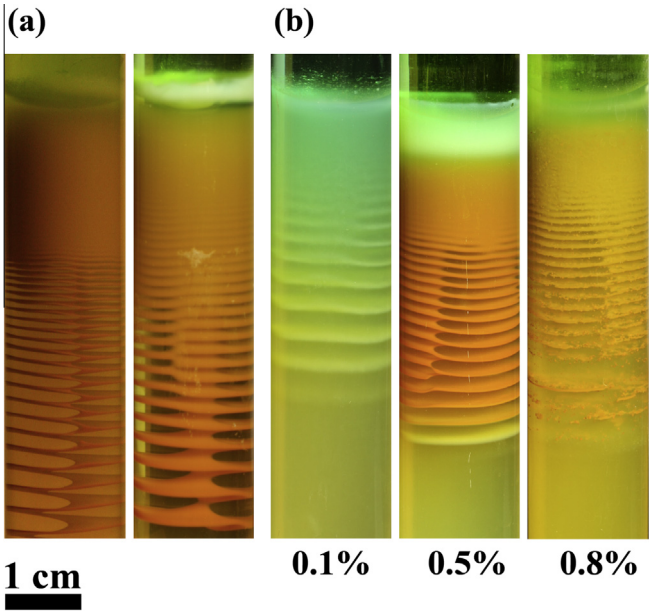


**Figure 1.** Precipitation patterns in agarose, silica and mixed silica–agarose gels. (a) Helicoids in agarose gel (1%; left) and in silica gel (pH = 7; right). (b) Patterns in mixed silica–agarose gels (pH = 7), numbers below the test tubes indicate the amount of agarose in silica gels. The concentration of the outer ($CuCl_2$) and inner ($K_2CrO_4$) electrolytes were 0.5 M and 0.01 M, respectively.

We can now discuss how to fit our experimental findings into a theoretical framework. The theory of helix formation in the wake of a front combines the properties of moving reaction front with the dynamics of the generation of precipitation pattern through pre- and post nucleation processes [9,14]. Technically, reaction–diffusion equations provide the source for the phase separation described by the Cahn–Hilliard equation with noise added [9,21,30–32]. This theory has been successful in reproducing the established regularities of Liesegang patters, and it also provided guidance in developing methods of controlling patterns by external fields and boundary conditions [21,33,34]. As far as the gel is concerned in precipitation systems, the usual argument is that the gel just prevents the convection of solutions and the sedimentation of precipitate. However, recent works [22–24] have shown transparently that the gel has a strong influence on pattern formation in agreement with the present experiments.

Introducing gels in the theories is highly nontrivial and we know only a few attempts in this direction [24,35]. Basically, the gel provides internal interfaces where the nucleation threshold is lowered [25]. Thus internal surfaces facilitate nucleation in the same way as increasing noise helps crossing thresholds in the nucleation processes. Assuming that parallels may be drawn between the effects of internal surfaces and noise, we can shortcut the theoretical difficulties, and interpret our experiments in terms of earlier results relating the probability of the emergence of the helices, $P_H$, to the amplitude of the noise $\eta$ [9]. As can be seen in Figure 3b of [9], $P_H$ is negligible in the $\eta \to 0$ limit (Liesegang bands dominate; $P_L \approx 1$), it increases with $\eta$ to a point that $P_H > P_L$, and then $P_H$ declines because more complicated (distorted chiral and random) structures take over. As we can see in Figure 2, the same sequence of changes in $P_H$ occurs in the present experiments if only the noise is replaced by internal surface areas (appropriately interpreted through concentration of the agarose or 1/pH in case of silica). The above arguments are of course phenomenological and their validity could be judged only by developing of a more precise theoretical approach.

### 3.2. Effect of 'chemical impurity' in a mixed gel medium

One of the interesting aspect of the control and engineering of precipitation patterns is the variation of the purity (chemical composition) of the supporting medium. To our knowledge, there are only a few experimental papers where the effect of the gel composition/impurity on the morphology of patterns was investigated [22–24]. We carried out experiments in a mixed silica–agarose gel media containing various amounts of agarose in order to maximize the probability of the emergence of helicoids. Our experiments show that introducing the other gel can dramatically affect the formation of helicoids (Figures 1b and 2c). Increasing amount of agarose increases the probability of the emergence of helicoids up to 0.9, which means that helicoids practically appear with certainty. Further increase of the amount of agarose results in a decrease of $P_H$, however, it is still a high value (0.5).

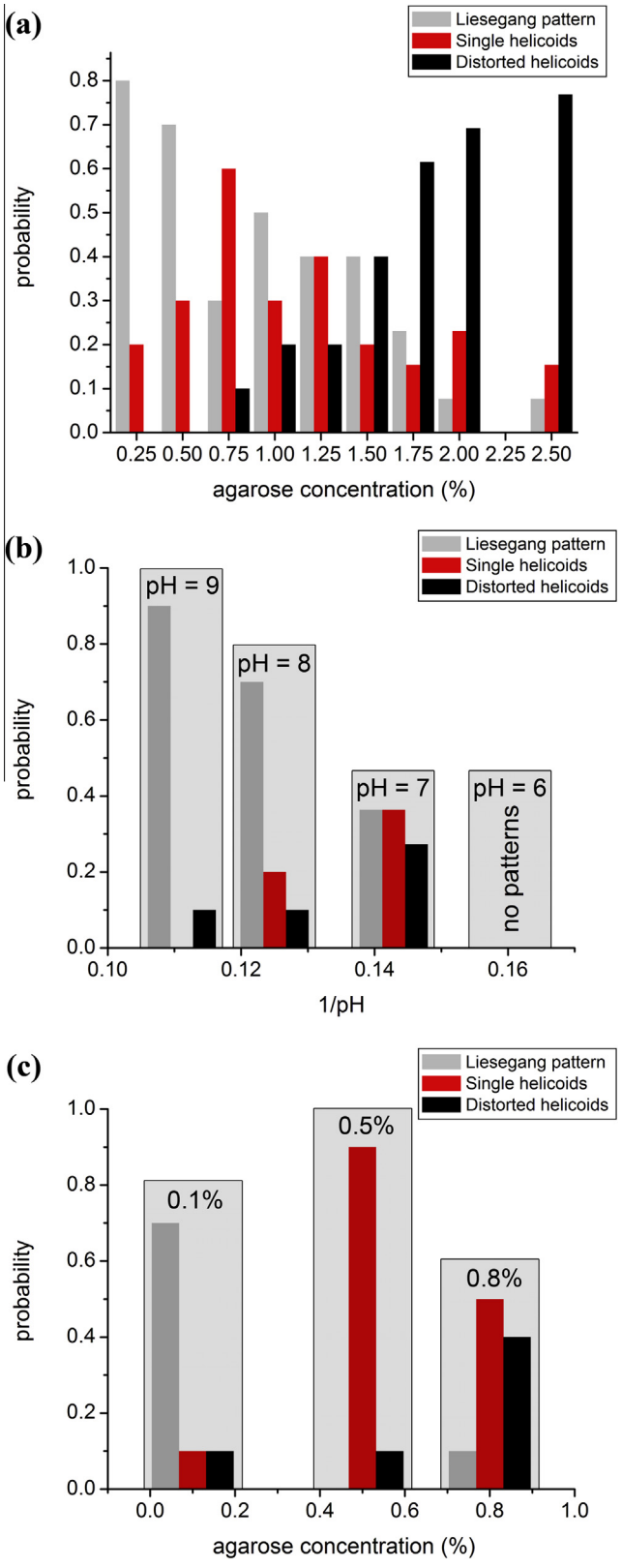


**Figure 2.** Dependence of the probability of the emergence of Liesegang patterns (obtained from 10 experiments for each set of parameters), single helicoids and distorted helicoids in agarose gel where the agarose concentration was varied (a), in silica gel with the pH changed (b) and in mixed silica–agarose gel, where the agarose concentration was varied (c).

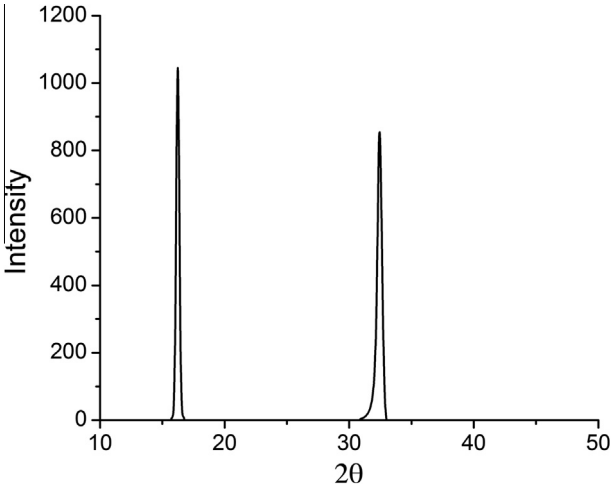


**Figure 3.** Powder XRD spectrum of precipitate particles collected from precipitation bands in silica gel. The wavelength of the X-ray was 1.5406 Å and the line broadening at half the maximum intensity was 0.29° and 0.42° for the first ($2\Theta$ = 16.23°) and second ($2\Theta$ = 32.39°) peak, respectively.

Explanation of this finding based on experimental and theoretical assumptions is problematic due to lack of the knowledge on physical and chemical properties of hybrid and mixed gels.

### 3.3. Scale of the building blocks

An interesting question related to helix formation is at what scale the symmetry breaking occurs. A lower limit of this scale is the size of the particles in the precipitate. In a previous study [13], we showed that, in agarose gel, the bulk precipitate of copper dichromate consists of ~1 μm particles (spherulites). Here we wanted to gather information on building blocks of the precipitate in silica gel. Therefore, we collected and dried solids from the helicoidal band regions and used powder XRD measurements to determine the particle size. The powdered sample was mounted on the sample holder and the XRD data were measured in a $2\Theta$ range from 10° to 80° in steps of 0.1°. We found the presence of crystals containing copper from the positions and intensities of the diffraction peaks (Figure 3). We estimated the average size of the crystallite ($d$) from the line broadening using the Scherrer equation, $d = \frac{0.9\lambda}{\beta \cos\Theta}$, where $\lambda$ is the X-ray wavelength (which was 1.5406 Å) and $\beta$ is the line broadening at half the maximum intensity (which were 0.29° and 0.42° for the first and second peak, respectively). We obtained the order of few tens of nanometers (~25 nm) for the average particle size. This is markedly different from the scale of the spherulites (~1 μm) observed in agarose gel [13]. We should emphasize, however, that the scale found above sets only a lower limit for the scale of the emergence of chirality.

## 4. Conclusion

We investigated the formation of helicoidal precipitation patterns in silica and agarose gel by varying the internal surface area of the gel through its concentration and pH. The probability of the emergence of helices in agarose and silica gel were found to follow similar trends with the maximum probability occurring at intermediate internal surface areas. We also found that the probability may be significantly increased ($P_H$ = 0.9) by mixing silica and agarose in an appropriate ratio. These results strongly suggest that the

properties of the gel media on pattern formation are highly relevant in understanding the process.

Our XRD experiments revealed the presence of particles of the size of ~20–30 nm in the precipitation bands of the silica gel. This finding suggests that the supporting media may have a more pronounced effect on particle size than it has been believed, and nanoparticles with various sizes can be produced in this novel way using reaction–diffusion processes.

## Acknowledgments

This research was supported by the Hungarian Research Fund (OTKA K104666 and NK100296), CSIR - Government of India for SRF Fellowship and by the European Union and the State of Hungary, co-financed by the European Social Fund in the framework of TÁMOP 4.2.4.A/1-11-1-2012-0001 'National Excellence Program'. We thank J. Kubica and Z.E. Horváth for the helpful discussions.

## References

[1] S.C. Müller, S. Kai, J. Ross, Science 216 (1992) 635.
[2] R.V. Suganthi, E.K. Girija, S.N. Kalkura, H.K. Varma, A. Rajaram, J. Mater. Sci. Mater. 20 (2009) 131.
[3] O. Giraldo, S.L. Brock, M. Marquez, S.L. Suib, H. Hillhouse, M. Tsapatsis, Nature 405 (2000) 38.
[4] P.X. Gao, Y. Ding, W.J. Mai, W.L. Hughes, C.S. Lao, Z.L. Wang, Science 309 (2005) 1700.
[5] H. Imai, Y. Oaki, Angew. Chem. Int. Ed. 43 (2004) 1363.
[6] Y. Fukui, S. Nakada, K. Fujimoto, RSC Adv. 4 (2014) 6027.
[7] J.H. Jung, Y. Ono, K. Hanabusa, S. Shinkai, J. Am. Chem. Soc. 122 (2000) 5008.
[8] Y. Oaki, H. Imai, J. Am. Chem. Soc. 126 (2004) 9271.
[9] S. Thomas, F. Molnár, I. Lagzi, Z. Rácz, Phys. Rev. Lett. 110 (2013) 078303.
[10] S.-Y. Ju, Nat. Nanotechnol. 3 (2008) 356.
[11] B.A. Grzybowski, K.J.M. Bishop, C.J. Campbell, M. Fialkowski, S.K. Smoukov, Soft Matter 1 (2005) 114.
[12] G. Varghese, M.A. Ittyachen, J. Mat. Sci. Lett. 11 (1992) 916.
[13] S. Thomas, F. Molnár, Z. Rácz, I. Lagzi, Chem. Phys. Lett. 577 (2013) 38.
[14] S. Thomas, I. Lagzi, F. Molnár, Z. Rácz, Phys. Rev. E 88 (2013) 022141.
[15] R.E. Liesegang, Naturwiss. Wochenschr. 11 (1896) 353.
[16] H.K. Henisch, Crystals in Gels and Liesegang Rings, Cambridge University Press, Cambridge, 1988.
[17] G.T. Dee, Phys. Rev. Lett. 57 (1986) 275.
[18] M.E. LeVan, J. Ross, J. Phys. Chem. 91 (1987) 6300.
[19] D.S. Chernavskii, A.A. Polezhaev, S.C. Muller, Phys. D 54 (1991) 160.
[20] M. Chacron, I. L'Heureux, Phys. Lett. A 263 (1999) 70.
[21] Z. Rácz, Phys. A 274 (1999) 50.
[22] A. Toramaru, T. Harada, T. Okamura, Phys. D 183 (2003) 133.
[23] I. Lagzi, D. Ueyama, Chem. Phys. Lett. 468 (2009) 188.
[24] I. Lagzi, Langmuir 28 (2012) 3350.
[25] J. Rahbani, A.R. Behzad, N.M. Khashab, M. Al-Ghoul, Electrophoresis 34 (2013) 405.
[26] M. Maaloum, N. Pernodet, B. Tinland, Electrophoresis 19 (1998) 1606.
[27] M. Maaloum, N. Pernodet, B. Tinland, Electrophoresis 18 (1997) 55.
[28] S. Ülkü, D. Balköse, H. Baltacboğlu, Colloid Polym. Sci. 271 (1993) 709.
[29] D. Dollimore, G.R. Heal, J. Appl. Chem. 12 (1962) 445.
[30] J.W. Cahn, J.E. Hilliard, J. Chem. Phys. 28 (1958) 258.
[31] T. Antal, M. Droz, J. Magnin, Z. Rácz, Phys. Rev. Lett. 83 (1999) 2880.
[32] A. Volford, I. Lagzi, Phys. Rev. E 80 (2009) 055102(R).
[33] I. Bena, M. Droz, I. Lagzi, K. Martens, Z. Rácz, A. Volford, Phys. Rev. Lett. 101 (2008) 075701.
[34] T. Antal, I. Bena, M. Droz, K. Martens, Z. Rácz, Phys. Rev. E 76 (2007) 046203.
[35] L. Chen, Q. Kang, Y.L. He, W.Q. Tao, Langmuir 28 (2012) 11745.

PRAMANA — journal of physics



Vol. 78, No. 1
January 2012
pp. 135–145

# The width of Liesegang bands: A study using moving boundary model and simulation

SHIBI THOMAS[1], GEORGE VARGHESE[1,*] and ISTVÁN LAGZI[2,3]

[1]Department of Physics, University of Calicut, Malappuram 673 635, India
[2]Department of Meteorology, Eötvös University, H-1117 Pázmány sétány 1/A, Budapest, Hungary
[3]Department of Chemical and Biological Engineering, Northwestern University, 2145 Sheridan Road, Evanston, Illinois 60208, USA
*Corresponding author. E-mail: gvphysics@gmail.com

MS received 24 September 2010; revised 16 June 2011; accepted 28 June 2011

**Abstract.** The pattern formation in reaction–diffusion systems was studied by invoking the provisions contained in the moving boundary model. The model claims that the phase separation mechanism is responsible for separating the colloidal phase of precipitants into band and non-band regions. The relation between the band separation and its width are invariably related to the concentration of the reacting components. It was observed that this model provides critical condition for the band formation in semi-idealized diffusion systems. An algorithm for generating the band structure was designed, and the simulated pattern shows a close resemblance with the experimentally observed ones.

**Keywords.** Reaction–diffusion systems; Liesegang bands; pattern formation; moving boundary; simulation.

**PACS Nos 64.75.Xc; 64.75.Yz**

## 1. Introduction

Nature has a wide storage of colourful patterns which are originated mostly by self-organized processes without the intervention of external templates [1]. The patterns tell us much about the dynamics, both at the macroscopic as well as at the microscopic levels of the underlying system. Because of its importance, pattern formation has received wide attention from people working in different areas of biology, chemistry, physics and geology. The spatio-temporal patterns observed in many reaction–diffusion systems provide an excellent area to study these phenomena, and the advanced computer techniques give scope for simulating the structures based on theoretical models. The quasiperiodic structure, reported first by Liesegang in 1896, is regaining its importance due to its applicability in engineering mesoscopic and microscopic structures [2]. These studies are opening up new possibilities in the control and design of structures by reversing the processing

**DOI: 10.1007/s12043-011-0204-2**; ***e*Publication: 12 December 2011**

order from the bottom-up approach to top-down methods in microelectronic device fabrications [3]. In recent years the interest in self-organized structures is growing, triggered by the idea of cheap and fast production of nanoscaled devices. One of the promising effects for obtaining such devices in Liesegang pattern formation is based on reaction and diffusion processes. In addition, the Liesegang phenomenon is an interesting research topic on its own due to the simple patterns arising out of complicated reaction and diffusion processes. A scientific understanding of pattern formation seems to be one of the most exciting aspects of non-linear dynamics.

The diffusion of a chemical reagent into a medium, most generally a gel medium, and the subsequent precipitation with another component that the gel medium contains, will generate periodic patterns under favourable conditions. Pattern formation in a reaction–diffusion system is considered as a self-organization phenomenon and the patterns are stationary in the sense that the bands are 'locked' in the position once they are formed. In this context, some researchers have considered the Liesegang structures as Turing-type patterns [4–10]. Since the 1952 theoretical work of Alan Turing, it is known that self-activated reactions with long-range inhibition process can spontaneously lead to the formation of stationary symmetry breaking patterns [11]. Under appropriate conditions, a spatially homogeneous state can be stable in the absence of diffusion and unstable in the presence of diffusion. An appropriate reaction network is capable of exhibiting spatially inhomogeneous state, i.e. pattern. The phenomenon in which diffusion destabilizes a spatially homogeneous steady state is termed as diffusion-driven or Turing instability. But many experimental observations support the argument that the initial form of the precipitants appears as colloids and its coagulation plays a vital role during the early stages of Liesegang ring formation [12,13]. Flicker and Ross [14] describe the mechanism of chemical instability as a reason for the periodic pattern formation. In mean-field theories, reaction–diffusion (partial differential) equations can describe the dynamics of the system taking into account diffusion of electrolytes and nucleation and aggregation of the precipitant species. Randomizing impacts like thermal fluctuation, presence of impurities, etc., are usually ignored in these models. Altogether, it is evident that quite diverse mechanisms can be at the helm of affairs of chemically generated patterns. They may also include even more physical aspects like buoyancy instabilities, surface tension, non-linear colloidal dynamics, etc., as the list of attributes.

The patterns usually consist of a set of clearly separated zones of colloidal precipitants, the shape of which depends on the geometry of the system. In typical systems that produce Liesegang patterns, the reacting components diffuse from outside to the gel medium impregnated homogeneously with the oppositely charged electrolyte species. The sparingly soluble precipitate of the chemical reaction coagulates at specific locations resulting in a sequence of precipitate bands. Precipitate moves diffusively into the zone and the dynamics can be described by a set of equations. Earlier investigators have framed four quantitative relations characterizing the pattern structure.

The first one relates the position of the ring ($x_n$) and its formation time ($t_n$) by a relation often called time law [15,16].

$$x_n = \alpha t_n^{1/2} + \beta, \tag{1}$$

where $\alpha$ and $\beta$ are the constants. This relation is analogous to Einstein–Smoluchowski relation for Brownian motion, interpreted in terms of random walk in homogeneous space [17].

The time law reflects the diffusive behaviour of the electrolyte into the gel matrix. The second one called the spacing law, is due to Jablczynski [18], which relates another important property of the bands

$$\frac{x_{n+1}}{x_n} = (1 + p), \tag{2}$$

where $(1 + p)$ is the spacing coefficient and the factor $p$ depends on the initial concentration of the reacting components. It has been observed in many experimental cases that $p$ varies from 0 to 0.5 [19]. A detailed study of the dependence of $p$ on concentration was made by Matalon and Packter [20,21].

According to them,

$$p = \Omega(b_0) + a_0^{-1}\Gamma(b_0), \tag{3}$$

where $\Omega(b_0)$ and $\Gamma(b_0)$ are two decreasing functions of their argument. Also the width or thickness $(w_n)$ of the bands has some functional regularity [22]:

$$w_n = \varepsilon x_n, \tag{4}$$

where $\varepsilon$ is a constant.

Many models, that provide theoretical prediction on the band formation was failed to provide conclusive suggestions on the domain size of the coagulated precipitants. Using cellular automata simulations, Chopard *et al* [23] have proposed

$$w_n = \varepsilon x_n^{\phi}, \tag{5}$$

where the width exponent $\phi$ depends on two constants $a_0$ and $b_0$. They have obtained theoretically the band structure for $\phi$ varying between 0.49 and 0.61. Later, Droz *et al* [24], combining the scaling properties of the density of precipitates in the bands, found that $\phi$ ranges from 0.90 to 0.99, which almost coincides with the linear dependence as suggested by eq. (4). Our goal here is to present an algorithm on pattern formation and predict the structure quantitatively with reasonably minimum inputs.

## 2. Theoretical methods

Several competing theories have been developed for describing the mechanism of Liesegang phenomena. All the theories share some common features to show how the diffusive reagents A and B turn into a final immobile precipitate D.

$$\mathrm{A} + \mathrm{B} \rightarrow \mathrm{D}. \tag{6}$$

Some theorists strongly prefer to place an intermediate compound (C′) as an inevitable component formed before the end product is reached [25].

$$\mathrm{A} + \mathrm{B} \rightarrow \mathrm{C}' \rightarrow \mathrm{D}. \tag{7}$$

Theoretical models can be grouped into two main categories. The first termed the pre-nucleation model, suggest that band formation can be treated on the basis of a feedback mechanism between the nucleation and diffusion transport [26–28]. Nucleation is a non-equilibrium process, and it occurs when the local product of the ion concentrations of

the reacting species reaches a saturation threshold value. The precipitation results in the reduction of the level of the supersaturation and no further nucleation is possible when the concentration product is less than the threshold limit. While the front proceeds further into the medium, the concentration product reaches the threshold level again and the nucleation of the precipitate is continuous. Repetition of this sequence results in periodic patterns. Theoretical predictions based on this model were made earlier by Wagner and Prager, and they assumed the existence of sharp periodic bands.

The second category, using Lifshitz–Sloyzov instability mechanism [29–31], suggests a post-nucleation droplet coarsening processes. The continuously advancing nucleation front produces an intermediate compound, which may be a homogeneous haze of colloids. The rate of production of colloid species is supposed to be proportional to the product of the local concentration of reactants. A first-order phase separation mechanism is assumed to take place inside the colloid-filled domain, separating them into regions of different matter densities. Such a process has the potential to generate a bunch of bands in a system when continuous domains of identical systems are perturbed. The precipitation bands arise by coagulation of the intermediate colloidal haze if certain critical electrolyte concentrations are exceeded [32]. The spatially distributed colloidal particles are unstable against perturbations [33]. Venzl [34] summarizes the process of Liesegang banding by three characteristic stages: the production of a continuous homogeneous colloid, the coarsening of the colloid and the dynamics of colloid particles resulting in pattern formation.

The moving boundary model [35] was suggested to deal with the problem slightly differently. Though it supports the formation of intermediate colloidal particles, it describes effectively the patterning process by considering a virtual migration of the boundary of the outer and the inner electrolytes. It also envisages a phase separation mechanism for the formation of the bands in the medium. The idea of formation of intermediate colloidal haze prior to patterning along with moving boundary model proved to be efficient in predicting the concentration dependence of the width of the spatio-temporal patterns. When the Liesegang patterns were studied by computer simulation, the usual method is to solve a set of coupled reaction–diffusion equations. We approach the task differentially by employing the results obtained directly from the moving boundary model. Once the boundary migration concept was introduced, the theory straight away upheld all the existing laws. Thus the moving boundary model is safer and simpler in many respects. It delineates scenery with distinctive assumptions and boundary conditions. Thus a better understanding of the basic facts of pattern formation and geometrical positioning of the bands is made possible with this model. The following are the basic approximations used in the moving boundary model.

(1) The initial concentration of the outer electrolyte $C_{A0}$ is assumed to be much larger than the initial concentration $C_{B0}$ of the inner electrolyte and it is also assumed that $C_A(x = 0, t)$ is kept fixed at the junction point of the electrolytes. For experiments, $0.005 \leq C_{B0}/C_{A0} \leq 0.1$.
(2) The boundary which separates the outer and inner electrolytes (gel–solution interface) is located at $x = 0$, in the $y$–$z$ plane. Also the type B ions are assumed to be uniformly distributed inside the gel medium and the initial concentrations are

$$C_A = C_{A0},\ C_B = 0; \quad x < 0,\ t = 0 \tag{8}$$

and

$$C_{\mathrm{A}} = 0,\ C_{\mathrm{B}} = C_{\mathrm{B0}};\quad x > 0,\ t = 0. \tag{9}$$

(3) As the reaction front advances into the medium in the positive $x$-direction, the concentration of type A ions varies and at the position of a band

$$C_{\mathrm{A}} = C_{\mathrm{A0}};\qquad 0 < x \leq x_n,\ t \sim t_n. \tag{10}$$

This assumption holds well as the reservoir concentration $C_{\mathrm{A0}}$ of type A ions is sufficiently large compared to the initial concentration $C_{\mathrm{B0}}$ of type B ions.

(4) The motion of the particles from one band to the other is assumed to be more or less uniform and therefore it can be assumed that the boundary layer shifts from one band to the next with uniform speed.

The concentration profile of type A ions in the gel is assumed to be [16]

$$C_{\mathrm{A}}(x,t) = C_{\mathrm{A0}} \exp\{-\beta(x - x_n(t))/\xi_{n+1}\},\quad x_n \leq x \leq x_{n+1}, \tag{11}$$

where $\beta > 0$, is a constant for a given system and $\xi_{n+1}$ is the separation between the $n$th and $(n+1)$th bands. For type B ions, the homogeneity of its concentration profile inside the gel column has been disturbed by the reaction process. It can be taken as

$$C_{\mathrm{B}}(x,t) = \eta C_{\mathrm{B0}} \exp\{-\gamma(x_n(t) - x)/\xi_n\} + C_{\mathrm{B0}}(1 - \eta' \exp\{-\gamma(x - x_n(t))/\xi_{n+1}\}). \tag{12}$$

Here $\gamma$ is another constant. The first term on the right side of eq. (11) represents those components of B which have successfully penetrated the band in the negative $x$-direction. Since this fraction is very small, the coefficient $\eta$ will be a very small positive quantity. The coefficient $\eta'$ appearing in the second term signifies the factor of $C_{\mathrm{B0}}$ which had been eliminated from its initial level due to the formation of the reaction product C$^*$. Applying the condition for band formation as stated in the ion product theory,

$$C_{\mathrm{A}}(x,t) C_{\mathrm{B}}(x,t) \mid x_n, t_n = \mathrm{C}^* \tag{13}$$

and

$$\partial/\partial x\{C_{\mathrm{A}}(x,t) C_{\mathrm{B}}(x,t)\} \mid x_n, t_n = 0. \tag{14}$$

Substituting the values of $C_{\mathrm{A}}(x,t)$ and $C_{\mathrm{B}}(x,t)$ from eqs (10) and (11) in eqs (12) and (13), we get

$$(\eta - \eta' + 1) C_{\mathrm{A0}} C_{\mathrm{B0}} = \mathrm{C}^* \tag{15}$$

and

$$\eta'(\beta/\gamma + 1) = \beta/\gamma + \eta(\beta/\gamma - \xi_{n+1}/\xi_n). \tag{16}$$

Writing $\xi_{n+1}/\xi_n = 1 + p$ and $\beta/\gamma = \alpha$, one obtains

$$\eta(\alpha - (1 + p)) + \alpha = \eta'(\alpha + 1). \tag{17}$$

Eliminating $\eta'$ from eq. (14) and by substituting in eq. (16),

$$p = K\mathrm{C}^*/\eta C_{\mathrm{B}0}^2 + K\alpha C^* - (1+2\eta)C_{\mathrm{B}0}^2/C_{\mathrm{A}0}(K\eta C_{\mathrm{B}0}), \tag{18}$$

where $K = C_{\mathrm{A}0}/C_{\mathrm{B}0}$ which obviously is the Matalon–Packater law. It is now desirable to calculate the values of the positive constants $\eta$ and $\eta'$ which were mentioned earlier. For this, substitute the value of $\mathrm{C}^*$ in eq. (17) and approximate the two concentration profile indices as the same. This will lead to

$$p = C_{\mathrm{B}0}^2\alpha(\eta - \eta' + 1) - (1+2\eta)/\eta C_{\mathrm{B}0}^2 \tag{19}$$

and finally to

$$p = (1-2\eta')/\eta. \tag{20}$$

If we assume the upper limit for $p$ as 0.5, then the two constants $\eta$ and $\eta'$ will become 0.05 and 0.493 respectively. On the other hand, if $p$ assumes the lowest range, i.e., $p \sim 0$ as in the case of equidistant band system, one of the constants becomes $1/2(\eta)$ and the other ambiguous. Thus the limiting ranges of the two new constants involved in the above calculation can be fixed. Using this value we may get a picture of the reaction mechanism. When $\eta'$ approaches 0.493, 49.3% of $C_{\mathrm{B}0}$ had been eliminated from its initial level, due to the formation of the reaction product ($\mathrm{C}^*$). This seems to be a large value, but generally in the precipitation band structure thick bands observed near the interface, nevertheless signifies this approximation. The value of $\eta$ which is small describes the intensity of penetration of type B ions into the negative direction. Here, in the approximation, $\eta \sim 0.05$ proposes a very low penetration of the B ions in the backward $(-x)$ direction.

An analysis of the width law is also possible at this juncture using the moving boundary concept. One of the main features of the intermediate species theory is that the substance to be precipitated is formed first as a continuous homogeneous colloidal dispersion [32,36,37]. A phase separation mechanism, the reason for which is not yet clear, occurs in the medium which segregates, the colloidal precipitants into a band. Different techniques were proposed to explain the phenomenon of phase separation. Droz *et al* analysed the phenomenon by employing spinoidal decomposition processes [38,39] and by the action of a moving reaction front. The reaction front produces colloidal particles and small clusters of particles nucleate and aggregate behind the front. The phase separation mechanism distributes the homogeneous colloidal particles of uniform initial concentration $c_0$ into two parts: a band having concentration $c_{\mathrm{b}}$ and a gap having concentration $c_{\mathrm{g}}$. Applying the rules of matter conservation we write

$$w_n c_{\mathrm{b}} + (\xi_n - w_n)c_{\mathrm{g}} = \xi_n c_0, \tag{21}$$

where $w_n$ is the width of the $n$th band.

The width of the $n$th band as a function of the concentration is

$$w_n = (c_0 - c_{\mathrm{g}})/(c_{\mathrm{b}} - c_{\mathrm{g}})\xi_n, \tag{22}$$

or

$$w_n = f_{\mathrm{c}}\xi_n, \tag{23}$$

where

$$f_{\mathrm{c}} = (c_0 - c_{\mathrm{g}})/(c_{\mathrm{b}} - c_{\mathrm{g}}) \tag{24}$$

is the width coefficient, which will be more or less constant for a steady pattern. Thus the width of the precipitation bands depends exclusively on the concentration of the intermediate colloidal particles.

For the evaluation of the values of $f_c$, the following approximations are useful:

(1) During the diffusion processes, type A particles will move towards the positive $x$-direction and a fraction of type B particles will move towards the negative $x$-direction. The remaining type B particles with concentration $(1-\eta)C_{B0}$, available in the diffusion zone, are capable of initiating the reactions.
(2) The quantity of colloidal precipitants formed will be a further fraction of the available electrolytes. Hence we proceed to assume $\mu(1-\eta)C_{B0}$ as the amount of the colloidal particles generated.
(3) The colloidal particles which segregate on the band is yet another fraction $\lambda(1-\eta)C_{B0}$ of the total colloidal particles generated.
(4) All the remaining particles will present in the gap.

Also from these assumptions, we equate the total concentration of colloidal precipitants produced $c_0$ and the concentration of the precipitants on the band $c_b$ as,

$$c_0 = \mu(1-\eta)C_{B0}, \tag{25}$$

$$c_b = \lambda(1-\eta)C_{B0}. \tag{26}$$

Upon substituting these values in eq. (23) it becomes,

$$f_c = \lambda/(2\lambda - \mu). \tag{27}$$

Majority of the colloidal particles appear to segregate on the bands and the void region contains practically very few colloidal particles. When $\lambda = 0$, $f_c$ also becomes zero, which gives the no-band condition. Between the values $0 \leq \lambda \leq 0.5$, $f_c$ becomes negative and band formation is forbidden. The width coefficient $f_c$ has an anomalous behaviour at $\lambda = 0.5$ and it takes the value 0.5 asymptotically. We may conclude that for sustained band formation, $\lambda \geq 0.5$, which is somewhat a critical condition. Hence it may be safer to approximate

$$f_c \approx 1/2 \tag{28}$$

when $\mu \ll \lambda$ and $\lambda = 1$ as special case and we simulate the patterns for this case. This gives an immediate conclusion

$$w_n = \xi_n/2. \tag{29}$$

The widths of the bands become half the separation distance and this is true only for small values of $n$. When $n$ becomes larger, the contribution of $\mu$ in eq. (26) becomes considerably large and the widths of the bands become lesser than this value.

## 3. Experimental methods

An experiment was carried out to obtain precipitation bands. This consists of silver dichromate precipitation bands in gelatin gel. The concentration of the outer (silver nitrate) and

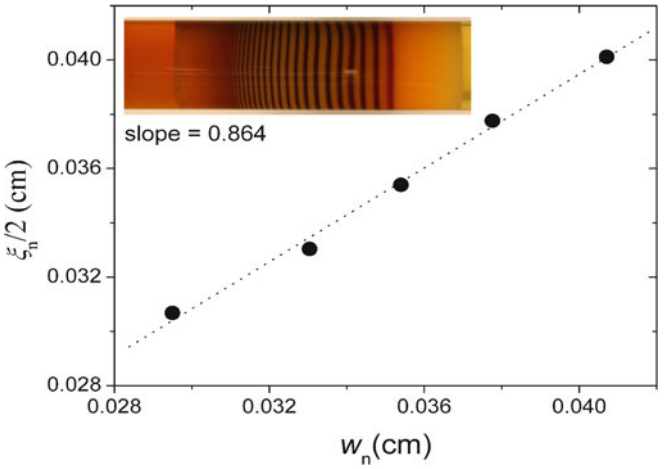


**Figure 1.** Dependence of the half-separation distance on the width of the band for the first five bands in silver dichromate system in 12.5 wt% gelatin gel. The concentration of the outer (silver nitrate) and the inner (potassium dichromate) electrolytes are 0.25 M and 0.0036 M, respectively. The obtained spacing coefficient is 0.074. The size of the experimental picture is 5.6 cm × 1.7 cm.

the inner (potassium dichromate) electrolytes are 0.25 M and 0.0036 M, respectively. Well-defined bands were seen at regular intervals in the gel column depicting the geometric sequence of Liesegang patterns. The width of the bands was approximately half of the interband separation (figure 1), supporting the theoretical predictions made on the basis of the moving boundary model.

## 4. Simulation

The algorithm of the program for simulation contains the following procedures:

(1) Assuming the values of $p$, compute the constants $\eta$ and $\eta'$.
(2) Compute the position of the first band using spacing law, assuming $x_0 = 1$.
(3) Continue the process for ten successive steps by assuming the concentration $C_{A0}$ as fixed.
(4) Compute the separation distance for each band and hence calculate the width of the bands using eq. (29).
(5) Then plot the bands using the above steps.

On the basis of this algorithm, two-dimensional band structures were generated by a Matlab programme, resembling Liesegang-type patterns. The geometry of the pattern bears all distinguishable features of the experimentally observed structure. These two-dimensional patterns are obtained for $p = 0.077$ and 0.5, respectively (figures 2 and 3). The pattern in the figure shows fixed values for $y$-axis, maximum or zero. The maximum corresponds to the initial concentration of outer diffusant ($C_{A0}$). This parameter does not vary between $x_n$ and $x_n + w_n$ (shown as the shaded region) as envisaged in the moving boundary model.

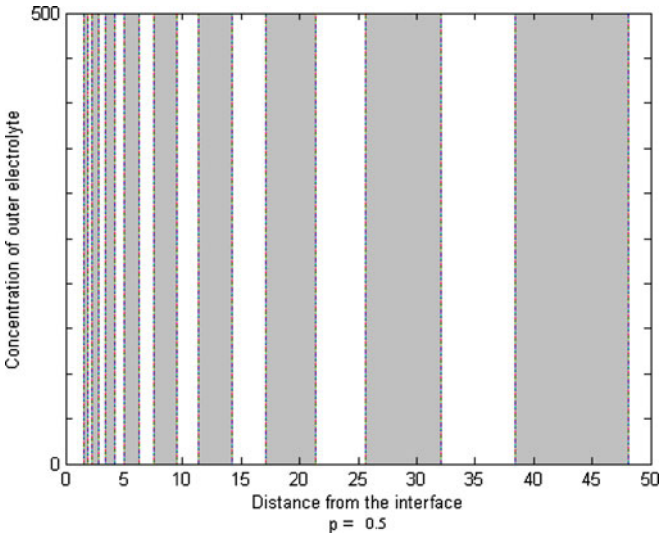


**Figure 2.** Computer simulated pattern for spacing coefficient $p = 0.5$. The concentrations taken on $y$-axis represent millimoles per litre and the distance on $x$-axis is in cm.

Beyond this point the concentration of type A ions falls to zero (blank region). This repeats periodically in space and hence the system is obtained. However, it does not mean that concentration of type A ions has a discontinuous regime before the precipitation zone. As $p$

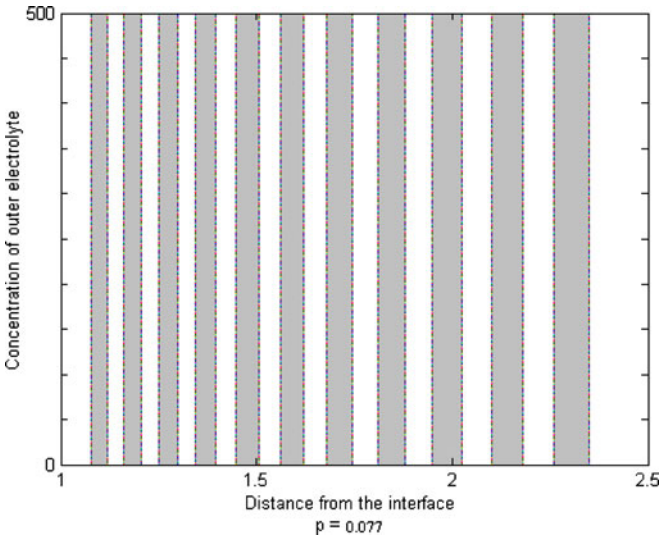


**Figure 3.** Computer simulated pattern for spacing coefficient $p = 0.077$. The concentrations taken on $y$-axis represent millimoles per litre and the distance taken on $x$-axis is in cm.

increases, the spacing and hence the width of the bands increases. Hence different patterns may be obtained for different concentrations of electrolytes. Plotting may also be possible for $\lambda$ values ranging from 0.5 to 1. Three-dimensional patterns can also be obtained by a similar analysis.

## 5. Conclusions

The moving boundary model provides a reasonable conclusion on the spatial positioning of the periodic band structure observed in reaction-limited diffusion systems. The theoretical calculations based on the model suggest that the width of the precipitation bands depends exclusively on the concentration of the intermediate colloidal particles. Also the theory could stipulate a critical condition for sustained band formation in the reaction–diffusion systems. This idea was sequentially developed to generate patterns in a Matlab program. The algorithm for this was prepared entirely on the basis of moving boundary concept and the simulated patterns bear the characteristic nature of the experimentally observed Liesegang patterns. The intermediate colloid formation hypothesis was once again ascertained in the model and it seems to be useful in illustrating many other phenomena, in particular, the self-sustained steady patterns.

## Acknowledgements

The authors gratefully acknowledge financial support from the Indo–Hungarian bilateral research fund of both the Governments. This research is partially supported by Hungarian Research Found (OTKA K68253 and K81933) and by the European Union and co-financed by the European Social Fund (Grant Agreement No. TAMOP 4.2.1./B-09/1/KMR-2010-0003).

## References

[1] E J Crampin, W W Hackborn and P K Maini, *Bull. Math. Biol.* **64**, 747 (2002)
[2] R E Liesegang, *Naturwiss. Wochenschr.* **11**, 353 (1896)
[3] I Bena, M Droz, I Lagzi, K Martens, Z Rácz and A Volford, *Phys. Rev. Lett.* **101**, 075701 (2008)
[4] A M Turing, *Phil. Trans. R. Soc.* **B237**, 37 (1952)
[5] M Al-Ghoul and R Sultan, *J. Phys. Chem.* **A105**, 8053 (2001)
[6] T Antal, I Bena, M Droz, K Martens and Z Rácz, *Phys. Rev.* **E76**, 046203 (2007)
[7] Q Ouyang and H L Swinney, *Nature* **352**, 610 (1991)
[8] K J Lee, W D McCormick, H L Swinney and Z Nosticziusz, *J. Chem. Phys.* **96**, 4048 (1992)
[9] V K Vanag and I R Epstein, *Phys. Rev. Lett.* **87**, 228301 (2001)
[10] J Ross, Adam P Arkin and Stefan C Mueller, *J. Phys. Chem.* **99**, 10417 (1995)
[11] J Horvath, I Szalai and P D Kepper, *Physica* **D239**, 776 (2010)
[12] E S Hedges and R V Hanley, *J. Chem. Soc.* Article no. CCCLX, 2714 (1928)
[13] D N Ghosh, *J. Indian Chem. Soc.* **1**, 509 (1930)
[14] M Flicker and J Ross, *J. Chem. Phys.* **60**, 3458 (1974)
[15] H W Morse and G W Pierce, *Z. Phys. Chem.* **45**, 589 (1903)
[16] H W Morse and G W Pierce, *Proc. Am. Acad. Arts Sci.* **38**, 625 (1903)
[17] A Einstein, *Ann. Phys. 4th Ser.* **xvII**, 549 (1905)

[18] K Jablczynski, *Bull. Soc. Chim. Fr.* **33**, 1592 (1923)
[19] T Antal, M Droz, J Magnin, Z Rácz and M Zrinyi, *J. Chem. Phys.* **109**, 9479 (1998)
[20] A Packter, *Kolloid Zeitschrift.* **142**, 109 (1955)
[21] A Packter and R Matalon, *J. Colloid Sci.* **10**, 46 (1955)
[22] K M Pillai, V K Vaidyan and M A Ittyachen, *Colloid Polym. Sci.* **258**, 831 (1980)
[23] B Chopard, P Luthi and M Droz, *Phys. Rev. Lett.* **72**, 1384 (1994)
[24] M Droz, J Magnin and M Zrinyi, *J. Chem. Phys.* **110**, 9618 (1999)
[25] M Droz, *J. Stat. Phys.* **101**, 509 (2000)
[26] W Ostwald, *Z. Phys.* **23**, 365 (1897)
[27] C Wagner, *J. Colloid Sci.* **5**, 85 (1950)
[28] S Prager, *J. Chem. Phys.* **25**, 279 (1956)
[29] R Lovett, P Ortoleva and J Ross, *J. Chem. Phys.* **69**, 947 (1978)
[30] R Feeney, S L Schmidt, P Strickholm, J Chadam and P Ortoleva, *J. Chem. Phys.* **78**, 293 (1983)
[31] I M Lifshitz and V V Slyozov, *J. Phys. Chem. Solids* **19**, 35 (1961)
[32] S Shinohara, *J. Phys. Soc. Jpn* **29**, 1073 (1970)
[33] G Venzl and J Ross, *J. Chem. Phys.* **77**, 1308 (1982)
[34] G Venzl, *J. Chem. Phys.* **85**, 1996 (1986)
[35] J George and G Varghese, *Chem. Phys. Lett.* **362**, 8 (2002)
[36] J George and G Varghese, *J. Colloid Interface Sci.* **282**, 397 (2005)
[37] D A B Young, *Colloid Polym. Sci.* **278**, 464 (2000)
[38] D Gunton, M S Miguel and P S Sahni, *Phase transition and critical phenomena* edited by C Domb and J L Lebowitz (Academic Press, New York, 1983)
[39] T Antal, M Droz, J Magnin and Z Rácz, *Phys. Rev. Lett.* **83**, 2880 (1999)